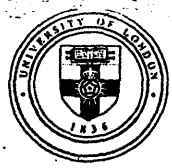

REFERENCE ONLY

UNIVERSITY OF LONDON THESIS

Degree PhD Year 2006 Name of Author TONG, H

MODULATION OF NMDA RECEPTOR ACTIVITY BY DOPAMINE RECEPTORS IN THE RAT STRIATUM

HUAXIA TONG

A thesis submitted for the degree of

Doctor of Philosophy

in the

University of London

Department of Pharmacology

University College London

March 2006

ProQuest LLC
789 East Eisenhower Parkway
P.O. Box 1346
Ann Arbor, MI 48106-1346

Abstract

NMDA receptors are of particular importance in the control of synaptic strength and integration of synaptic activity. Dopamine receptor modulation of NMDA receptors in the striatum may influence the efficacy of synaptic transmission in the cortico-striatal pathway (Calabresi et al., 2000c; Centonze et al., 2003) and if so, this modulation will be lost in Parkinson's disease. This change may be an important factor in the changes in the basal ganglia neural network that occur in Parkinson's Disease. In this thesis I have studied dopamine D1 and D2 receptor modulation of NMDA receptors in medium spiny neurons of 7-21 day old rat striatum.

The dopamine D1 receptor agonist, SKF-82958, significantly decreased rat striatal NMDA receptor currents in patch-clamp whole-cell recordings from 7 day old rats. This inhibition was not abolished by application of a G protein inhibitor (GDP-β-S) or irreversible activator (GTP-γ-S) suggesting a G protein-independent mechanism. In addition, intracellular application of protein tyrosine kinase inhibitors (lavendustin A or PP2) abolished D1 inhibition of NMDA currents. Functional NR2A receptors were absent in 7 day old rat striatum according to my experiments. Single-channel recordings showed that direct D1 receptor inhibition of NMDA receptors can not be observed in isolated membrane patches, which may indicate that D1 inhibition in whole-cell recordings is mediated by a change in NMDA receptor trafficking. Consistent with this hypothesis, intracellular application of a dynamin inhibitory peptide (QVPSRPNRAP) abolished D1 inhibition of NMDA receptor currents. I therefore conclude that a tyrosine kinase–dependent alteration of NMDA receptor trafficking underlies D1 dopamine receptor-mediated down-regulation of NMDA receptor currents in the striatum.

The D2 class dopamine receptor agonist, quinpirole, significantly inhibited the NMDAR responses at 1 μM, but at a lower concentration (40 nM) there was no significant effect in 7 day old rat striatum. Replacement of GTP with GDP-β-S in the pipette solution abolished the inhibition induced by 1 μM quinpirole suggesting a G protein-dependent mechanism underlies the D2 family dopamine receptor modulation of NMDA receptors in the striatum.

TABLE OF CONTENTS

LIST OF FIGURES

Chapter 1

Chapter 3

Chapter 4

Chapter 5

Chapter 6

LIST OF TABLES

Chapter 1

Chapter 3

Acknowledgements

I would like to express heartily my thankfulness to my supervisor Alasdair J. Gibb. He brought me to the amazing world of neuroscience and electrophysiology and created such a great opportunity for me to become a young scientist. He is the greatest teacher I have ever met for his invaluable guidance, constant support and encouragement, patience and friendship. I really enjoyed my PhD in his lab.

I would like to thank Beth Rycroft for her precious help during the first year of my PhD. I would also like to thank Michiko Takahashi for her great suggestions and support, Veronica Gee, Zhuo Huang and other members of the lab for making the lab friendly and enjoyable.

I would like to thank everyone in the Pharmacology Department because they are helpful and very friendly which makes me feel at home.

I am grateful for the Graduate School Research Scholarship from University College London that has allowed me to finish the PhD

I would like to express my deep appreciation to my parents for their steady support and love.

Finally I can not be thankful enough to my husband Lin Li for his love, support and understanding. I am so fortunate to have him.

Chapter 1

Introduction

1.1 Why is this project important?

N-methyl-D-aspartate (NMDA) receptors are one type of glutamate receptor and play a crucial role in excitatory synaptic transmission. Understanding how NMDA receptors behave and how they are regulated is important for a number of reasons. As a cellular model for learning and information storage in the central nervous system, NMDA receptor dependent long-term potentiation (LTP) and long-term depression (LTD) have been described in several brain areas including the striatum (Calabresi et al., 1992; Charpier et al., 1997). Moreover NMDA receptor mediated excitotoxicity has been shown to contribute to the death of striatal neurons under some pathological conditions (Koroshetz et al., 1990; Cepeda et al., 1998b; Li et al., 2003 and Zeron et al., 2002).

NMDA receptor activity can be regulated by protein kinases (PKA, PKC and tyrosine kinases) (Blank et al., 1997; Lu et al., 1999; Xiong et al., 1999; Lei et al., 2002) and protein phosphatases (PP1 and calcineurin) (Lieberman and Mody, 1994; Morishita et al., 2002; Krupp et al., 2002; Rycroft and Gibb, 2004). There is substantial evidence showing that G protein-coupled receptors such as dopamine receptors modulate NMDA receptor activity (Blank et al., 1997; Chen et al., 2004). Therefore dopamine receptor modulation of NMDA receptors in the striatum could result in a change of the efficacy of synaptic transmission in the cortico-striatal pathway, and this modulation may be lost

during the progress of Parkinson's disease. In addition the interaction between glutamatergic and dopaminergic input in the striatum is crucial for movement control. Imbalance of this interaction may contribute to motor abnormalities in Parkinson's disease (Hallett & Standaert, 2004).

1.2 Basal Ganglia

1.2.1 Overview

Movements are produced by spatial and temporal muscular contractions mediated by the brain and spinal cord. There are several levels of movement control ensuring that movements are executed properly; for instance, they are from the lower motor neurons in the spinal cord and brainstem to the upper motor neurons locating in several brainstem centers and cortical areas in the frontal lobe (Purves et al., 2001). Moreover, the basal ganglia, lying in the basal telencephalon, receive information primarily from the cerebral cortex and thalamus, and influence motor behavior by regulating the activity of upper motor neurons mostly locating in the cortex. The basal ganglia are a large and functionally various set of interconnected nuclei including the caudate nucleus, putamen, globus pallidus, subthalamic nucleus and substantia nigra.

1.2.2 The five individual nuclei

The caudate and putamen together make up the largest part of the striatum, which is the main input structure of the basal ganglia circuit (Blandini et al., 2000). The striatum

receives most of the excitatory projection from virtually the whole area of the cortex, and the main targets of striatal projections are the globus pallidus and the substantia nigra pars reticulata (Parent and Hazrati 1995a).

Globus pallidus consists of internal (medial globus pallidus) and external (lateral globus pallidus) divisions. The internal part passes the basal ganglia output onto the thalamus and eventually onto the motor cortex. The external part projects to a number of structures, but principally to the subthalamic nucleus.

The subthalamic nucleus is the only glutamatergic nucleus in the basal ganglia (Smith and Parent, 1988). Cortical input to the subthalamic nucleus can interact with information processed in the striatum to determine the excitatory action on basal ganglia output neurons (Adel et al., 1998).

The substantia nigra is made of two different structures, the substantia nigra pars compacta (SNc) and the substantia nigra pars reticulata (SNr). They both receive information from the striatum and the subthalamic nucleus. Neurons in the substantia nigra pars compacta contain neuromelanin and use dopamine as neurotransmitter (Blandini et al., 2000), and they offer dopaminergic inputs to the striatal neurons. However, neurons in the reticulata part use gamma-aminobutyric acid (GABA) as neurotransmitter and they mainly project to the thalamus.

1.2.3 The basal ganglia circuitry

The normal functional circuitry of the basal ganglia receives the information from the cortex, and transmits as well as influences its return to the cerebral cortex via a direct and an indirect pathway. This conceptual model of basal ganglia function (Albin et al., 1989; Alexander and Crutcher 1990) is useful in understanding the action of dopamine in Parkinson's disease, although it is still being revised and refined (Cheselet and Delfs, 1996; Bolam et al., 2000; Smith et al., 1998).

1.2.3.1 The original model of the circuitry

According to the conceptual model (Albin et al., 1989; Alexander and Crutcher 1990), the information received from the cortex is sent out by the striatum via the direct and the indirect pathway. The direct pathway starts from striatal GABAergic neurons, containing dynorphin and substance P (the substance P neurons mainly project to SNr) and expressing both DA receptor classes but predominately D1 receptors (Webster, 2001). They make monosynaptic contact with the internal globus pallidus (IGP, medial globus pallidus) and to a lesser extent the substantia nigra reticulata (SNr). In the indirect pathway, the striatal GABAergic neurons contain enkephalin and express D2 receptors. They then project to the external globus pallidus (EGP, lateral globus pallidus), which sends GABAergic projections to the subthalamic nucleus. The subthalamic nucleus (STN) sends its glutamatergic efferents to the globus pallidus and substantia nigra. From the output nuclei (IGP, SNr) GABAergic projections reach the ventral lateral and ventral anterior nuclei of the motor thalamus. The thalamic nuclei then send glutamatergic

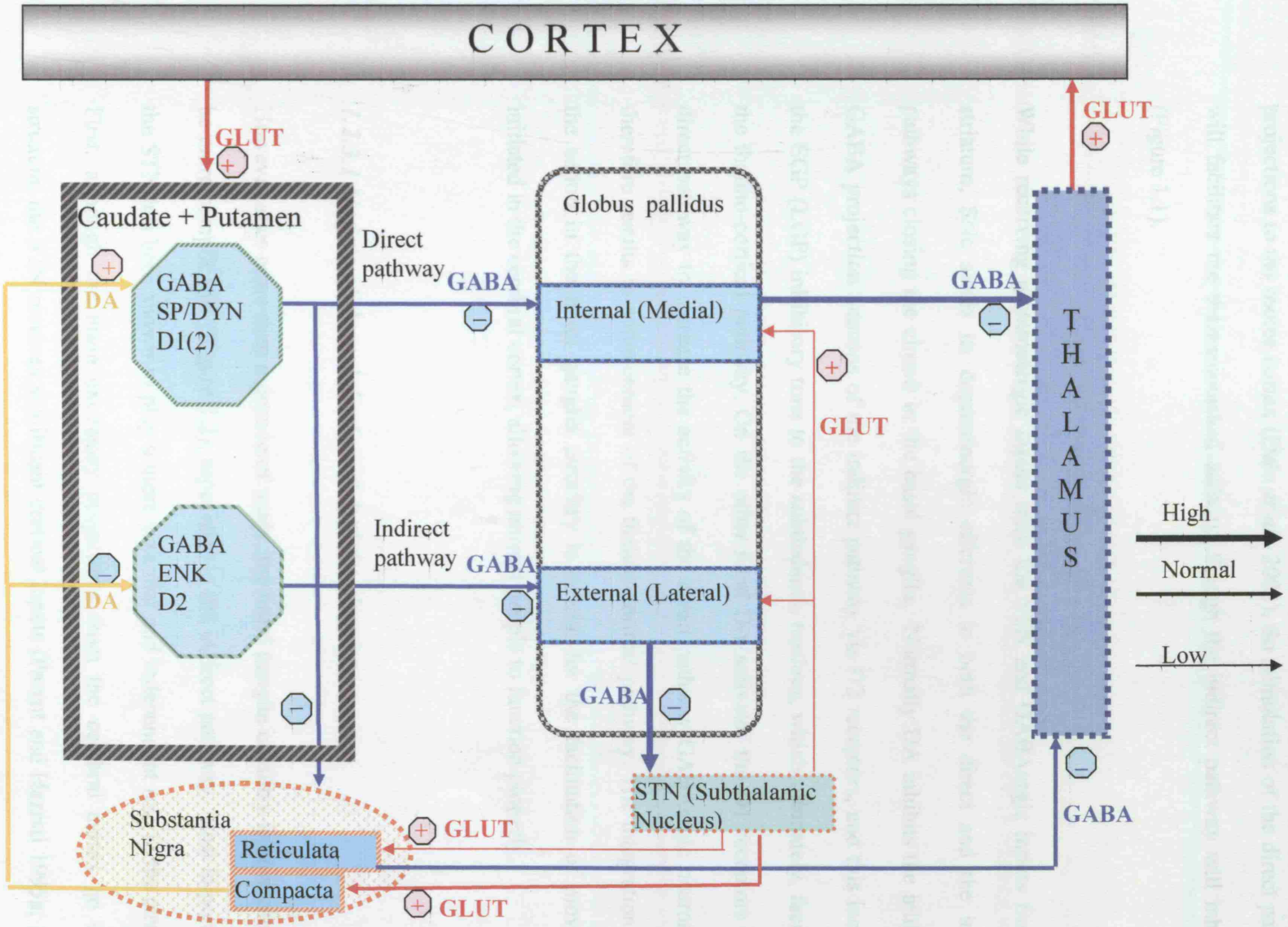

Figure 1.1 Schematic presentation of the normal functional basal ganglia circuitry (direct and indirect pathways). Modified from Alexander and Crutcher, 1990.

projections to the motor cortex (Dale *et al.*, 2001). So stimulation of the direct pathway will facilitate the thalamocortical activity, though the indirect pathway will inhibit it (Figure 1.1).

While receiving glutamatergic inputs from the STN and GABAergic inputs from the striatum, SNc sends its dopaminergic efferents to both the direct and the indirect pathways closing the circuit in the basal ganglia. Normally DA inhibits the inhibitory GABA projection neurons of the indirect pathway via D2 receptors, and this increases the EGP (LGP) inhibitory tone to the subthalamic nucleus, which ultimately, facilitates the thalmo-cortical pathway. On the other hand DA activates the D1 receptors of the direct pathway to increase the activity of the direct pathway GABAergic neurons and therefore results in enhancement of the thalmo-cortical pathway. The integration of all the action in the basal ganglia circuitry is crucial for the facilitation of movement initiated in the cerebral cortex, allowing normal people to function properly.

1.2.3.1 Update of the original model of the circuitry

However after more than a decade of study, the basal ganglia circuitry is now known to be more complicated (Figure 1.2), especially in the indirect pathway. Most importantly, the STN has been shown to play a more essential and independent role in the circuitry. First, although the main excitatory projections from the cerebral cortex go to the striatum, the STN receives significant cortical inputs (Parent and Hazrati 1995a; Smith et al., 1998; Chesselet and Delfs 1996; Mchaffie et al., 2005). Secondly the STN and the

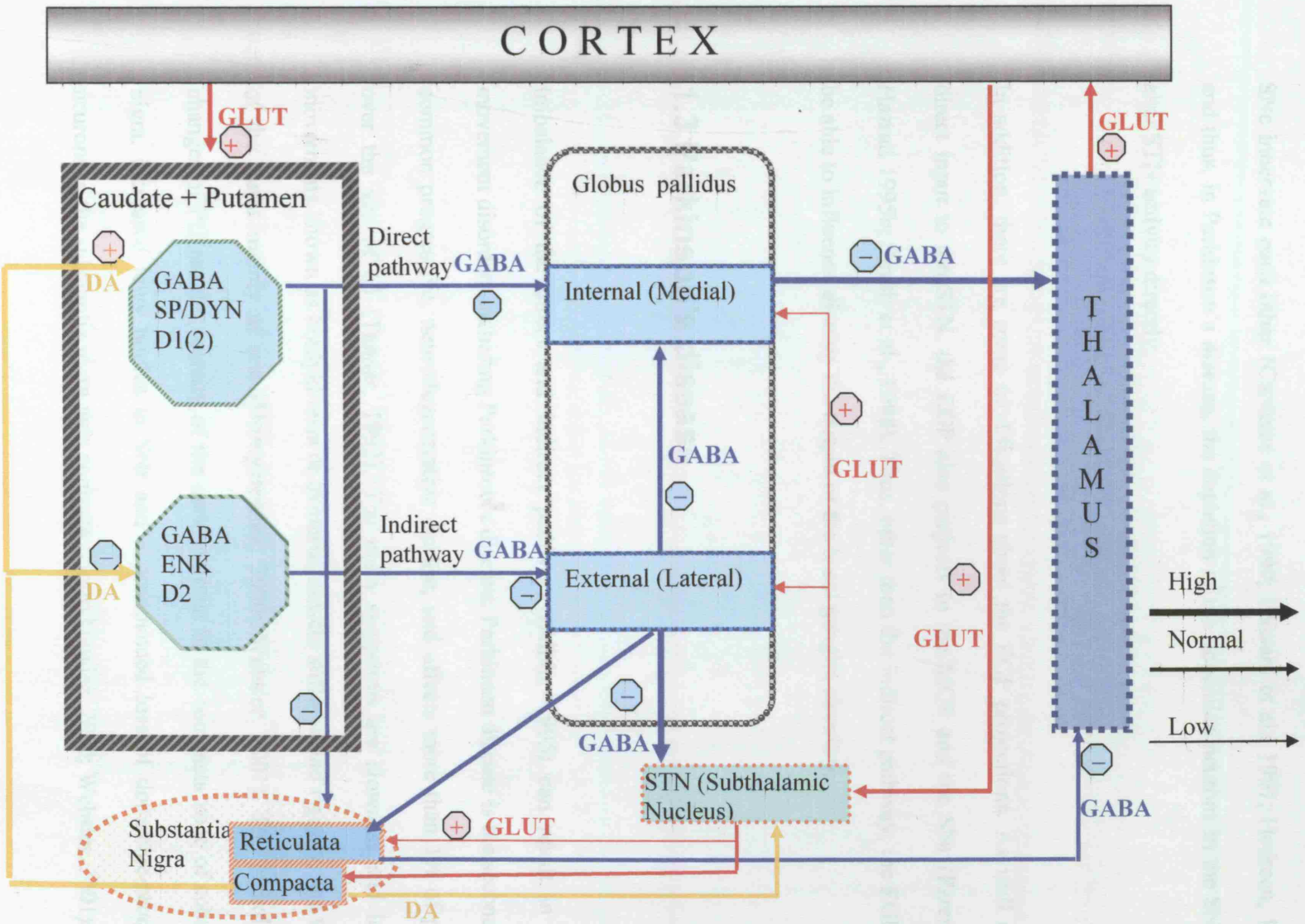

Figure 1.2 Schematic presentation of the updated basal ganglia circuitry (direct and indirect pathways).
Modified from Alexander and Crutcher, 1990 and Chesselet and Delfs, 1990.

SNc innervate each other (Canteras et al., 1990; Hassani et al., 1997; Hedreen, 1999), and thus, in Parkinson's disease, the depletion of the dopamine neurons in the SNc can alter STN activity directly.

In addition, there are some modifications about the EGP projections. As well as the direct input to the STN, the EGP also projects to the MGP and the SNr (Parent and Hazrati 1995b; Smith et al., 1998). Thus, other than the indirect pathway, the EGP may be able to influence directly the output of the basal ganglia circuitry.

1.3 Parkinson's disease

Imbalance of the direct and indirect pathways (Albin, 1995) can result in many movement disorders including Parkinson's disease. Parkinson disease is the second most common progressive, neurodegenerative disease, and affects more than 1% of people over the age of 65 (Tanner, 1992). The main symptoms are slowness and loss of movements known as bradykinesia or akinesia, muscle stiffness and rigidity, and tremor of the limbs mainly at rest (Hornykiewicz, 2000; Webster, 2001). The pathological changes of PD are the scarcity of the dark pigment in the compacta zone of substantia nigra, increased lewy bodies in SNr and a pronounced loss of dopamine-producing neurons in the substantia nigra pars compata (Hornykiewicz, 2000; Webster, 2001)

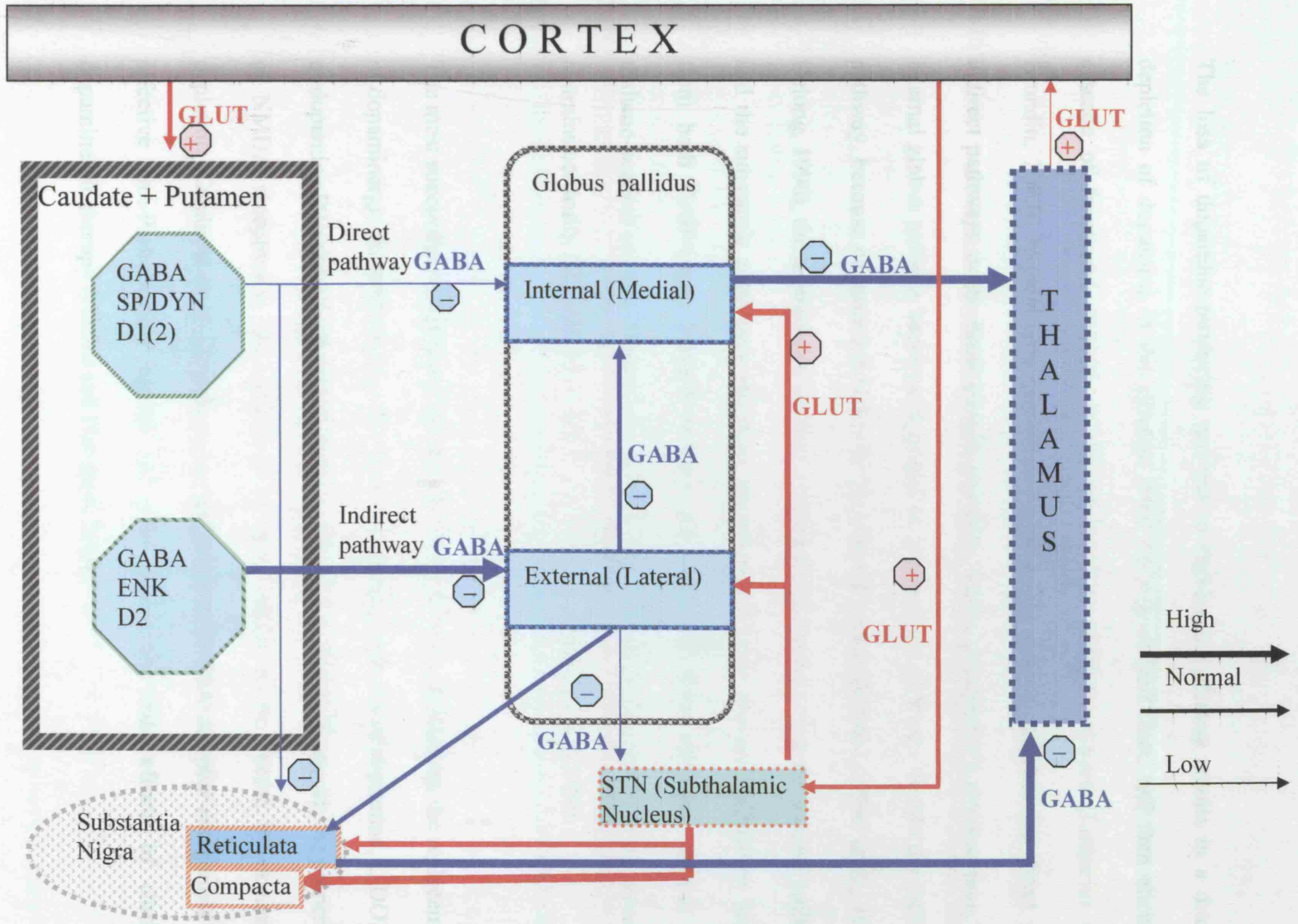

Figure 1.3 Schematic presentation of the changes in the basal ganglia circuitry in the Parkinson's disease. Modified from Alexander and Crutcher, 1990 and Chesselet and Delfs, 1990.

The loss of dopamine-producing neurons in Parkinson's disease results in a drastic depletion of dopamine in the striatum from the nigrostriatal tract, and then elicits a cascade of functional changes in the whole basal ganglia network (Lotharius and Brundin, 2002). Nigrostriatal dopamine regulates the activity of both the direct and indirect pathways in the basal ganglia circuitry. Under the disease's circumstance, the internal globus pallidus becomes hyperactive in the direct pathway. Within the indirect pathway, because of more inhibition to the external globus pallidus (Albin et al., 1989; Delong, 1990), the subthalamic nucleus glutamatergic inputs to both the internal pallidus and the substantia nigra pars reticulata are enhanced. Thus increased inhibitory drive, from both GABAergic internal pallidus and nigra reticulata neurons, reduces the thalamo-cortical activity (Figure 1.3). Therefore, the dopaminergic deficit in the striatum restrains cortically initiated movement (hypokinesia) (Hornykiewicz,2000).

The most successful symptomatic treatments for Parkinson's disease are the replacement of dopaminergic stimulation by either the biosynthetic precursor of dopamine, L-DOPA, or dopamine D1 receptor agonists (Hallett and Standaert, 2004). However, the properties of NMDA receptors in the striatum have been shown to be altered by dopamine depletion (Calabresi et al., 2000b). In animal models, NMDA receptor antagonists are effective anti-Parkinsonian agents and can reduce the side effects of chronic dopaminergic therapy (Hallett and Standaert, 2004).

1.4 Striatum

1.4.1 Anatomy and function

The striatum is mainly defined by the caudate nucleus and putamen. Due to different locations and connections each part has different functions. The caudate nucleus can be divided into head and body. The ventromedial part of the head of the caudate nucleus is involved in motivation, reward and emotion, because it connects to the lateral orbitofrontal cortex, which works in the normal function of the limbic system. The dorsolateral part of the head of the caudate is part of the dorsolateral prefrontal circuit and so is involved in cognitive functions. The putamen is located lateral to the globus pallidus and medial to the external capsule (Adel K. et al.,1998) and links with the supplementary motor area and premotor cortex so it is chiefly involved in motor control (Jain et al., 2001).

There are three main projections that go to the striatum, and they are the cortico-striatal projection, thalamo-striatal projection, and mesencephalo (substantia nigra)-striatal projection. Glutamatergic projections from cortical areas are the major excitatory inputs, and some excitatory inputs also arise from thalamus and amygdala to the striatum (Groenewegen and Berendse, 1990; Kelley et al, 1982). The principal mesencephalo-striatal projection originates from dopamine-containing cells of the substantia nigra pars compacta. The projection neurons of the striatum mainly send the GABAergic fibers to

Figure 1.4 Horizontal rat brain slice The picture is from Laboratory of NeuroImaging, UCLA. http://www.loni.ucla.edu/Research/Atlases

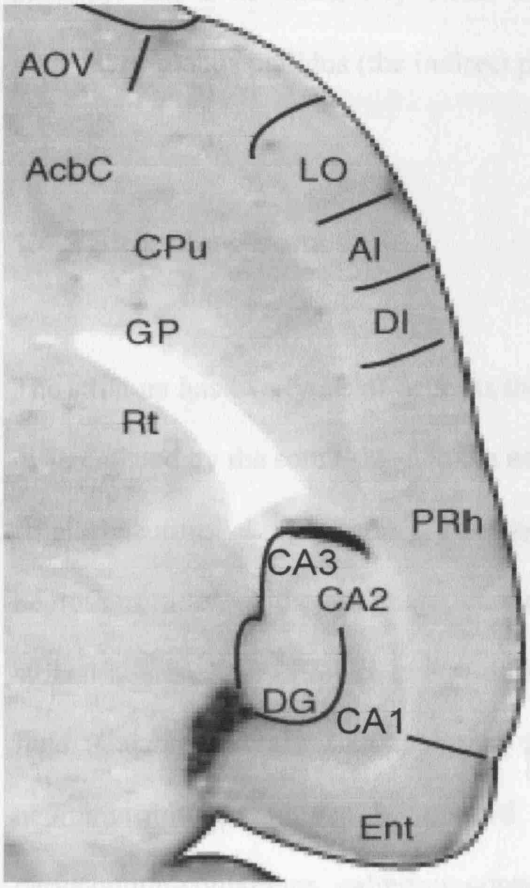

Acbc accumbens nucleus, core
AI agranular insular cortex
AOV anterior olfactory
CA1 field of CA1 of hippocampus
CA2 field of CA2 of hippocampus
CA3 field of CA3 of hippocampus
Cpu caudate putamen
DG dentate gyrus
DI dysgranular insular cortex
Ent entorhinal cortex
GP globus pallidus
LO lateral orbital cortex
PRh perirhinal cortex
Rt reticular thalamic nucleus

the globus pallidus and the substantia nigra pars reticulata. In addition dopaminergic inputs from SNc have a net excitatory effect on striatal neurons that project to the internal segment of globus pallidus and substantia nigra pars reticulata (the direct pathway) and a net inhibitory effect on striatal neurons that project to the external segment of globus pallidus (the indirect pathway)（Adel K. *et al.*, 1998）.

1.4.2 Striatal neurons

The striatum has two types of neurons that are aspiny and spiny. Aspiny neurons can be differentiated by the soma size and the neuropeptide, and they make up about 10% of the striatal neurons. Large aspiny interneurons (around 30 μm) use acetylcholine as neurotransmitter. Although these cholinergic cells compose only 1-2% of the total striatal neurons, they project to a wide area in the striatum with their extensive axonal field (Calabresi et al., 2000a). Some of the medium aspiny neurons use GABA as neurotransmitter, and can be divided into subtypes: the calcium binding proteins parvalbumin-containing, calretinin-containing and somatostatin /neuronal nitric oxide synthase containing neurons (kawaguchi et al., 1995). These GABAergic interneurons make projections to medium spiny neurons and modulate their activity.

Spiny neurons constitute most of the striatal neuron population (about 90%), and their size is medium about 10-15 μm in diameter. They are the main projection neurons of the striatum and use GABA as their basic transmitter, as well as synthesize a number of neuropeptides. Those projecting to the external globus pallidus express enkephalin as a

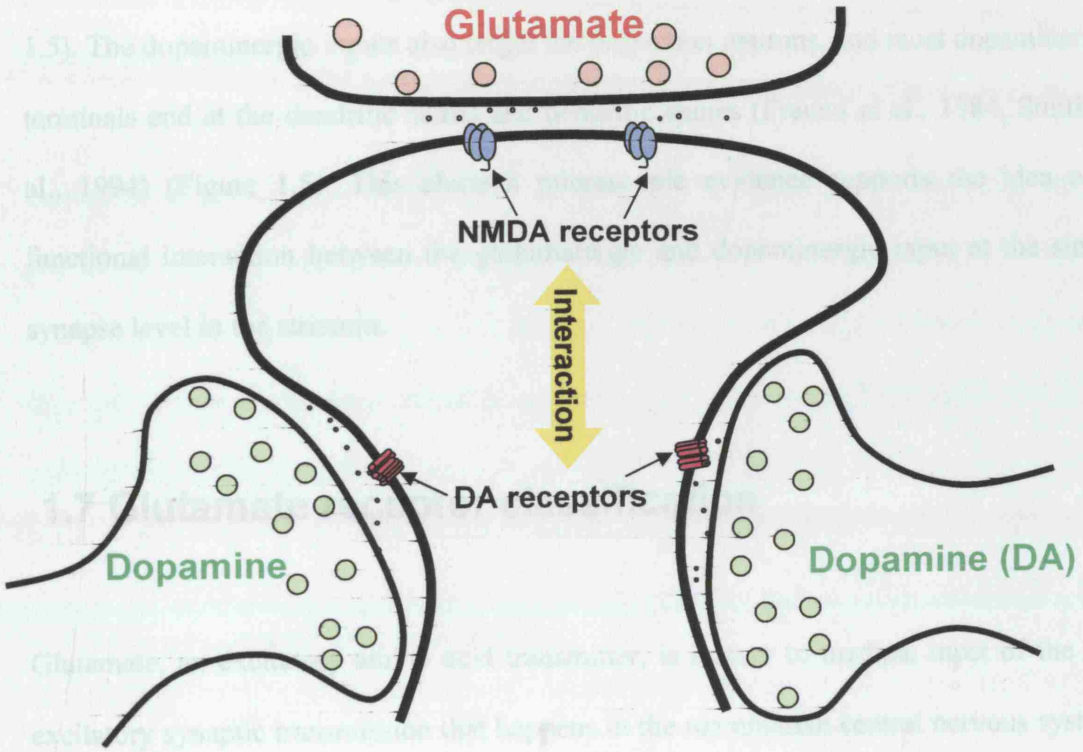

Figure 1.5 A cartoon of the dendritic spine of the medium spiny neuron

Dopaminergic inputs project from substantia nigra pars compacta to the neck of the spine, and glutamatergic inputs from cortex project to the head of the spine.

co-transmistter, while those projecting to the substantia nigra and internal pallidum utilize substance P and dynorphin (Beckstead, 1985; Gerfen et al., 1990). Most of the glutamatergic inputs from the cortex project to the medium spiny neurons and terminate on the heads of the dendritic spines (Smith et al., 1994; Yung and Bolam 2000) (Figure 1.5). The dopaminergic inputs also target the projection neurons, and most dopaminergic terminals end at the dendritic shafts and dendritic spines (Freund et al., 1984, Smith et al., 1994) (Figure 1.5). This electron microscopic evidence supports the idea of a functional interaction between the glutamatergic and dopaminergic input at the single synapse level in the striatum.

1.7 Glutamate receptor classification

Glutamate, an excitatory amino acid transmitter, is known to mediate most of the fast excitatory synaptic transmission that happens in the mammalian central nervous system. Beside the neurotransmission, glutamate receptors also contribute to the synaptic plasitcity underlying learning and memory (Bliss and Collingridge, 1993; Riedel et al., 2003) and neuronal signaling during the central nervous system development (Lujan et al., 2005). Paradoxically, glutamate can be toxic to the central nervous system. The excessive activation of glutamate receptors during some pathological conditions, such as ischemia, brain trauma, epileptic seizures, as well as neurodegenerative conditions such as Huntington's chorea, leads to the death of neurons (Arundine and Tymianski, 2004; Hossain 2005; Li et al., 2003). The synaptic actions of glutamate are mediated by two types of receptors, ionotropic and metabotropic receptors.

1.7.1 Metabotropic glutamate receptors

Glutamate activates metabotropic glutamate receptors (mGluRs) coupled to GTP-binding proteins (G-proteins). G-protein coupled mGluRs cause slower postsynaptic actions via second messenger cascades that either increase or decrease the excitability of postsynaptic cells (Purves et al., 2001). There are eight different subtypes (mGluR1-mGluR8) of mGluRs, and they are categorized into three groups because of the homology of their amino acid sequences, pharmacology and different intracellular transduction pathways (Conn and Pin 1997): group 1 (mGluR1 and mGluR5; coupled to G_q); group 2 (mGluR2 and mGluR3; coupled to Gi) and group 3 (mGluR4, mGluR6, mGluR7, mGluR8; coupled to Gi).

1.7.2 Ionotropic glutamate receptors

Ionotropic glutamate receptors are glutamate-gated cation channels that mediate the fast excitatory synaptic transmission. Ionotropic glutamate receptors are subdivided into three families and named after their selective agonists: AMPA (a-amino-3-hydroxy-5-methyl-4-soxazolepropionic acid) receptors, NMDA (N-methyl-D-aspartate) receptors and kainate receptors. When these receptors are activated by glutamate they allow cation passage (mainly Na^+ and sometimes also Ca^{2+}) and depolarize neurons within milliseconds (Dingledine et al., 1999). In this section only the non-NMDA receptors (AMPA receptors and kainate receptors) will be introduced, and NMDA receptors will be discussed in detail later.

AMPA receptors are composed of various combinations of four subunits GluR1, GluR2, GluR3 and GluR4; while kainate receptors consisted of two subunit families, GluR5, GluR6 and GluR7; KA1 and KA2. Some members of AMPA and kainate receptors can be activated by both agonists.

Gating of AMPA and kainate receptors by glutamate is extremely fast in contrast to the slow gating of NMDA receptors, and these two groups exhibit much lower affinity for glutamate when compare with NMDA receptors (Dingledine et al., 1999). With these characteristics, AMPA receptors are activated rapidly by glutamate, and channels only open briefly. Consequently, AMPA receptor activation facilitates unblock of NMDA receptors by Mg^{+2} when these two receptors are colocalized together on the post-synaptic membrane. At many excitatory synapses in the central nervous system, the EPSCs (excitatory postsynaptic currents) have both AMPA and NMDA receptor-mediated components, and the NMDA component has much slower rise and decay times when compared to the AMPA component (Ozawa et al., 1998). Much less is known about kainate receptor function, and they seem to play a relatively subtle role in neurotransmission regulation (Lerma, 2003).

1.8 NMDA receptors

1.8.1 Overview

NMDA receptors exhibit unique properties that distinguish themselves from other ionotropic glutamate receptors and underlie their vital physiological role in the brain.

First, NMDA receptors are highly permeable to Ca^{2+} in addition to Na^{+} and K^{+}. Calcium influx through NMDA receptors leads to a series of intracellular events that may initiate long-term potentiation (LTP) and long-term depression (LTD) in postsynaptic neurons. However when NMDA receptors are intensely or chronically activated (Lipton et al., 1994) following acute trauma or during chronic neurodegenerative disorders, extensive calcium entry can lead to neuron death (Hardingham and Bading 2003). Second, NMDA receptors are characterized by voltage-dependent block by physiological levels of extracellular Mg^{2+} (Nowak et al 1984; Mayer et al., 1984). Only when neurons are depolarized, can the Mg^{2+} block can be partially released and ions enter through activated NMDA receptors (Dingledine et al., 1999). Thirdly, activation of NMDA receptors needs the concerted action of glutamate and a co-agonist, glycine (Johnson and Ascher 1987), and they bind of different sites on the receptor. Finally, NMDA receptors synaptic currents exhibit unusual kinetics with a slow rise and decay time, reflecting a high affinity for glutamate and glycine (Behe et al., 1999; Dzubay and Jahr 1996).

1.8.2 NMDA receptor structure

1.8.2.1 Transmembrane architecture

NMDA receptors have been shown to have three transmembrane domains (M1, M3, and M4) in addition to a M2 domain forming a re-entrant loop facing the intracellular surface of the plasma membrane (Kunner et al; 1996; Wood et al., 1995). The C-terminus is intracellular, while the N-terminus is positioned extracellularly (Figure 1.6). The C-terminus of the NR2 subunit is longer than that of the NR1 subunit,

Figure 1.6

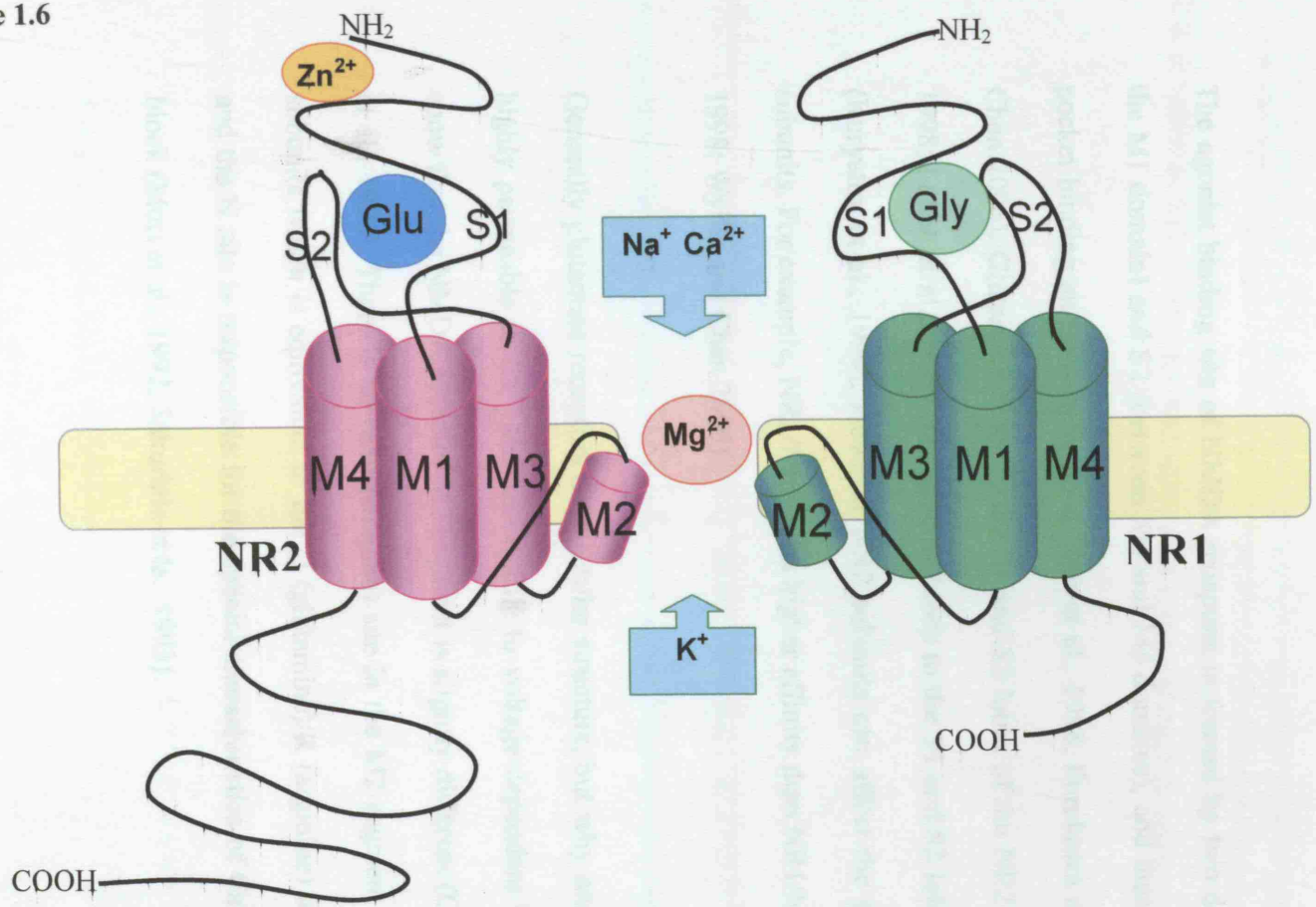

Figure 1.6 Schematic representation of the NMDA (N-Methyl D-Aspartate) receptor transmembrane architecture. Modified from Stephenson, 2001 and Cull-Candy and Leszkiewicz, 2004.

and this extra peptide sequence has been suggested to associate synaptic proteins (PSD95 and PSD93) in the postsynaptic density linked with the membrane cytoskeleton (Kennedy et al., 2005; Niethammer et al., 1996).

The agonist binding site of NMDA receptors is formed by two domains S1 (adjacent to the M1 domain) and S2 (between M3 and M4 domains), and these two structures form a pocket binding site for the agonist (Sun et al., 1998, Furukawa et al., 2005; Wyllie and Chen 2006). Glutamate binds to the S1 and S2 lobes of the NR2 subunits (Anson et al., 1998; Laube et al., 1997), and glycine binds to the S1 and S2 lobes of the NR1 subunits (Kuryatov et al., 1994). However NR2 subunits can affect the glycine affinity of NR1 subunits. For example, NR1/NR2B has higher affinity than NR1/NR2A does (Honer et al., 1998; Wyllie and Chen 2006).

Generally glutamate receptors have similar structure, but why only NMDA receptors are highly permeable to Ca^{2+} and susceptible to voltage-dependent block by Mg^{2+}. Studies show that the NMDA receptor M2 segment is slightly different (Ozawa et al., 1998; Mori et al., 1992). There is an N (asparagine) site in the M2 segment of the NMDA receptor subunits which is equivalent to the Q (glutamine)/R (arginine) site of AMPA receptors, and the N site is responsible for the special characteristics of Ca^{2+} permeation and Mg^{2+} block (Mori et al., 1992; Sakurada et la., 1993).

1.8.2.2 The NMDA receptor complex

NMDA receptors are made of a mixture of three subunit families: NR1 (has eight splice isoforms), NR2 (NR2A, NR2B, NR2C, NR2D) and NR3 (has two subunits A and B), and the receptor properties depend upon the subunit composition. Although, only the NR1 subunit itself can form functional NMDA receptors in Xenopus oocytes, the channel properties are not the same as the NMDA receptor obtained with brain mRNA (Moriyoshi et al., 1991). Several pieces of evidence suggests a most popular model of NMDA receptor involved a tetrameric protein consisting of two glycine-binding NR1 and two glutamate-binding NR2 subunits (Benveniste and Mayer., 1991; Behe et al 1995; Wyllie and Chen 2006), while NR1 subunits are essential for functional receptors and NR2 subunits serve as a regulator for the NMDA receptor.

There are eight different isoforms expressed from a single NR1gene because of three alternatively spliced exons: exon 5 in the amino terminus (N1 cassette), exon 21 in the C terminus (C1 cassette) and exon 22 in the C terminus (C2 cassette) (Dingledine) (Table 1.1). The C2 cassette contains an alternate splice site which can cut part of exon 22 and encode a cassette C2'. Native NMDA receptors can contain different NR1 splice variants (Blahos and Wenthold 1996).

The NR2 dimer of functional NMDA receptors can be composed of identical or different NR2 subunits (Cull-Candy and Leszkiewicz, 2004). Evidence from immunoprecipita-tion have suggested, beside diheteromeric complexes NR1/NR2A, NR1/NR2B, NR1/NR2C, and NR1/NR2D, triheteromeric complexes NR1/NR2A/NR2B, NR1/NR2A/NR2C,

Table 1.1 Nomenclatures of NR1 isoforms

Nomenclature	Explanation
NR1-1a	**1**: Containing both C1 (exon 21) and C2 (exon 22) cassettes **a**: Lack of N1(exon 5) cassette
NR1-1b	**1**: Containing both C1 (exon 21) and C2 (exon 22) cassettes **b**: Presence of N1cassette
NR1-2a	**2**: Containing only C2 (exon 22) cassette **a**: Lack of N1(exon 5) cassette
NR1-2b	**2**: Containing only C2 (exon 22) cassette **b**: Presence of N1cassette
NR1-3a	**3**: Containing both C1 (exon 21) and C2'(partial deletion of exon 22) cassette **a**: Lack of N1(exon 5) cassette
NR1-3b	**3**: Containing both C1 (exon 21) and C2'(partial deletion of exon 22) cassette **b**: Presence of N1cassette
NR1-4a	**4**: Containing only C2'(partial deletion of exon 22) cassette **a**: Lack of N1(exon 5) cassette
NR1-4b	**4**: Containing only C2'(partial deletion of exon 22) cassette **b**: Presence of N1(exon 5) cassette

From Hollmann et al., 1993

NR1/NR2A/NR2D, and NR1/NR2B/NR2D have also been found in native NMDA receptors (Sheng et al., 1994; Blahos and Wenthold, 1996; Chazot and Stephenson 1997; Stephenson, 2001). NR3 subunits are not a necessary component for functional NMDA receptors but coexpression of NR3A subunit with NR1/NR2 complex can control the receptor surface expression and reduce Ca^{2+} permeability (Perez-Otano et al., 2001).

1.8.3 NMDA receptor subunit distribution and functions

1.8.3.1 NR1 isoforms

NR1 mRNA has been detected in nearly every examined neuron both in the adult and the developing rat central nervous system (Moriyoshi et al., 1991, Monyer et al., 1994). According to Laurie et al. (1995), the isoforms lacking the N1 cassette (NR1-a) and those containing only the C2 cassette (NR1-2) are expressed all over the brain; the isoforms with the N1 cassette (NR1-b) and with only the C2' cassette (NR1-4) are also distributed widely but to fewer areas. The variants including both C1 and C2' cassettes (NR1-3) are not abundant in any brain area. Overlapping expression patterns of NR1 splice variant distribution have been shown (Laurie et al., 1995; Blahos and Wenthold, 1996; Chazot and Stephenson 1997), and at least two NR1 isoforms can be expressed in the same receptor complex. Moreover the C1 cassette is reported to be required for localizing the NR1 subunit to receptor-rich domains associated with the plasma membrane (Ehler et al., 1995; Perez-Otano and Ehlers., 2005).

In the striatum, NR1-a variants are intensively expressed, but NR1-b isoforms are less abundant (Laurie et al.1995). Kuppenbender et al. (1999) demonstrated that only the

parvalbumin-containing interneurons were N1 cassette immunopositive. Both NR1-1 and NR1-2 are strongly and evenly expressed, but NR1-3 and NR1-4 isoforms are weakly expressed as in other brain regions.

These NR1 splice variants influence NMDA receptor function. For instance isoforms containing exon5 (NR1b) relieve the tonic proton inhibition at physiological pH (Traynelis *et al.,* 1995) and they increase the IC_{50} for voltage-independent Zn^{2+} inhibition by more than 3-fold (Traynelis *et al.,* 1998). In great contrast the receptors, whose NR1 subunits lack exon 5 (NR1-a), are more sensitive to Zn^{2+} inhibition especially when NR1-1a is co-assembled with NR2A (Paoletti et al., 1997), but the receptors comprise of NR1-1a with NR2C or NR2D are much less sensitive to Zn^{2+} (Hatton and Paoletti, 2005). When expressed in Xenopus oocytes NR1 isoforms present different channel properties especially with the difference in the N terminus. Durand et al. (1993) have shown that NR1-a exhibit higher affinity for NMDA and has bigger potentiation by spermine. Moreover exon 5 insertion gives rise to a four times faster deactivation time of NR2-1b/NR2B receptors than of NR1-1a/NR2B receptors (Vicini 1998; Cull-Candy et al., 2001).

1.8.3.2 NR2 family

The NR2 family of NMDA receptor subunits consists of four members: NR2A, NR2B, NR2C and NR2D. Compared with the ubiquitously expressed NR1 subunit, NR2 subunit expression is under tight temporal and spatial regulation. They do not form functional NMDA receptors unless coexpressed with NR1 subunits, and they are the major

determinants of the functional and pharmacological properties of NMDA receptors (Monyer et al., 1994; Dingledine et al., 1999; Cull-Candy and Lieskiewitz 2004).

Distribution in adult brain

In the adult rat brain, NR2A subunits are widely expressed and are prominent in cerebral cortex and hippocampus, and moderately expressed in striatum, thalamus, olfactory bulb, and cerebellum (Jin et al., 1997; Goebel and Poosch 1999). The NR2B subunits are found selectively in cerebral cortex olfactory bulb, hippocampus and striatum (Jin et al., 1997; Goebel and Poosch 1999; Kupperbender et al., 2000). NR2C has been detected predominantly in the granule cell layer of the cerebellum with a lower expression in olfactory bulb (Laurie et al., 1997; Ozawa et al., 1998). The highest level of NR2D expression has been identified in superior colliculus followed by thalamus and brainstem (Laurie et al., 1997; Goebel and Poosch 1999). The different distribution of the NR2 subunits in each brain area suggests there are different ingredients for NMDA receptor complex formation in each region

Distribution in the developing brain

Within the NR2 family only NR2B and NR2D mRNA has been detected during the embryonic period. The former is expressed in the cortex, thalamus and spinal cord, while the latter mainly locate in midbrain structures (diencephalons, mesencephalon and spinal cord) (Watanabe et al., 1993; Monyer et al., 1994). Soon after birth NR2B and NR2D gene expression is still widespread. By postnatal day 7 (P7) NR2B shows strongest expression among the NR2 family in the cortex, hippocampus, striatum, thalamic nuclei

and cerebellum. At the same time NR2A and NR2C mRNA only weakly appears (Monyer et al., 1994). NR2D is reaching its peak expression at P7 mainly in thalamic and hypothalamic nuclei but soon decreases to a very low level while the brain is maturing (Monyer et al., 1994; Laurie et al., 1997). During the second and third postnatal weeks, NR2A gene expression increases and occurs in the largest number of brain regions predominantly in cortex, hippocampus and striatum (Portera-Cailliau et al., 1996; Laurie et al., 1997). To summarize, a gradually increasing distribution of NR2A and a decline of NR2B expression occurs while the brain is developing and NR2C replaces the NR2B in the cerebellum (Watanabe *et al.*, 1993)

NR2 subunit distribution in the striatum

In 7-day-old rat striatum, NR1 and NR2B mRNA is highly expressed, a lower NR2D expression can be found. The other members of the NR2 family are very faintly expressed. In adult rat striatum, NR2A expression is moderate in all striatal neurons except cholinergic interneurons, and NR2B shows strong labeling in projection neurons and cholinergic interneurons. NR2C shows scarce labeling; only some interneurons (somatostatin or acetylcholine containing) express NR2D mRNA (Standaert et al., 1999; Landwehrmeyer et al., 1995). Furthermore binary NMDA receptors containing NR1 and either NR2A or NR2B are widely expressed in the striatum, but ternary receptors (composing of NR1, NR2A and NR2B) are found exclusively in the synaptosomal membranes (Dunah and Standaert 2003).

Variation in properties of different receptor complexes

NR2 subunits confer variability to the functional and pharmacological properties of NMDA receptors. During synaptic transmission NMDA receptors mediate the excitatory postsynaptic currents with a slow gating character (Forsythe and Westbrook, 1987; Behe et al., 1999; Dzubay and Jahr 1996). A wide deactivation time range has been found in different NR2 subunits containing diheteromeric NMDA receptors (NR1/NR2) (Monyer et al., 1994). NR1/NR2A receptors have the shortest deactivation time of tens of milliseconds, while NR1/NR2D receptors have the longest of around several seconds (Monyer *et al.*, 1994; Wyllie et al., 1998). NR2A or NR2B containing NMDA receptors are more sensitive to voltage-dependent block by extra cellular Mg^{2+} than NR1/NR2C and NR1/NR2D receptors (Monyer et al., 1994; Kuner and Schoepfer, 1996; Qian et al., 2004). In terms of single-channel properties, NR1/NR2A and NR1/ NR2B combinations produce higher conductance channel openings (around 50 and 40 pS) than NR1/NR2C or NR1/NR2D (around 16 to 36 pS) (Stern et al., 1992; Wyllie et al., 1996; Cull-Candy et al., 2001).

A number of pharmacological agents have been developed to distinguish some NMDAR subtypes. Ifenprodil is a NR2B subunit selective non-competitive antagonist that acts by increasing the receptor sensitivity to proton inhibition (Mott et al., 1998). For NR2B the concentration of ifenprodil producing half maximal inhibition (IC_{50}) is around 400-times lower than for other NR2 subunits (Williams, 1993). Spermine induces potentiation exclusively to the NR1-a/NR2B receptor complex by relieving the tonic proton inhibition at physiological pH (Traynelis et al., 1995; Dingledine et al., 1999). Also NR1/NR2A receptors can be identified by Zn^{+} and TPEN (a highly specific heavy metal chelating agent). Zn^{+} is a non-competitive inhibitor of NR2A with IC_{50} around 20 nM, and its tonic

inhibition of NR2A containing receptors can be selectively reversed by using the Zn^{2+} chelator TPEN (Paoletti *et al.,* 1997). PPDA is a competitive blocker of NR2C and NR2D containing NMDA receptors (Hrabetova *et al.*, 2000).

Triheteromeric NMDA receptors have been reported in native NMDA receptors (Sheng et al., 1994; Blahos and Wenthold, 1996; Chazot and Stephenson 1997; Dunah et al., 1998; Brickley et al., 2003; Jones and Gibb, 2005), and they may have different channel properties compared to diheteromeric NMDA receptors. Vicini et al. (1998) has demonstrated that recombinant NMDA receptors with NR1, NR2A and NR2B present an intermediate deactivation time course between NR1/NR2A (~80 ms) and NR1/NR2B (~300 ms), moreover NR1/NR2A/NR2B receptors display lower ifenprodil sensitivity than that of diheteromeric NMDA receptors (NR1/NR2B) (Tovar and Westbrook, 1999).

1.8.3.3 NR3 family

The NR3 subfamily of NMDA receptor subunits consists of NR3A and NR3B, and they do not form functional NMDA receptors unless they unite with both NR1 and NR2 subunits (Nishi et al., 2001; Perez-Otano et al., 2001).However, when NR3A or NR3B co-assembles with NR1 in Xenopus oocytes, NR1/NR3A or NR3B constitute excitatory glycine receptors that are unaffected by glutamate or NMDA. (Chatterton et al., 2002) The NR3A subunit is expressed in several areas of the central nervous system such as spinal cord, brainstem, hypothalamus and thalamus (Ciabarra et al., 1995; Goebel and Poosch, 1999) and the expression changes during development. Coexpression of NR3A subunits with NR1 and NR2A gives rise to smaller conductance channel openings with

reduced Ca^{2+} permeability (Perez-Otano et al.,2001), and more interestingly in mice, knock-out of NR3A expression leads to enhancements of both NMDA responses and dendritic spines (Das et al., 1998). NR3B subunits have been found to be restricted to somatic motoneurons of brainstem and spinal cord in mouse brain (Nishi et al., 2001). NR3B also suppressed the NMDA current when coexpressed with NR1 and NR2A and reduced the Ca^{2+} permeability (Nishi et al., 2001; Matsuda et al., 2003).

1.9 Dopamine Receptors

1.9.1 Structure and classification

Dopamine receptors are one type of G protein-coupled receptor, which play a very important role in the brain in modulation of coordinated motor movements. These receptors are classified into two families: D1-like receptors and D2-like receptors. All dopamine receptors belong to the superfamily of G protein-coupled seven transmembrane domain receptors. However the C terminal for D1 family receptors is about seven times longer than for D2 family receptors. D1-like receptors are coupled to Gs proteins and like many Gs coupled receptors they contain a short third intracellular loop, while like other Gi coupled receptors, D2 family receptors have a long third intracellular loop (Missale et al., 1998).

The main criteria for dopamine receptor classification is whether the receptor stimulates adenylate cyclase (AC) or inhibits it. D1-like receptors (D1, D5) have been shown to

stimulate AC in most dopaminergic brain areas (striatum, nucleus accmbens and olfactory tubercle) (Memo et al., 1986), and consequently stimulate cAMP accumulation. The D2-like receptors (D2, D3, and D4) have the ability to inhibit AC in the central nervous system (Onali et al., 1985). Besides regulating AC activity, dopamine receptors can also influence various ion channels. For example, D1-like receptors appear to stimulate release of calcium from intracellular stores as well as increase calcium currents by L-type calcium channels (Missale et al., 1998). Moreover D2 receptors have been shown to suppress calcium currents though L-type Ca^{2+} channels in striatal medium spiny neurons (Hernandez-Lopez et al., 2000; Olson et al., 2005) and olfactory receptor neurons (Okada et al., 2003).

1.9.2 Expression of dopamine receptors in the brain

D1 receptor mRNA is expressed in many brain areas but predominantly in striatum, nucleus accumbens, and olfactory tubercle and in addition is distributed throughout the cerebral cortex, limbic system, hypothalamus, and thalamus (Fremeau et al., 1991). D5 receptor expression is restricted to the hippocampus, the lateral mamillary nucleus and hypothalamus, and barely detectable in striatum and nucleus accumbens (Missale et al., 1998). The distribution of D2 receptors is very similar to D1's distribution, and most D2 receptors are also expressed in striatum and nucleus accumbens and olfactory tubercle but some are found in substantia nigra and ventral tegmentum. D3 receptors are specially localized in limbic regions and hypothalamus, and D4 are found highly expressed in the frontal cortex, amygdala, hippocampus, hypothalamus and mesencephalon but have very low expression in the basal ganglia (Webster, 2001; Missale et al., 1998).

In the striatum most D1 receptors are expressed in the medium spiny neurons containing substance P, and more than 80% of the substance P neurons exhibit D1 receptor mRNA (Le Moine et al., 1991). D2 receptor mRNA has been found in the medium spiny neurons where enkephalins are expressed (Le Moine et al., 1995). However there are controversial results about colocalization of D1 and D2 receptors in the striatum. Some studies claimed D1 and D2 mRNA are only co-localized in approximately 30% of striatal cells (Meador-Woodruff et al., 1991; Wong et al., 1999), whereas Surmeier et al. (1996) demonstrated that functional D1 and D2-like receptors are co-localized in nearly 50% of medium spiny projection neurons and Aizman et al. (2000) even indicated that virtually all striatal projection neurons contained both D1 and D2 family receptors. Both of these groups claimed the small overlap of D1 and D2 subclass receptors shown by other studies is due to inadequate sensitivity of the analytical procedures.

1.9.3 Pharmacology of dopamine receptors

There are drugs that can distinguish the D1 family from the D2 family, but so far it has not been possible to pharmacologically distinguish between D1 and D5 receptors with no more than 10-fold selectivity and there is little to distinguish between D2, D3 and D4 (Missale et al., 1998; Sibley 1999). For instance, SKF-38393, SKF-81297, SKF-82958 are all agonists for D1-like receptors, while SCH-23390 selectively inhibits D1 receptors. Quinpirole is a classical D2-like receptor agonist, and spiperone is an antagonist for D2 receptors. In table 1 the affinity of selected compounds which were used in this thesis to distinguish the two dopamine receptor families is shown (Kebabian *et al.*, 1997, Mottola et al., 1996).

Table 1.2 Dissociation equilibrium constants (Ki, nM) of drugs at dopamine receptors (Kebabian et al., 1997; Mottola et al., 1996)

	D1	D2	D3	D4	D5
Agonist					
SKF-82958	4	73	ND	ND	ND
Quinpirole	1900	3.3	4.0	18	ND
Dopamine	0.80	7.5	3.9	28	ND
Antagonists					
SCH-23390	0.30	1430	780	3560	0.35
Spiperone	220	0.08	0.60	0.08	4500

ND: not determined

1.9.4 Dopamine receptor modulation of NMDA receptor

In prefrontal cortex, dopamine D1 receptor activation has been shown to potentiate NMDA receptor synaptic currents (Seamans et al., 2001). In the striatum, dopamine D1 receptors couple to Gs G proteins with stimulation of the classical adenylate cyclase pathway resulting in phosphorylation of DARPP-32 (dopamine and cyclic AMP-regulated phosphoprotein of M_r 32000) and an inhibition of protein phosphatase-1 (Greengard, 2001), and dopamine has been shown to increase NR1 subunit phosphorylation in the nucleus accumbens (Snyder et al., 1998). In addition deletion of the gene for DARPP-32 abolished dopamine-induced increase in NR1 phosphorylation, while inhibition of protein phosphatase 1 (PP1) produced a prominent increase in NR1 phosphorylation (Snyder et al., 1998).

Some other studies also suggested the classical pathway (Figure 1.7) contributes to D1 enhancement of NMDA receptor currents; however they introduced different downstream effectors. Blank et al. (1997) reported D1 receptors increased NMDA-mediated currents in oocytes injected with hippocampal and striatal mRNA, and potentiation of striatal NMDA responses was mediated by PKA which phosphorylates DARPP-32 resulting in inhibition of PP1. Cepeda's group (Cepeda et al., 1998a) has shown that L-type Ca^{2+} channel blockers reduced D1-induced potentiation markedly but did not completely abolish the D1 effect suggesting an involvement of Ca^{2+} channels in D1 potentiation of NMDA receptor currents. However in acutely isolated striatal neurons, L-type Ca^{2+} channels are not required for D1 receptor potentiation of NMDA receptor currents

Figure 1.7 A cartoon for D1 receptor modulation of NMDA receptors via the classical pathway (based on Blank et al., 1997).

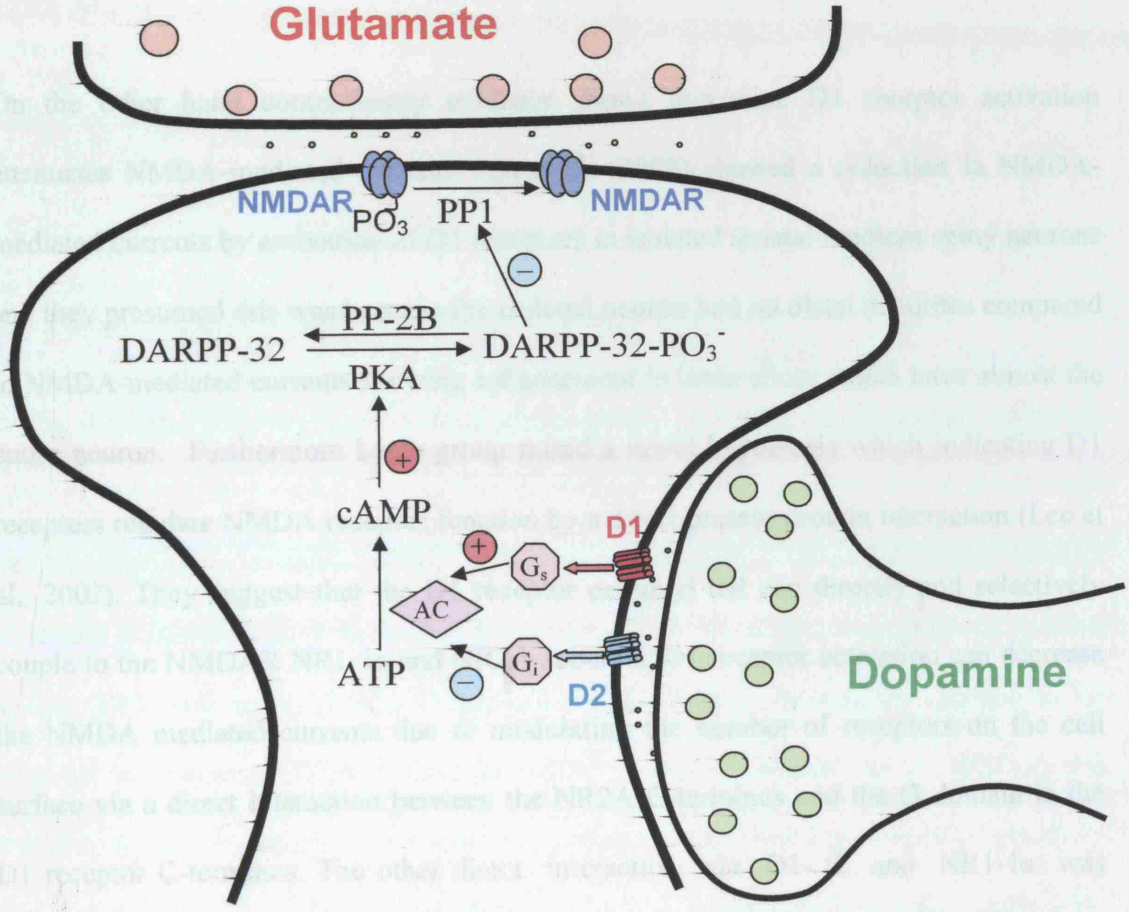

perhaps due to the loss of dendrites during cell isolation (Flore- Heranadez et al., 2002). Moreover, D1 receptor activation has been demonstrated to enhance the abundance of NR1, NR2A and NR2B subunits in the synaptosomal membrane fraction of striatal homogenates, and deletion of the gene for the protein tyrosine kinase, Fyn, abolishes this D1 effect (Dunah et al., 2004, Dunah et al., 2001).

On the other hand contradictory evidence shows dopamine D1 receptor activation attenuates NMDA-mediated currents. Lin et al. (2003) showed a reduction in NMDA-mediated currents by activation of D1 receptors in isolated striatal medium spiny neurons and they presumed this was because the isolated neuron had no distal dendrites compared to NMDA-mediated currents showing enhancement in brain slices which have almost the entire neuron. Furthermore Lee's group raised a novel hypothesis which indicating D1 receptors regulate NMDA receptor function by a direct protein-protein interaction (Lee et al., 2002). They suggest that the D1 receptor carboxyl tail can directly and selectively couple to the NMDAR NR1-1a and NR2A subunits. D1 receptor activation can decrease the NMDA mediated currents due to modulating the number of receptors on the cell surface via a direct interaction between the NR2A C-terminus and the t3 domain in the D1 receptor C-terminus. The other direct interaction via D1- t2 and NR1-1a was suggested to be involved in NMDA-mediated excitotoxicity. D1 activation may promote the connection between NR1 and calmodulin (CaM) instead of NR1 and D1 receptors, and by increasing PI-3 kinase activity may result in more cell survival (Lee et al., 2002).

There are also some reports of D2 family dopamine receptor inhibition of NMDA receptor transmission (Kotecha et al., 2002). They suggested stimulation of D2-like

receptors in CA1 neurons depressed NMDA receptor activity and excitatory NMDAR-mediated synaptic transmission via the transactivation of PDGFRs (PDGF: platelet-derived growth factor) followed by mobilization of intracellular Ca^{2+} and Ca^{2+}- dependent inactivation of NMDA receptors. In prefrontal cortex Wang et al. (2002) showed D4 receptor activation decreases the NMDA receptor-mediated current by means of the inhibition of PKA followed by the activation of PP1 and the ensuing inhibition of Ca^{2+}-calmodulin-dependent protein kinase II (CaMKII).

1.9.5 Dopamine receptors in striatal synaptic plasticity

In the striatum, there are both cortical glutamatergic and nigral dopaminergic afferents targeting projection neurons. Repetitive activation of cortical input can produce long-lasting changes in synaptic transmission in the striatum, and activation of NMDA receptors is required for long-term potentiation (LTP) but not for long-term depression (LTD) (Calabresi et al., 1992). Dopamine and DARPP-32 have been claimed to be essential to generate LTP and LTD in striatal neurons (Calabresi et al., 2000c), and chronic dopamine denervation severely damages corticostriatal synaptic plasticity (Centonze et al., 2001). D1-like receptor activation has been shown to be required for LTP induction (Calabresi et al., 2000c), while D2 receptor antagonist enhanced LTP (Calabresi et al., 1997; Centonze et al., 2001). However the cellular mechanisms for the LTD are not fully appreciated. It has been suggested nitric oxide production following D1 receptor activation might cooperate with D2 receptors to induce LTD in medium spiny neurons (Calabresi et al., 2000c; Centonze et al., 2001).

1.10 Internalization of NMDA receptors

NMDA receptors are thought to be stable at the excitatory postsynaptic membrane with a very slow turnover rate (Luscher et al., 1999), However, recent studies showed that the synaptic expression of NMDA receptors can be changed rapidly by internalization (Grosshans et al., 2002; Roche et al., 2001; Snyder et al., 2001), and this may provide a new aspect of NMDA receptors in regulating synaptic transmission and strength.

Most functional NMDA receptors are likely to be tetrameric in structure with both NR1 and NR2 subunits. Unless assembled with NR2 subunits, NR1 subunits do not reach the cell surface and are degraded rapidly (Huh and Wenthold, 1999), and this suggests an essential role for NR2 subunits to regulate receptor expression on the cell surface. Temporal variation of NR2 subunit expression may underlie the developmental changes observed in NMDA receptor trafficking and synaptic expression. Lavezzari et al. (2004) showed distinct intracellular pathways for NR2A and NR2B endocytosis, and in mature neurons internalization of NR2B is more robust than of NR2A. Roche et al. (2001) reported a progressive decrease of NMDA receptor endocytosis as neurons mature.

NMDA receptors can interact with many proteins such as the PSD-95 family and AP-2 adaptor protein, which may potentially influence the targeting of the receptor to the synapse and the receptor localization at the synapse. In addition some proteins can also target phosphorylation sites of NMDA receptors and affect receptor trafficking as well as functions (Wenthold et al., 2003).

1.10.1 The PSD-95 family of PDZ scaffolds

The PSD-95 family of membrane-associated guanylate kinase (MAGUK) proteins consists of 4 members: PSD-95 (postsynaptic protein 95)/SAP90 (synapse-associated protein 90), PSD-93/chapsyn-110, SAP102 and SAP97 (Kim and Sheng 2004), and they make a major component of the postsynaptic density (PSD). These proteins have three PDZ domains, Src homology-3 domain, and a guanylate kinase-like (GK) domain (Kim and Sheng 2004). The first two PDZ domains of these proteins (except SAP97) have been reported to associate with the last four amino acids (ESDV or ESEV) of NR2 subunits (NR2A and NR2B) (Sheng and Sala, 2001, Kornau et al., 1995, Niethammer et al., 1996) and consequently the PSD-95 family serve as a scaffold to assemble specific signaling proteins associated with NMDA receptors to influence the receptor properties and to respond to calcium influx through the NMDA receptor channel (Sheng and Pak, 2000; Kennedy et al., 2005).

Many studies have shown that association of PSD-95 with NMDA receptors regulates the stability of NMDA receptors at the cell surface (Roche et al., 2000; Rutter and Stephenson, 2000; Lin et al., 2004; Chung et al., 2004; Lavezzari et al., 2004). Roche et al. (2001) showed coexpression with PSD-95 blocked the NR2B-mediated internalization in Hela cells. In great contrast when cultured hippocampal neurons were transfected with truncated NR2B (lacks PDZ binding domain), receptors exhibited robust internalization. Thus they concluded that disruption of the NMDA receptor-PSD-95 complex destabilized the NMDA receptor allowing receptor internalization. Chung et al. (2004) also revealed phosphorylation of a serine residue within the PDZ ligand domain of the NR2B subunit

disrupts the interaction with PSD-95 and SAP102 and decreases surface NR2B expression. Moreover the PDZ binding motif in the NR2A subunit has been reported to be crucial for the PSD-95 potentiation of NMDA current and the ability of PSD-95 to increase NMDA receptor surface expression (Lin et al., 2004).

1.10.2 Clathrin-mediated endocytosis

Clathrin-coated vesicles mediate endocytosis of many transmembrane receptors such as $GABA_A$ receptors (Kittler et al., 2000), AMPA receptors (Carroll et al., 1999) and NMDA receptors (Nong et al., 2003). In this endocytosis process, the adaptor protein complex (AP) is one of the major constituents and promotes clathrin assembly under more physiological conditions (Schmid, 1997). The AP family consists of at least two complexes: AP1 and AP2. Also dynamin, a GTPase, plays an essential role for the budding of Clathrin-coated vesicles (Schmid, 1997).

Many studies have reported a clathrin-dependent mechanism for NMDA receptor endocytosis. NMDA receptor internalization can be blocked by coexpression of receptor with dominant-negative dynamin (Roche et al., 2001). Lavezzari et al. (2003) showed that the medium chain of AP2 (μ2) interacts with NR2B C-terminus directly, and mutation of tyrosine motif (YEKL) wipes out the interaction. Unlike NR2B, NR2A binds to a different adaptor medium chain (μ1) of AP1, and it traffics to distinct intracellular compartments (Lavezzari et al., 2004).

1.10.3 Non-receptor tyrosine kinases and NMDA receptors

The Src family of non-receptor tyrosine kinases consists of Src, Fyn, Lyn, Lck and Yes (Ali and Salter 2001). These kinases have been shown to have the ability to regulate NMDA receptor function and expression.

In recombinant NMDA receptors, Kohr and Seeburg (1996) showed that Src potentiated whole cell currents mediated by NR1/NR2A, but had no effect on receptors composed of NR1 and other NR2 subunits. In cultured rat central neurons activation of Src family kinases increased the NMDA channel activity, and Src could be coprecipitated with NMDA receptors (Yu et al., 1997).

Tyrosine motifs in the NR2 C-terminus are suggested to regulate NMDA receptor internalization. Roche et al (2001) demonstrated that the removal of the tyrosine motif (YEKL) of NR2B subunits dramatically inhibited the receptor internalization. Moreover Dunah et al. (2004) showed that deletion of the gene for the protein tyrosine kinase Fyn remarkably reduces the basal content of tyrosine-phosphorylated NR2A and NR2B in the striatum, and inhibits dopamine D1 receptor-induced enhancement of the abundance of NR1, NR2A and NR2B subunits in the synaptosomal membrane fraction.

NR2B has been reported to be the most prominently tyrosine phosphorylated protein in the postsynaptic density (Moon et al., 1994), and its interaction with PSD proteins may serve to hold NMDA receptors at the synapse. Also PSD-95 has been revealed to promote the tyrosine phosphorylation of NR2A significantly in 293T cells (Tezuka et al., 1999).

More importantly, phosphorylation of NR2B subunit has been suggested to disrupt the interaction with PSD-95 and SAP102, and therefore decreases surface NR2B expression (Chung et al., 2004). Hence, these pieces of evidence make the Src family non-receptor tyrosine kinase an excellent candidate to regulate NMDA receptor trafficking.

1.11 Experiments conducted in this study

In this study, I have used whole cell and outside-out patch clamp recordings to investigate D1 and D2 modulation of NMDA receptors in striatal medium spiny neurons. There was a decrease of NMDA receptor whole cell currents during D1 receptor activation. This decrease was not G protein-dependent but was abolished by intracellular application of tyrosine kinase inhibitors (lavendustin A and PP2). Furthermore, intracellular application of a dynamin inhibitory peptide prevented D1 inhibition of NMDA currents. However, in outside-out patches, the NMDA receptor single channel properties were not changed by application of a D1 agonist. Based on these results, I conclude that G protein-independent D1 inhibition of NMDA responses in whole-cell recordings is mediated by a tyrosine kinase-induced change in NMDA receptor trafficking.

D2 receptor activation significantly decreased the NMDA receptor whole-cell currents in a concentration-dependent manner. Intracellular application of a general G protein inhibitor (GDP-β-S) abolished the D2 inhibition suggesting a G protein-dependent mechanism underlies the D2 receptor modulation of NMDA receptors in the striatum.

Chapter 2

Materials and Methods

2.1 Solutions

2.1.1 Slicing solution

A modified Krebs solution (Edwards et al., 1989) with the following composition was used for slicing (in mM): sucrose, 206 (instead of NaCl because of better preservation of slice cells); KCl, 2.5; $CaCl_2$, 1.0; $MgCl_2$, 1.0; NaH_2PO_4, 1.25; $NaHCO_3$, 26; glucose, 25; at pH 7.4 when bubbled with 95% O_2 and 5% CO_2.

2.1.2 External solution

A magnesium-free Krebs solution with the following composition was used for the external recording solution (in mM): NaCl, 125; KCl, 2.5; $CaCl_2$, 1.0; NaH_2PO_4, 1.25; $NaHCO_3$, 26; glucose, 25; pH 7.4. The free Mg^{2+} concentration in this solution has been estimated to be around 4 μM (Gibb & Colquhoun, 1992). The slicing and external solution for recording were continuously gassed with a mixture of O_2 (95%) and CO_2 (5%) (BOC Gases, Manchester, UK). In most experiments the TTX, 100nM, was added to the external recording solution to block voltage-gated Na^+ currents (Xie et al., 2001).

2.1.3 Pipette solution

In order to minimize potassium currents, patch pipettes were filled with caesium chloride (CsCl) internal solution. The composition of the internal solution was (in mM): $CsCl_2$, 140; EGTA, 10; HEPES, 10; NaCl, 10; $MgCl_2$, 1; adjusted to pH 7.4 with NaOH. This solution was stored frozen in 1 ml aliquots. ATP 1mM, GTP 1mM or GDP-β-S (GDP-β-S inhibits receptor mediated activation of G proteins) 0.5 mM or GTP-γ-S (irreversible activator of G-proteins) 0.5 mM were added to each 1ml aliquot at the start of the experiment as the different experiments demand.

2.2 Drugs and chemicals

NaCl, NaOH, NaH_2PO_4, $NaHCO_3$, KCl, $CaCl_2$, $MgCl_2$, sucrose, CsCl and glucose were purchased from BDH (Poole, England). HEPES (N-[2-hydroxyethyl]piperazine-N'-[2-ethanesulfonic acid]), EGTA (ethylene glycol-bis(β-aminoethyl ether) N,N,N',N'-tetraacetic acid), R-(+)SCH-23390, SKF-82958, spiperone, ATP (adenosine 5'-triphosphate (ATP) disodium salt), GTP (guanosine 5'-triphosphate sodium salt), GDP-β-S (guanosine 5'-[β-thio] diphosphate trilithium salt), GTP-γ-S (guanosine 5'-[γ-thio] triphosphate tetralithium salt), DMSO (dimethyl sulfoxide), H-89 (N-[2-(p-bromocinnamylamino) ethyl]-5-isoquinolinesulfonamide dihydrochloride), $ZnCl_2$ (zinc chloride), and TPEN (N,N,N'N'-tetrakis(2-pyridylmethyl) ethylenediamine) were purchased from Sigma (St. Louis, MO, USA). NMDA (N-methyl-D-aspartic acid), glycine, 7-Cl-K (7-chloro-hydroxyquinoline-2-carboxylic acid), (-)-quinpirole hydrochloride, PP2, dynamin inhibitory peptide (QVPSRPNRAP) and myristoylated scrambled dynamin inhibitory peptide were purchased from Tocris (Bristol, UK). TTX

(tetrodoxin) was purchased from Alomone Labs. Lavendustin A (5-Amino-[(N-2, 5-dihydroxybenzyl)-N'-2-hydroxybenzyl] salicylic Acid RG14355) and Lavendustin B (5-Amino-(N,N'-bis-2-hydroxybenzyl) salicylic Acid), and Genistein (4', 5, 7-Trihydroxyisoflavone) were purchased from Calbiochem (EMD Biosciences, Inc.)

2.3 Brain slice preparation

Striatum slices were prepared as described elsewhere (Edwards et al., 1989; Gibb & Edwards, 1994). 7 day-old or 21 day-old Sprague-Dawley rats were killed by decapitation in accordance with the Animals Scientific Procedures Act (1984) using a pair of surgical scissors (RS6930, Roboz, Germany). The skin was cut along the midline with a pair of small scissors. The skull was cut along the midline with a pair of fine scissors and the skull bones were removed using fine curved forceps. Within 60 seconds of decapitation the exposed brain was submerged in a 100 ml plastic weighting boat (Fisher Scientific, Loughborough, UK) containing ice-cold slicing solution continuously bubbled with a mixture of O_2 (95%) and CO_2 (5%). Then the brain was cut along the midline with a scalpel (N° 11, Swann-Morton, Sheffield, UK) and the cerebrum was isolated from the rostral part of the cerebellum and caudal part of the olfactory bulb. Then the brain was removed from the skull using a fine spatula. Both brain halves were allowed to cool down for 3-5 minutes in ice-cold slicing solution.

For striatal slices, a flat surface was cut across the dorsal side of a half brain with a scalpel. This surface was glued, using cyanoacrylate instant adhesive (Loctite UK Ltd, Watchmead, Welwyn Garden City), to the tissue block of the specimen bath of a vibroslicer (DTK 1000, Dosaka; Kyoto, Japan) with the medial side of the brain facing

the cutting blade. Immediately, the specimen bath was filled with oxygenated ice-cold slicing solution until the tissue was completely covered. Slices were cut using carbon steel blades or ceramic blades (Campden Instruments Ltd, UK) at a thickness of 300 μm. Hypodermic needles (Monoject, 26 guage Ballymoney, UK) were used to dissect out the striatum with the adjacent cerebral cortex from the rest of the brain slice. Slices were transferred into an incubation chamber (Edwards & Konnerth, 1992) using a plastic disposable Pasteur pipette (Scientific Laboratory Supplies Ltd, Nottingham) cut to a tip opening of 3-5 mm. The incubation chamber contained 100 ml external recording solution with additional 1 mM $MgCl_2$ added and was continuously bubbled with a mixture of O_2 (95%) and CO_2 (5%). Slices were incubated at room temperature (20 – 24 °C) for a period that ranged from 45 minutes to 8 hours before experimenting. Each slice was transferred in the same way to a recording chamber fitted to the stage of an upright microscope (Axioscope-FS, Zeiss-Oberkochen, Germany).

2.4 Cell visualisation and identification

The cell bodies of individual neurons in brain slices were visualised under Normaski differential interference contrast optics (Yamamoto, 1975; Takahashi, 1978; Edwards et al., 1989) using an upright microscope with an infinity corrected Achromat 40X water immersion objective with a numerical aperture of 0.75 and a working distance of 1.6 mm at a total magnification of 600X. Visualisation was carried out on a monochrome video monitor (VM-902K, Hitachi-Denshi, Tokyo, Japan) connected to CCD monochrome camera (RS Components, Corby, UK) mounted on top of the microscope trinocular head. Slice health was visually checked before patching and the presence of a considerable

proportion of neurons with a smooth surface readily evident on the surface of the slice was used as an indicator of a good healthy slice. Individual healthy cells were identified by the smooth appearance of their surface. Striatal medium spiny neurons were identified by their location, size and morphology (Gotz et al., 1997). Medium spiny neurons comprise approximately 90% of the striatal neurons (Jain et al., 2001), and they are about 15 μm in diameter which is about half of the interneuron's size (Gotz et al., 1997).

2.5 Patch pipette fabrication

Patch pipettes were made in a vertical pipette puller (MF-83, Narishige, Tokyo, Japan) from thick-walled borosilicate glass capillaries containing an internal filament (GC150F-7.5, outer diameter 1.5 mm, inner diameter 0.86 mm, Harvard Apparatus Ltd). The tip of the pipette was cleaned, smoothed and reduced by fire polishing on a microforge (MF-83, Narishige, Tokyo, Japan) to a final resistance of 6-15 MΩ. For single channel recordings, pipettes were coated with an insulating silicone resin (Sylgard 184® Dow Corning, USA). Pipettes were back-filled with pipette solution and the level in the pipette was kept to a minimum to reduce electrical interference produced by solution creeping up the electrode or going into the suction line.

2.6 Patching procedure

2.6.1 Whole-cell recordings

2.6.1.1 Procedure

Patch pipettes were positioned on an electrode holder connected to the head-stage of a patch-clamp amplifier (Axopatch 200A, Axon Instruments, Foster City, CA, USA) and

some positive pressure was applied to the inside of the pipette to generate a tiny stream of solution at the tip of the pipette that prevented the accumulation of debris at the tip and the mixing of the pipotte solution inside the pipette with the external solution in the recording chamber. The patch pipette was then lowered into the recording chamber. Once in solution, the pipette resistance was measured by passing a 5 mV rectangular pulse through the input using the patch clamp amplifier. Patch pipettes usually had a final resistance of 10 - 15 MΩ for single channel recordings and 5 – 10 MΩ for whole cell recordings. Positioning of the patch pipette was carried out under the optic field of the microscope using a micromanipulator (sutter-np225) and under visual control the patch pipette was lowered until visual contact with the slice was made. Contact between the patch pipette and the cell was visually confirmed by the formation of a characteristic dimple on the cell surface caused by flow of solution from the pipette tip. Immediately, the positive pressure was released and a small amount of suction was applied to the back of the electrode. Then the cell membrane and the tip of the electrode begin to form a high resistance gigaohm seal. The membrane under the patch pipette was held at -60 mV and suction was applied through the tubing connected to the back of the electrode holder to break the membrane and gain electrical access to the cell interior (Hamill et al., 1981), and then a whole-cell current can be recorded.

2.6.1.2 Compensation of series resistance

In order to reduce the voltage error due to the series resistance existing in whole-cell experiments, more than 80 percent of the series resistance was compensated by the Axopatch-200A before starting recordings. The voltage error can be calculated by Ohm's

law ($V = I R_s$).The average series resistance (R_s) before compensation from my experiments was 33 mΩ (n = 150). The holding current (I_h) was usually less than 50 pA. So originally the voltage error ($V_e = I_h Rs$) was -1.65 mV and reduced to -0.3 mV after 80% compensation. Although during the NMDA response, the currents increased to 300 pA, the voltage error would be -1.8 mV after compensation. Therefore in these experiments series resistance errors had little impact on the whole cell recordings.

2.6.2 Single-channel recordings

After gaining electrical access to the cell interior, the patch electrode was very slowly withdrawn away from the cell using the manipulator until an outside out patch was obtained. Electrical noise was reduced by bringing the patch pipette towards the surface of the bath leaving only its tip in the solution. The patch pipette was also brought toward the inlet of the recording chamber to improve contact between the patch and the incoming solutions. Before recording was attempted, the noise level was checked and an RMS noise level below 0.300 pA at a bandwidth of 5 kHz (Bessel filter) was considered acceptable for recording. The presence of spontaneous single channel openings was also checked and patches with spontaneous single channel activity were discarded.

2.7 Drug application and experimental design

All solutions were superfused into the recording chamber by gravity. The exchange between solutions was made by manually switching a two-way tap. Solution was

removed from the recording chamber by suction supplied by a suction pump connected to a solution reservoir.

2.7.1 Whole-cell recordings

In each slice only one whole cell recording was made in the presence of SKF-82958 or quinpirole. After a slice had been exposed to SKF-82958 or quinpirole, the slice was discarded.

2.7.1.1 Dopamine receptor experiments

NMDA currents were evoked by 2 minute applications of NMDA (10 μM) and glycine (10 μM) followed by a 5 minute application of either the dopamine D1 receptor agonist SKF-82958 (20 nM) with the D2 receptor antagonist spiperone (2 nM), or the D2 receptor agonist quinpirole (40 nM or 1 μM) in the presence of the D1 receptor antagonist SCH-23390 (10 nM). Finally we applied NMDA (10 μM) and glycine (10 μM) accompanied by SKF-82958 (20 nM) and spiperone (2 nM) or quinpirole (40nM) and SCH-23390 (10 nM) for 2 minutes. Genistein (100 μM), lavendustin A (10μM), lavendustin B (10 μM), H-89 (5 μM), PP2 (10 μM) and intracellular dynamin inhibitory peptide (QVPSRPNRAP, 50 μM) were applied individually to the pipette solution as the experiments required.

The concentration of SKF-82958, 20 nM, was chosen to give 83% occupancy of the dopamine D1 receptors in the presence of 2 nM spiperone which would block 95% of the D2 receptors (Mottola et al., 1996; Kebabian et al., 1997). In control experiments, SCH-

23390 (300 nM) was applied together with SKF-82958 (20 nM) to block 99% of the D1 receptors from activation.

Receptor occupancies were calculated using the Gaddum equation:

$$P_{AR} = \frac{[A]}{[A] + K_A\left(1 + \frac{[B]}{K_B}\right)}$$

$[A]$: agonist concentration

$[B]$: antagonist concentration

K_A: agonist dissociation equilibrium constant

K_B: antagonist dissociation equilibrium constant

The concentration of quinpirole, 40 nM were chose to activate 92% of the D2 receptors in the presence of D1 receptor antagonist, SCH-23390, which would block 97% of the D1 receptors. In another experiment the concentration of quinpirole was increased to 1 μM which would activate almost all the D2 receptor (99.7%), and in this case 10 nM SCH-23390 would block 95% of the D1 receptor (Kebabian et al., 1997)

2.7.1.2 $ZnCl_2$ and TPEN experiments

To evoke the first NMDA response NMDA (10 μM) and glycine (10 μM) were applied until the response reached a steady state followed by control solution to wash out the response. NMDA, glycine and $ZnCl_2$ 100nM were then applied. The NMDA response

again reached a steady state followed by control solution to wash out. Finally TPEN (1 μM), NMDA and glycine were applied for another steady state the NMDA response.

2.7.1.3 Calcium channel experiments

$BaCl_2$ (5 mM) was applied in the recording solution instead of $CaCl_2$ (1 mM) to record Ba^{2+} currents through Ca^{2+} channels, and the solution was bubbled with 95% O_2 and 5% CO_2 to avoid precipitate. The medium spiny neurons were voltage clamped at -80 mV in these experiments. The stimulus protocol was 100 ms voltage step pulses between -70 mV and 20 mV in 10 mV increments. Before each test voltage step, 4 leak subtraction pulses were applied and each of them is equivalent to ¼ of the voltage change induced by the followed voltage step.The control calcium channel current-voltage relationship was obtained from these voltage steps first, followed by 5 minutes incubation in the D2 receptor agonist quinpirole (40 nM or 1μM) and D1 receptor antagonist SCH-23390 (10 nM). Finally a second calcium channel current-voltage relationship was recorded from the same voltage step protocol in the presence of quinpirole (40 nM or 1μM) and SCH-23390 (10 nM).

2.7.2 Single channel recordings

In the single channel experiments each outside-out patch was firstly exposed to a constant lower concentration of NMDA (1 μM) for 2 minutes in the presence of saturating concentrations of glycine (10 μM). Then SKF-82958 (20 nM) and spiperone (2 nM) were applied together with NMDA and glycine for 2 minutes. ATP (1 mM) and GDP-β-S (0.5 mM) were present in the pipette solution.

2.8 Whole cell data acquisition and analysis

2.8.1 Whole-cell NMDA responses – WinEDR

Whole-cell current was evoked by NMDA (10μM) and glycine (10 μM) application. Currents were recorded using an Axopatch 200A patch-clamp amplifier (Axon Instruments). Signals were amplified and filtered at 2 kHz (8 pole Bessel) and digitised at 20 kHz using an analogue-to-digital converter (CED micro 1401, Cambridge Electronics Design, UK). Whole-cell currents were stored on computer using the program WinEDR (V2.2.3) (available at http://spider.science.strath.ac.uk/PhysPharm/showPage.php?page Name=software_ses).

After recording, whole cell current traces were printed out with the program WinEDR and then the mean maximum currents manually measured with a ruler, which illustrated in Figure 3.1 and Figure 3.2. I then used Excel to organize and analyze all the data obtained from manually measured current traces. An average current was calculated and the percentage change from each control response was calculated.

2.8.2 Voltage-gated calcium currents – WinWCP

For the calcium current experiments the program WinWCP (V3.4.6) was used to control the membrane potential and record membrane currents. (available at http://spider.science.strath.ac.uk/PhysPharm/showPage.php?page Name=software_ses). A current-voltage relationship curve was plot out by Excel after each recording.

2.9 Single channel data analysis

2.9.1 Steady-state single channel recordings – Consamwin

Steady state single channel activity was produced by a constant concentration of NMDA (1μM) and of glycine (10 μM), and recorded using an Axopatch 200A patch-clamp amplifier (Axon Instruments). Signals were amplified and filtered at 2 kHz (8 pole Bessel) and digitised at 20 kHz using an analogue-to-digital converter (CED micro 1401, Cambridge Electronics Design, UK). Single channel currents were stored on the computer using a continuous sampling program (consamwin or CONSAM) designed by Prof. D. Colquhoun and I Vais (Department of Pharmacology, University College London).

2.9.2 Detection and fitting of single channel date - SCAN

Each digitised single channel record was scanned and opening and closing transitions were detected, measured and fitted using an interactive computer program (SCAN) that carried out direct fitting of each event time-course based on the step response (calculated from a 2kHz Gaussian filter) of the recording system (Colquhoun & Sigworth, 1995). Briefly, the digitised recording was displayed and scanned by scrolling it across the computer screen under visual inspection. Segments of data containing obvious artifacts or "double" openings were set as unusable and excluded from further analysis. Events were detected after crossing a threshold placed close to the baseline. Once it was decided that the event could be fitted, the program made initial guesses for the positions of all the transitions and amplitudes and performed a least-squares fit on the basis of these guesses; finally, it displayed the fitted curve superimposed on the digitised event. If the step-

response function fitted poorly, the fit was adjusted to obtain the fit that best described the event. Fits were stored as a list of values with the amplitude and duration of each open period and the duration of each closed period. Incompletely resolved openings had their amplitude constrained to be the same as that of the closest opening longer than 2 filter rise-times if such an opening was present in the region of trace being fitted. If on the contrary, there were no openings with such characteristic in the section of trace being fitted, they were fitted as openings to the mean amplitude level. After the record was fitted, a data file containing all the values describing the lifetime and amplitude of all single channel events present in the record was created and stored as a computer file which was later used during the analysis of the single-channel data.

2.9.3 Analysis of single channel distribution – EKDIST

Display and analysis of single channel data distributions was done using the program 'EKDIST' designed by D. Colquhoun (Department of Pharmacology, University College London). Before analysis, a fixed resolution for open times and closed times that gave a false event rate less than 10^{-11} events per second was imposed, and a 'real' difference between adjacent amplitude levels defined as > 0.25 pA.

2.9.3.1 Stability plots

Stability plots for amplitudes were built by plotting the individual single-channel current amplitude of each opening against the interval number in which the opening was detected. The amplitude of each single opening longer than 2 filter rise-times (332 μs) was plotted. Each data point on the plot represented a single observation independently of its duration.

Before a patch was accepted for detailed analysis, the long term stability of the data records was checked by making stability plots for open times, shut times and P_{open} (Weiss and Magleby, 1989; Colquhoun and Sigworth, 1995). Stability plots for open and shut times were made by calculating a moving average of 50 consecutive open or shut time intervals with an overlap of 25 events and plotting this average against the interval number at the center of the averaged values. Stability plots for open probability were made by calculating a P_{open} value for each set of 50 open and shut times. Once the stability of the record was confirmed, open and closed time values were sorted into bins and used in the construction of frequency distribution histograms.

2.9.3.2 Distribution of fitted amplitudes

The amplitude of channel openings can be measured accurately only if the duration is at least twice the rise-time (T_r) of the recording system (Colquhoun & Sigworth, 1995). Frequency distribution histograms containing individual open-channel amplitudes longer than 2 filter rise-times (332 μs) were constructed and fitted with the sum of three Gaussian components with their standard deviations constrained to be the same. The relative area occupied by each Gaussian component represents the relative frequency of events to each particular amplitude level rather than the relative time spent at each level. Each single channel opening longer than 2 filter rise-times represented one observation independently of its duration.

2.9.3.3 Distribution of open times and shut times

As the duration of closed and open time intervals can vary from tens of microseconds to tens of seconds, frequency distribution histograms were constructed using a logarithmic transformation of the abscissa (McManus *et al.*, 1987; Sigworth & Sine, 1987) and a square root transformation of the ordinate (Sigworth & Sine, 1987). Distributions were fitted using the maximum likelihood method (Colquhoun and Sigworth, 1995) with probability density functions that were a mixture of three exponential components for open times and five exponential components for closed times (Gibb & Colquhoun, 1992).

2.10 Statistics

For statistical comparisons, two different procedures were used: students t-tests and a randomisation test that does not involve making any assumptions about the shape of the distribution of observations (this can be requested at http://www.ucl.ac.uk/Pharmacology/dcpr95.html). Statistical significance was set at $p<0.05$. The randomisation test works on paired or unpaired data with continuous variables with the advantage that avoid the effects that may be induced by grouping data. Randomized data sets are generated by drawing data values from control and test data sets at random and the difference in the mean values of each randomized sets calculated. This process was repeated 1000 times and the distribution of the difference in mean values compared with the original data. If the proportion of randomizations, giving a mean difference greater than or equal to that observed, was less than 5% the difference between control and test data sets was concluded to be significant.

Chapter 3

Dopamine D1 receptor inhibition of NMDA responses in medium spiny neurons

3.1 Introduction

Dopamine D1 receptor activation has been shown to regulate NMDA receptor activity in the striatum (Levine et al., 1996; Cepeda et al., 1998a; Flores-Hernandez et al., 2002, Lee et al., 2002; Lin et al., 2002). Some studies showed that D1 receptor activation enhanced NMDA receptor currents by the classical adenylate cyclase pathway (Levine et al., 1996; Blank et al., 1997; Cepeda et al., 1998a; Snyder et al., 1998; Flores-Hernandez et al., 2002). In this classical pathway, D1 receptors couple to Gs G proteins, raising cAMP and resulting in phosphorylation of DARPP-32 and inhibition of protein phosphatase-1 (Blank et al., 1997; Snyder et al., 1998; Greengard, 2001). In addition to the classical pathway, Dunah et al. (2004) have shown that deletion of the gene for the protein tyrosine kinase, Fyn, inhibits dopamine D1 receptor-induced enhancement of the abundance of NR1, NR2A and NR2B subunits in the synaptosomal membrane fraction of striatal homogenates.

On the other hand some other studies presented evidence that dopamine can attenuate NMDA-mediated currents (Lin et al., 2003; Lee et al., 2002). In particular Lee et al. (2002) demonstrated inhibition of NMDA responses by a direct protein-protein interaction between the dopamine D1 receptor and NR2A subunit C-termini. Thus there

are conflicting results about D1 receptor modulation of NMDA receptors in the striatum and more research needs to be done to clarify this issue.

In this study, I have used whole cell and outside-out patch clamp recordings to investigate D1 receptor modulation of NMDA receptors in striatal medium spiny neurons.

3.2 Results

Most of these experiments were carried out upon medium spiny neurons in striatal brain slices from 7 day old rats unless specified otherwise. Medium spiny neurons were voltage clamped at -60mV in the presence of TTX (100nM) to block voltage-gated Na^+ currents.

3.2.1 D1 receptor activation reduced NMDA receptor currents in striatal medium spiny neurons.

Figure 3.1 shows that the D1 receptor agonist, SKF-82958, significantly ($p< 0.05$) decreased the NMDA whole-cell current. Figure 3.1*A* illustrates a current trace from a whole-cell recording, where the first NMDA response was evoked by a 2 minute application of NMDA (10 μM) and glycine (10 μM) followed by a 5 minute application of SKF-82958 (20 nM) and spiperone (2 nM) in the absence of NMDA and glycine then for another 2 minutes in the presence of NMDA and glycine. Spiperone, a D2 receptor antagonist, was used to rule out the effect of D2 receptor activation on the NMDA responses. ATP (1 mM) and GTP (1 mM) was included in the pipette solution.

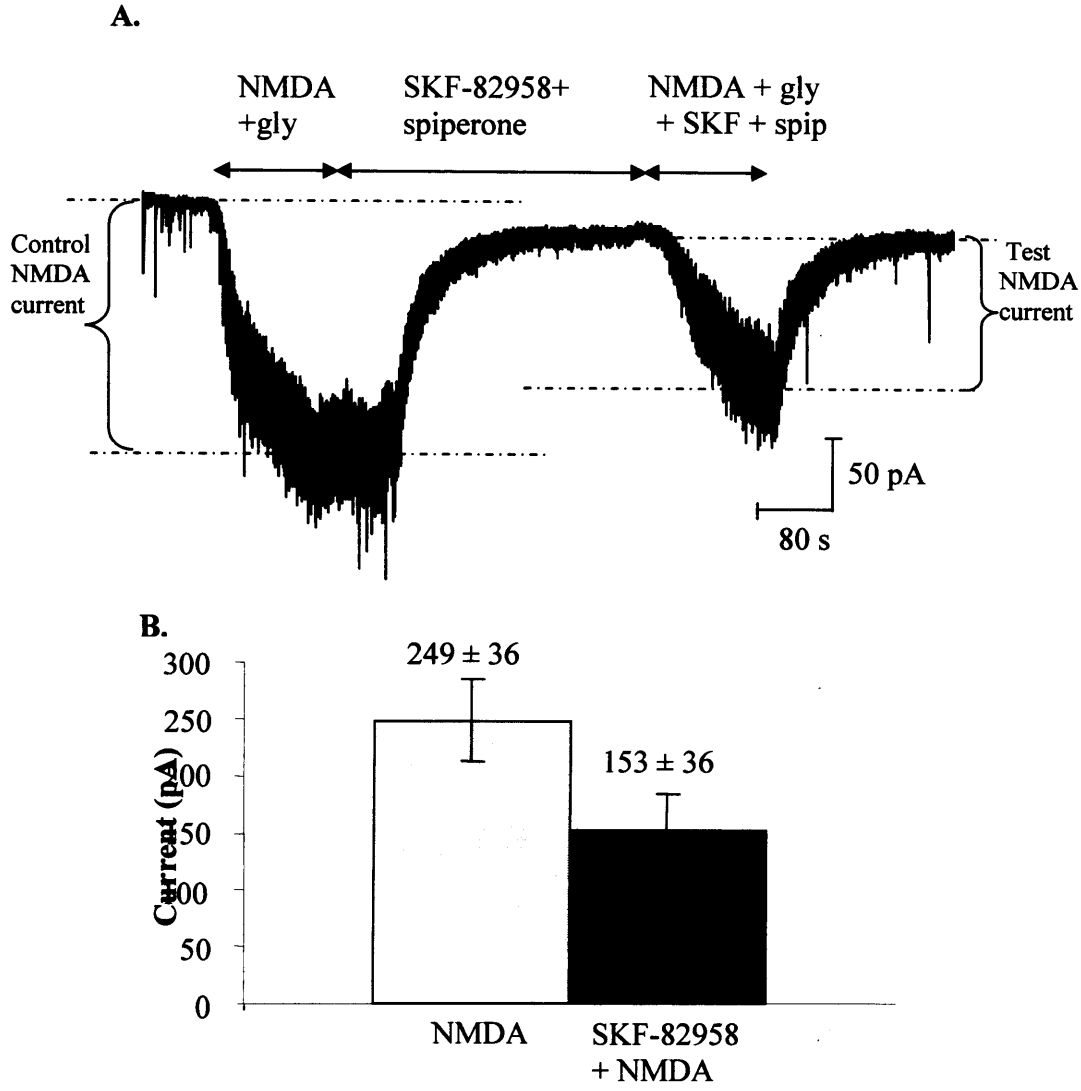

Figure 3.1 D1 receptor activation inhibits whole cell NMDA receptor currents recorded from 7 day-old rat striatal neurons voltage clamped at -60mV. A, Response to NMDA (10 μM) and glycine (10 μM) applied for 2 minutes, followed by 5 minutes SKF-82958 (20 nM) and spiperone (2 nM), and finally NMDA (10 μM), glycine (10 μM), SKF-82958 (20 nM) and spiperone (2 nM) for 2 minutes. Dashed lines show how currents and test NMDA current is measured. Brief downward deflections of the current trace show occasional miniature synaptic currents. The holding current was -39 pA prior to the control NMDA response. B, Mean current (± SE) of the second NMDA response, in the presence of SKF-82958 and spiperone, was significantly less than the first response. ($n = 10$, $p < 0.05$).

Cell number	I_{H1} (pA)	NMDA (pA)	I_{H2} (pA)	NMDA + SKF-82958 (pA)	% change	R_s (MΩ)	C_m (pF)
22-05-03#1	-80	67	-98	40.0	-76.0	22.0	19.9
22-05-03#2	-126	240	-230	347	44.4	21.2	29.3
22-05-03#3	-68	373	-87	240	-35.7	35.0	21.9
22-05-03#4	-15	127	-26	93.3	-26.3	34.2	9.60
22-05-03#5	-20	360	-52	240	-33.3	45.0	24.0
22-05-03#6	-35	367	-39	137	-62.7	32.1	16.6
22-05-03#7	-11	83.3	-35	100	20.0	15.6	14.6
27-05-03#1	-37.8	127	-51	46.7	-63.2	8.3	30.5
27-05-03#3	-40	317	-44	110	-65.3	26.0	12.2
27-05-03#4	-23	327	-80	180	-44.9	15.2	19.2
Count	10	10	10	10	10	10	10
Mean	-46	249	-74	153	-38.3	25.5	19.8
SE	11	36.0	34	30.9	12.3	3.5	2.2

Table 3.1 D1 receptor activation inhibited whole cell NMDA receptor currents. Details of each whole cell recording from ten neurons are given showing the holding currents (I_H), the steady state NMDA currents (10 μM NMDA and 10 μM glycine) in the absence and in the presence of SKF-82958 (20 nM) and spiperone (2 nM), the series resistance (R_s) and the capacitance (C_m) of each cell. A paired t-test and a randomization test show that SKF-82958 reduced the NMDA responses significantly ($p = 0.016$), and that the holding current prior to the NMDA response in the presence of SKF-82958 (I_{H2}) is significantly greater than prior to the control NMDA response (I_{H1}) ($p = 0.016$)

Figure 3.1B shows a comparison of the mean maximum currents, averaged from the ten neurons in this experiment (Table.3.1), between the NMDA responses in the absence and in the presence of SKF-82958 and spiperone. NMDA receptor currents decreased significantly from 249 ± 36 pA to 153 ± 31 pA (mean ± SE, n=10 neurons), although in two cells the NMDA currents increased in the presence of SKF-82958. The results indicated that dopamine D1 receptor activation reduced the NMDA receptor whole-cell currents significantly in striatal medium spiny neurons in 7 day-old rats.

To confirm this inhibition, in a separate group of slices I had made control experiments in 7 cells (Table.3.2), where two consecutive NMDA responses, 5 minutes apart, were recorded without application of SKF-82958 or spiperone (Figure 3.2*A*). There was no significant reduction in the mean value of the second NMDA responses (409 ± 78 pA) when compared with the mean value of the first NMDA responses (411 ± 89 pA) (Figure 3.2*B*), and the second NMDA response increased in 3 cells. When I averaged the percentage change of the two NMDA responses in each neuron, there was 3.1± 6.0% decrease in this control experiment, and in contrast SKF-82958 significantly decreased the second NMDA response by 34.2 ± 12.3% ($p< 0.05$) (Figure 3.2*C*).

Moreover in another control experiment, the D1 antagonist, SCH-23390 (300 nM), was tested in ten neurons (Table 3.3). After the first NMDA response, SCH-23390 was applied together with the SKF-82958 and spiperone throughout the rest of the experiment until the second NMDA response was washed out by the external recording solution (Figure 3.3*A*). SCH-23390 effectively blocked the SKF-82958 induced inhibition of the NMDA responses (NMDA; 173 ± 28 pA; SCH-23390 + SKF-82958 + NMDA; 167 ± 34 pA, n = 10) (Figure 3.3*B*). These results also demonstrate that the

Figure 3.2

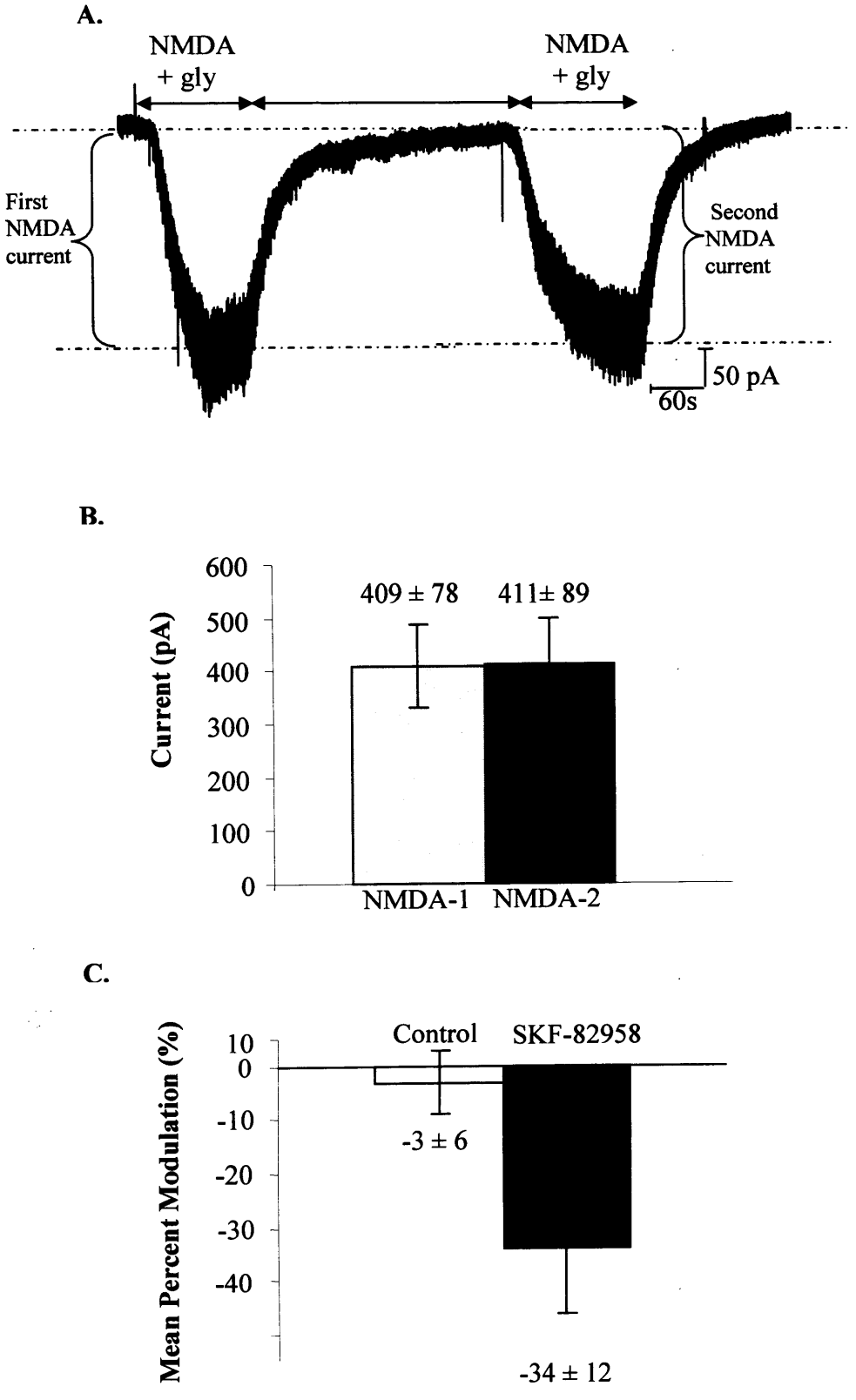
A.
NMDA
+ gly
NMDA
+ gly
First
NMDA
current
Second
NMDA
current
50 pA
60s
B.
Current (pA)
600
500
400
300
200
100
0
409 ± 78
411± 89
NMDA-1
NMDA-2
C.
Mean Percent Modulation (%)
10
0
-10
-20
-30
-40
Control
SKF-82958
-3 ± 6
-34 ± 12

Figure 3.2 No difference was observed between two consecutive NMDA responses in control experiments. **A,** Response to NMDA and glycine applied for 2 minutes, followed by 5 minutes of control recording solution, followed by NMDA and glycine for 2 minutes. Dashed lines show how currents and test NMDA current is measured. The holding current was -11 pA prior to the control NMDA response. **B,** Mean current (± SE) of the first NMDA response compared to the second NMDA response ($n = 7$, $p > 0.05$). **C,** mean percent change (± SE) in control experiments involving two successive NMDA responses compared to the inhibition in the presence of SKF-82598 and spiperone ($p < 0.05$).

Cell number	I_{H1} (pA)	NMDA-1 (pA)	I_{H2} (pA)	NMDA -2 (pA)	% change	R_s (MΩ)	C_m (pF)
04-02-05#4	-70	725	-210	750	3.45	28.5	39.00
04-02-05#5	-80	650	-280	675	3.85	24.9	29.40
10-02-05#1	-20	156	-20	138	-12.00	70.0	8.70
10-02-05#2	-11	375	-13	363	-3.33	80.1	11.00
10-02-05#6	-20	300	-30	269	-10.42	38.7	15.00
11-02-05#3	-80	256	-28	188	-26.83	43.5	12.70
11-02-05#5	-110	400	-80	494	23.44	34.6	24.00
Count	7	7	7	7	7	7	7
Mean	-56	400	-94	411	0.44	45.8	20.0
SE	15	78.4	42	89.8	6.0	8.0	4.2

Table 3.2 Results of control experiments investigating two consecutive NMDA responses. Details are given of each whole cell recording from seven neurons, which include the holding currents (I_H), the steady state NMDA currents in response to two successive NMDA applications, the series resistance (Rs) and the capacitance (C_m) of each cell. Comparing the two NMDA (10 μM) and glycine (10 μM) responses shows that there is no significant difference ($p = 0.931$) by both paired t-test and randomization test, and no significant difference between the holding currents prior (I_{H1}) and after (I_{H2}) the first NMDA responses ($p = 0.391$).

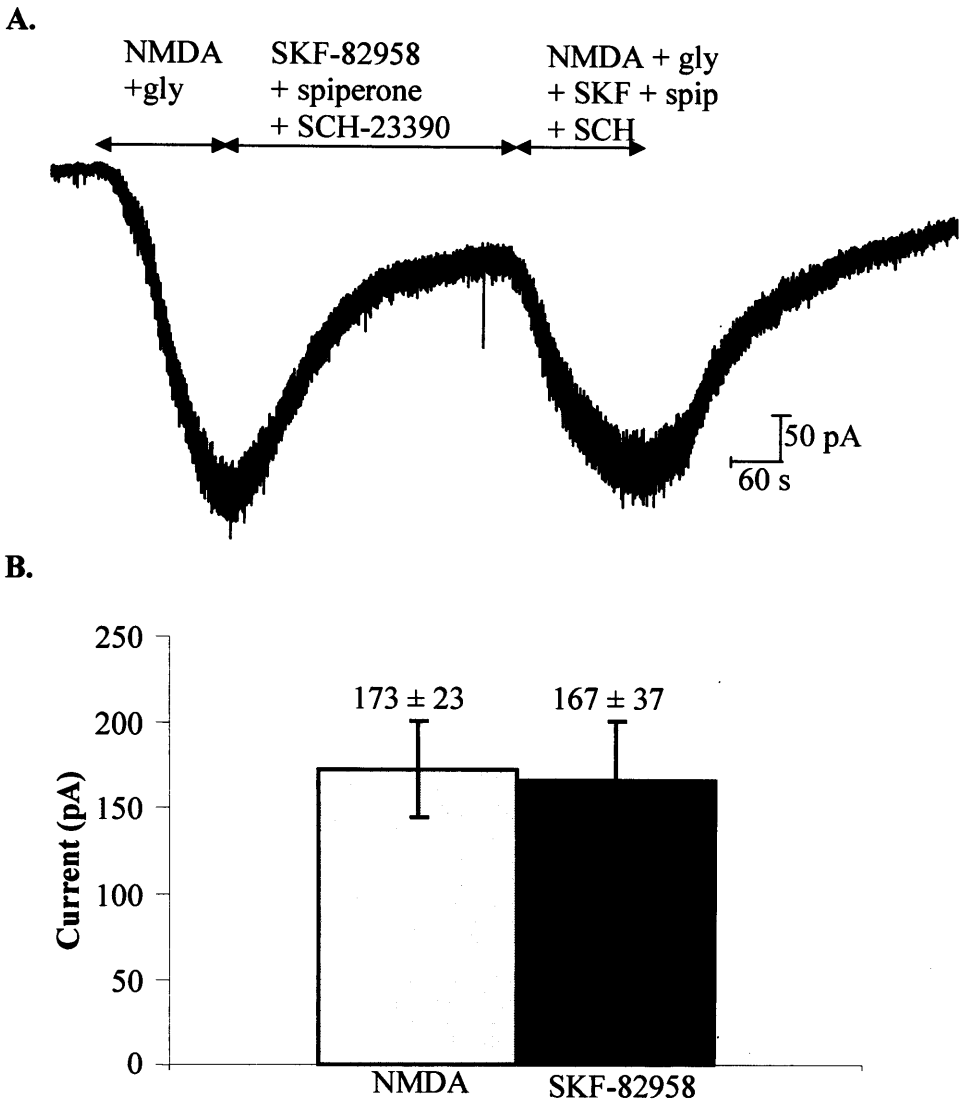

Figure 3.3 D1 receptor antagonist SCH-23390 blocked the D1 inhibition of NMDA receptor currents. A, Response to NMDA (10 μM) and glycine (10 μM) applied for 2 minutes, followed by 5 minutes SKF-82958 (20 nM), spiperone (2 nM) and SCH-23390 (300 nM), and finally NMDA (10 μM), glycine (10 μM), SKF-82958 (20 nM), spiperone (2 nM) and SCH-23390 (300 nM) for 2 minutes. The holding current was -100 pA prior to the control NMDA responses. B, Mean current (± SE) of the first NMDA response compared to the second response in the presence of SKF-82958, spiperone and SCH-23390 (300 nM) ($n = 10$, $p > 0.05$).

Cell number	I_{H1} (pA)	NMDA (pA)	I_{H2} (pA)	NMDA + SKF-82958 (pA)	% change	R_s (MΩ)	C_m (pF)
14-3-05#1b	-100	231.3	-97	200.0	-13.5	64.6	11.0
14-3-05#2b	-50	231.3	-158	246.9	6.8	45.5	21.0
14-3-05#4	-117	175.0	-200	143.8	-17.9	44.1	24.0
14-3-05#5	-13	150.0	-160	146.9	-2.1	42.8	31.2
14-3-05#6	-20	218.8	-170	225.0	2.9	53.2	20.6
15-3-05#1	-28	175.0	-60	118.8	-32.1	29.2	19.3
8-04-05#2	-4	87.5	-20	68.8	-21.4	58.2	10.7
8-04-05#3	-40	75.0	-78	68.8	-8.3	51.3	9.6
8-04-05#4	-50	343.8	-80	406.6	18.3	32.1	17.4
8-04-05#5	-14	46.9	-16	40.6	-13.3	24.6	6.6
Count	10	10	10	10	10	10	10
Mean	-43.6	173.4	-103.9	166.6	-3.9	44.6	17.1
SE	11.9	28.2	20.5	34.4	4.7	4.1	2.4

Table 3.3 SCH-23390, a D1 receptor antagonist, abolished the D1 inhibition of NMDA receptor currents. Details of each whole cell recording from ten neurons are given, which include the holding currents (I_H) steady state NMDA currents in the absence and in the presence of SKF-82958, spiperone and SCH-23390, the series resistance (R_s) and the capacitance (C_m) of each cell. In the presence of SCH-23390, no significant difference was found between NMDA responses in control and NMDA responses in the presence of SKF-82958 (20 nM), spiperone (2 nM) and SCH-23390 (300 nM) ($p = 0.52$) by both paired t-test and randomization test. The holding current prior to the NMDA response in the presence of SKF-82958 and SCH-23390 (I_{H2}) is significantly greater than prior to the control NMDA response (I_{H1}) ($p = 0.01$)

presence of the D2 receptor antagonist spiperone and hence block of any constitutive D2 tone in the slice did not significantly affect NMDA responses. It is clear that D1 receptor activation in striatal medium spiny neurons inhibited the NMDA receptor-mediated whole-cell currents.

My results are not consistent with the hypothesis of the classical adenylate cyclase pathway involving Gs G proteins, where D1 activation has been shown to enhance NMDA responses via the adenylate cyclase – protein kinase-A and DARPP-32 (Dopamine and cyclic adenosine 3',5'-monophosphate-regulated phosphoprotein, 32 kDa) cascade (Levine et al., 1996; Flores-Hernandez et al., 2002, Greengard, 2001). Therefore it is possible that the classical pathway is not involved in the D1 inhibition of NMDA receptors observed in my experiments. However these results are consistent with those of Lee et al. (2002) who demonstrated that D1 receptor activation inhibited NMDA currents via a direct protein-protein interaction between the D1 receptor and the NMDA receptor that did not involve the Gs G protein pathway. Consequently, I decided to test if Gs G protein activation was essential for the D1 inhibition of NMDA receptors observed in my experiments.

3.2.2 G protein was not involved in D1 inhibition of NMDA receptor currents

In order to test whether G proteins are required for D1 receptor inhibition of whole cell NMDA currents, intracellular GTP (1mM) was substituted with a general G protein inhibitor, GDP-β-S (0.5 mM). The rest of the experiment was executed using exactly the

same procedures as used in the former SKF-82958 experiments (Figure 3.1A). Figure 3.4*A* shows a current trace from this experiment. In the presence of GDP-β-S, SKF-82958 significantly decreased the mean value of the NMDA whole-cell currents from 162 ± 34 pA to 74 ± 12 pA (54 ± 12% inhibition) (Figure 3.4*B*), and only one cell showed increase. However intracellular GDP-β-S apparently reduced the first NMDA responses compared with NMDA responses with ATP and GTP in the pipette (control) (Control: 252 ± 27, n=32; GDP-β-S: 162 ± 34, n=9), although statistically this was not significant ($p = 0.1$).

Likewise, replacement of GTP with GTP-γ-S (0.5 mM) (Figure 5A), an irreversible activator of G proteins, did not occlude the SKF-82958 induced inhibition of NMDA responses (NMDA: 365 ± 52 pA, SKF-82958 + NMDA: 209 ± 27 pA, n = 10 cells, $p< 0.05$) (Figure 3.5*B*, Table.3.5). Although there was an apparent increase of the first NMDA responses in the presence of intracellular GTP-γ-S, GTP-γ-S did not significantly affect the NMDA responses ($p = 0.10$). Neither intracellular GDP-β-S nor GTP-γ-S significantly affected the holding currents (I_H) prior to the first NMDA response when compared with the I_H with intracellular ATP and GTP (control: -47 ± 7.1 pA, n = 32; GDP-β-S: -48 ± 8 pA, n = 25; GTP-γ-S: -33 ± 5 pA, n= 10, $p>0.05$).

These results suggest that G protein activation was not involved in D1 inhibition of NMDA responses. Nevertheless, since the mean NMDA response in the presence of G protein inhibition (GDP-β-S) is significantly smaller (162 ± 34 pA) than in the presence of an irreversible G protein activator, GTP-γ-S (365 ± 52 pA), these results indicate that G protein activation can potentiate NMDA responses.

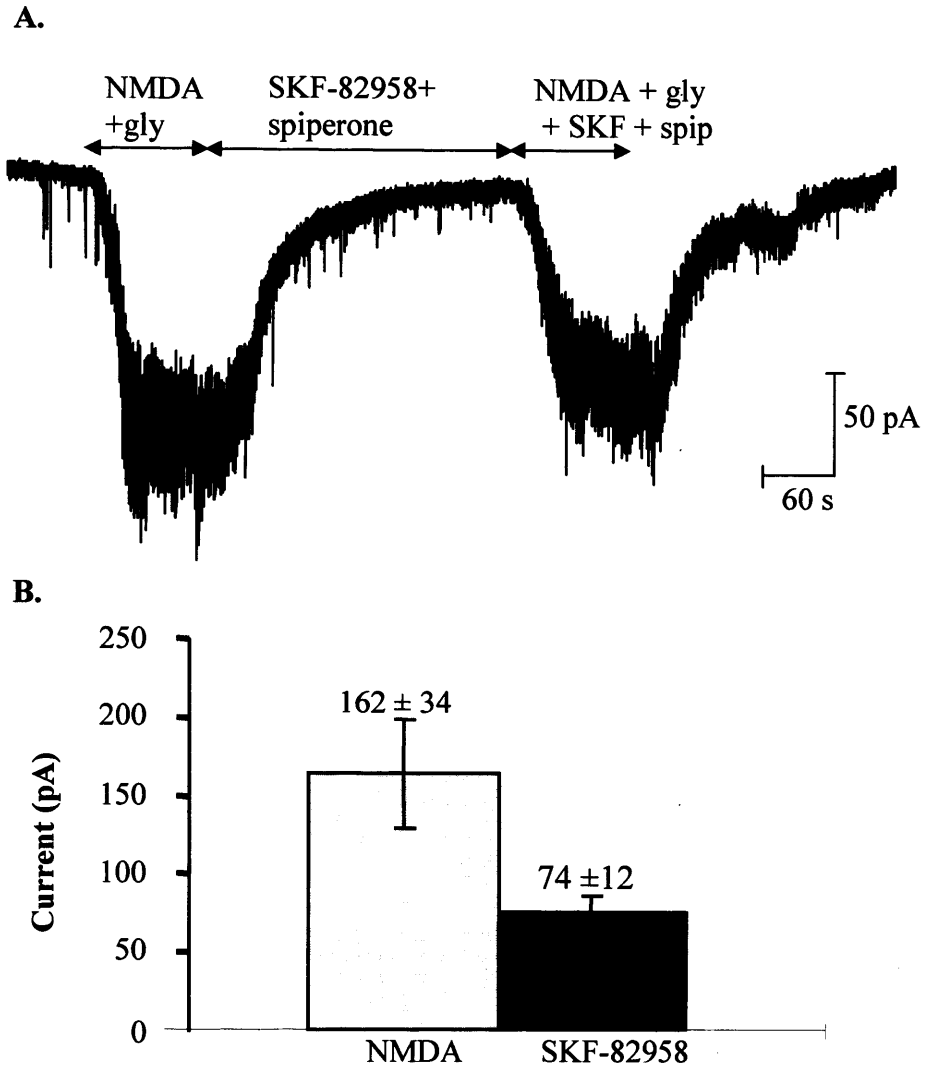

Figure 3.4 GDP-β-S, a G protein inhibitor, had no effect on D1 inhibition of NMDA responses. A, whole cell current recording with GDP-β-S (0.5 mM) and ATP (1 mM) in the pipette solution. NMDA (10 μM) and glycine (10 μM) were applied for 2 minutes, followed by 5 minutes SKF-82958 (20 nM) and spiperone (2 nM), and finally NMDA (10 μM), glycine (10 μM), SKF-82958 (20 nM) and spiperone (2 nM) for 2 minutes. The holding current was -18 pA prior to the control NMDA responses. **B**, The mean current (± SE) in the presence of intracellular GDP-β-S (0.5 mM) of the first NMDA response compared to the second response in the presence of SKF-82958 and spiperone ($n=9$, $p< 0.05$).

Cell number	I_{H1} (pA)	NMDA (pA)	I_{H2} (pA)	NMDA + SKF-82958 (pA)	% change	R_s (MΩ)	C_m (pF)
12-06-03#2	-18	131	-20	100	-23.8	32.0	12.0
12-06-03#3	-7	62.5	-20	36.9	-41.0	16.5	11.6
120603#4	-40	53.1	-37	22.5	-57.6	39.4	10.2
13-06-03#1	-60	244	-190	75.0	-69.2	27.0	54.5
13-06-03#2	-33	175	-50	138	-21.4	21.9	14.3
16-06-03#2	-70	331	-60	48.8	-85.3	28.5	25.9
17-06-03#1	-33	119	-70	113	-5.26	18.0	14.5
17-06-03#2	-23	281	-130	62.5	-77.8	22.9	25.8
17-06-03#3	-20	59.4	-52	68.8	15.8	27.1	18.0
Count	9	9	9	9	9	9	9
Mean	-33.8	162	-69.9	74	-54.4	25.9	20.8
SE	6.8	34	18.6	12	11.5	2.4	4.6

Table 3.4 G protein activation was not required for D1 inhibition of NMDA receptor responses. GDP-β–S (0.5 mM), a general G protein inhibitor, replaced GTP in the pipette solution. Details of each whole cell recording from 9 neurons are illustrated, which include the holding currents (I_H), the steady state NMDA currents in the absence and in the presence of SKF-82958 and spiperone, the series resistance (R_s) and the capacitance (C_m) of each cell. Comparing the NMDA (10 μM) and glycine (10 μM) responses with NMDA, glycine, SKF-82958 (20 nM) and spiperone (2 nM) responses shows that there is a significant decrease ($p = 0.038$) in the presence of GDP-β–S by both paired t-test and randomization test, and that the holding current prior to the NMDA response in the presence of SKF-82958 (I_{H2}) is not significantly greater than prior to the control NMDA response (I_{H1}) ($p = 0.06$)

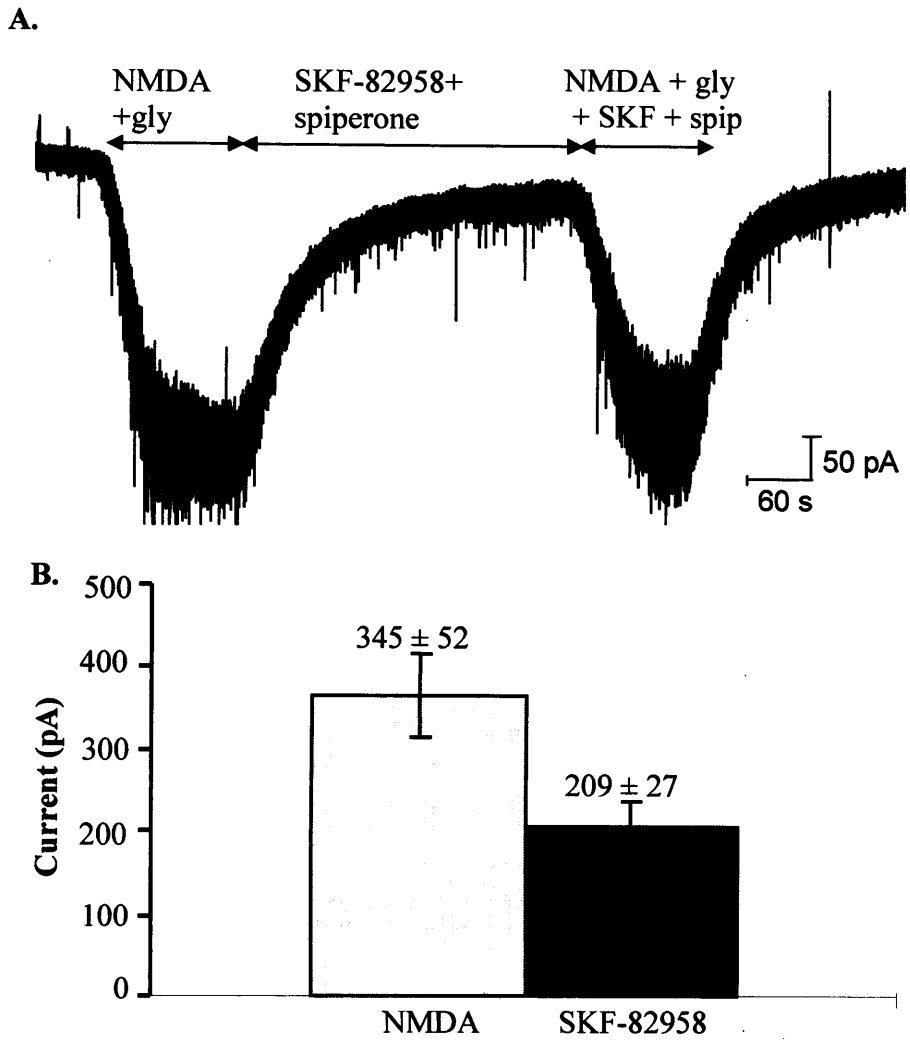

Figure 3.5 An inreversible G protein activator, GTP-γ-S, did not affect the D1 inhibition of NMDA receptor whole cell currents. A, whole cell current recording with GTP-γ-S (0.5 mM) and ATP (1mM) in the pipette solution. NMDA (10 μM) and glycine (10 μM) were applied for 2 minutes, followed by 5 minutes SKF-82958 (20 nM) and spiperone (2 nM), and finally NMDA (10 μM), glycine (10 μM), SKF-82958 (20 nM) and spiperone (2 nM) for 2 minutes. The holding current was -30 pA prior to the control NMDA responses. **B,** The mean current (± SE) in the presence of intracellular GTP-γ-S of the first NMDA response compared to the second NMDA response (n=10, $p<0.05$).

Cell number	I_{H1} (pA)	NMDA (pA)	I_{H2} (pA)	NMDA + SKF-82958 (pA)	% change	R_s (MΩ)	C_m (pF)
15-10-04#2	-50	193.75	-80	165.63	-14.52	64.70	22.6
15-10-04#3	-50	450.00	-50	150.00	-66.67	38.50	31.4
5-11-04#1	-60	462.50	-120	237.50	-48.65	30.00	31
8-11-04#1	-20	218.75	-80	162.50	-25.71	70.00	15.6
8-11-04#2	-30	487.50	-140	350.00	-28.21	45.20	27.5
8-11-04#3	-20	456.25	-74	262.50	-42.47	33.70	22.8
9-11-04#2	-36	312.50	-80	243.75	-22.00	33.70	25
9-11-04#3	-6	40.63	-10	34.38	-15.38	21.90	5.1
9-11-04#5	-40	487.50	-59	212.50	-56.41	35.50	26.3
9-11-04#6	-18.4	537.50	-55	268.75	-50.00	39.50	29
Count	10	10	10	10	10	10	10
Mean	-33.0	364.7	-74.8	208.8	-42.8	41.3	23.6
SE	5.4	52.0	11.5	27.2	5.8	4.8	2.5

Table 3.5 GTP-γ-S, an irreversible activator of G proteins did not affect D1 inhibition of NMDA receptor currents. Details of each whole cell recording from ten neurons are shown, which include the holding currents (I_H), the steady state NMDA currents in the absence and in the presence of SKF-82958 and spiperone, the series resistance (R_s) and the capacitance (C_m) of each cell. ATP (1 mM) and GTP-γ–S (0.5 mM) were in the pipette solution. Comparison of the two NMDA responses with intracellular GTP-γ–S shows that in the presence of SKF-82958 and spiperone the NMDA responses were significantly smaller ($p = 0.0161$) by both paired t-test and randomization test. The holding current prior to the NMDA response in the presence of SKF-82958 (I_{H2}) is significantly greater than prior to the control NMDA response (I_{H1}) ($p = 0.03$)

3.2.3 PKA is not required for D1 inhibition of NMDA receptor currents

Activation of cAMP-dependent protein kinase (PKA) was assumed to be also involved in D1 receptor modulation of NMDA receptors via the classical adenylate cyclase pathway (Snyder et al., 1998, Greengard 2001). To test for a role for PKA in D1 inhibition, H-89 (5 μM), a PKA inhibitor, was added to the pipette solution which contained ATP (1 mM) and GTP (1 mM) in 7 neurons (Figure 3.6*A*, Table.3.6).

In the presence of H-89, SKF-82958 again significantly reduced the mean maximum NMDA responses by 33 ± 9% (NMDA: 238 ± 27 pA, SKF-82958 + NMDA: 150 ± 15 pA n=7, $p<0.05$), although in one cell the NMDA response increased in the presence of SKF-82958. These results show that PKA activation is not required for D1 inhibition of NMDA receptor currents in medium spiny neurons. H-89 did not significantly affect the control NMDA response (the first NMDA response) (Table 3.7) and the holding currents (control: -47 ± 7.1 pA, n = 32; H-89: -81 ± 19 pA, n = 7, $p>0.05$), when compared with other control NMDA responses with ATP and GTP in the pipette.

Since neither G protein nor PKA were involved in D1 inhibition of NMDA responses in these experiments, I conclude an alternative mechanism may predominate here.

3.2.4 D1 inhibition is blocked by non-receptor tyrosine kinase inhibitors

3.2.4.1 General tyrosine kinase inhibitors lavendustin A and genestein

Besides the classical pathway and the possibility of a direct protein-protein interaction, Dunah et al. (2001) suggested that dopamine D1 receptor activation can enhance the

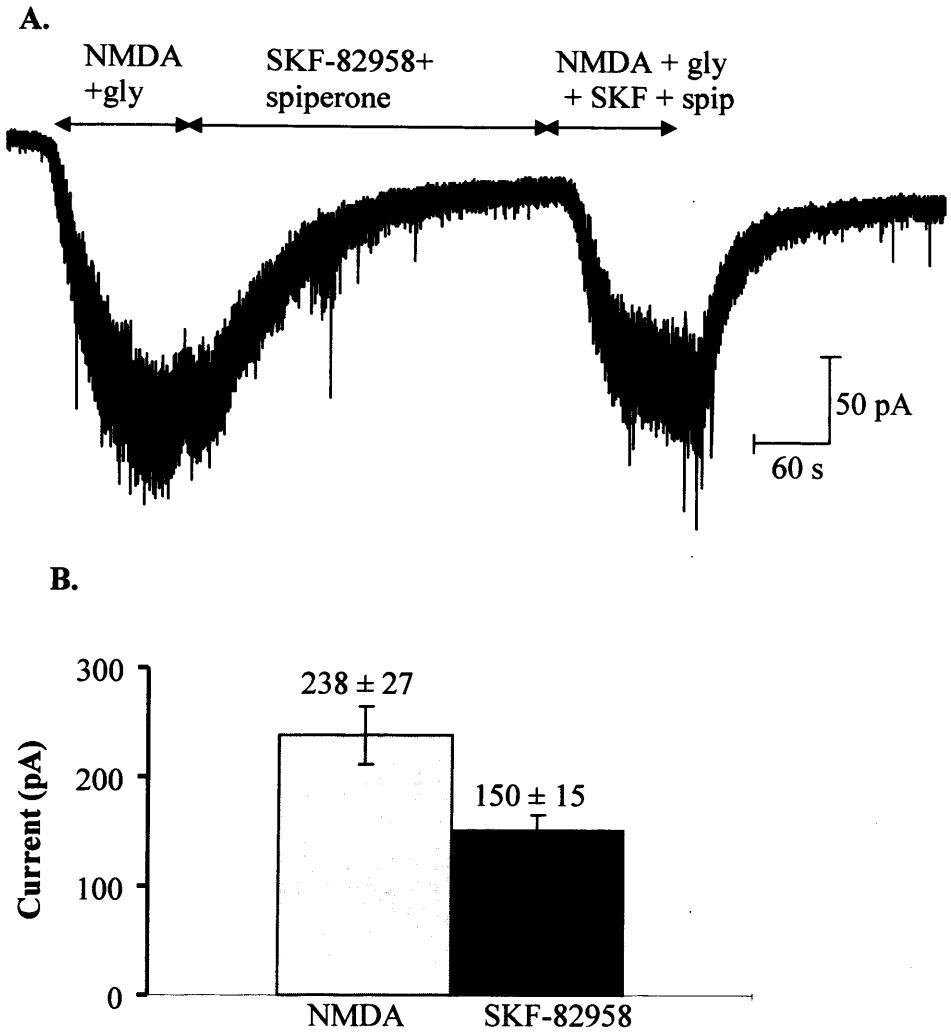

Figure 3.6 D1 inhibition of NMDA currents does not require PKA activation. A, whole cell current recording in the presence of intracellular H-89 (5 μM), ATP (1 mM) and GTP (1mM). NMDA (10 μM) and glycine (10 μM) were applied for 2 minutes, followed by 5 minutes SKF-82958 (20 nM) and spiperone (2 nM), and finally NMDA (10 μM), glycine (10 μM), SKF-82958 (20 nM) and spiperone (2 nM) for 2 minutes. The holding current was -3 pA prior to the control NMDA responses. **B,** The mean current (± SE) in the presence of intracellular H-89 (5 μM) of the first NMDA response compared to the second NMDA response in the presence of SKF-82958 and spiperone ($n=7$, $p< 0.05$).

Cell number	I_{H1} (pA)	NMDA (pA)	I_{H2} (pA)	NMDA + SKF-82958 (pA)	% change	R_s (MΩ)	C_m (pF)
14-12-04#2	-100	176.9	-180	195.2	10.3	50.2	19.7
15-12-04#2	-30	318.8	-70	206.3	-35.3	72.6	11.3
15-12-04#3	-68	225.0	-72	162.5	-27.8	63.0	8.5
17-02-05#1	-130	318.8	-102	106.3	-66.7	62.2	11.0
17-02-05#6	-3	150.0	-30	112.5	-25.0	28.9	12.5
17-02-05#7a	-100	187.5	-120	118.8	-36.7	33.8	17.7
17-02-05#9	-138	287.5	-380	150.0	-47.8	15.0	43.9
count	7	7	7	7	7	7	7
MEAN	-81.3	237.8	-136.3	150.2	-32.7	46.5	17.8
SE	19.0	26.6	44.3	15.2	8.9	8.0	4.6

Table 3.6 H-89, a PKA inhibitor, did not affect D1 inhibition of NMDA receptor currents. Details of each whole cell recording from ten neurons are shown, which include the holding currents (I_H), the steady state NMDA currents in the absence and in the presence of SKF-82958 and spiperone, the series resistance (R_s) and the capacitance (C_m) of each cell. ATP (1 mM), GTP (1 mM) and H-89 (5 μM) were in the pipette solution. Comparison of the two NMDA responses with intracellular H-89 shows that in the presence of SKF-82958 and spiperone the NMDA responses were significantly smaller ($p = 0.021$) by both paired t-test and randomization test. There is no significant difference between the holding current prior to the NMDA response in the presence of SKF-82958 (I_{H2}) and the holding currents prior to the control NMDA response (I_{H1}) ($p = 0.15$)

cell number	Control NMDA response (pA)	Cell number	NMDA response in H-89 (pA)
04-02-05#4	725.00	14-12-04#2	176.9
04-02-05#5	650.00	15-12-04#2	318.8
10-02-05#1	156.25	15-12-04#3	225.0
10-02-05#2	375.00	17-02-05#1	318.8
10-02-05#6	300.00	17-02-05#6	150.0
11-02-05#3	256.25	17-02-05#7a	187.5
11-02-05#5	400.00	17-02-05#9	287.5
22-05-2003#1	167		
22-05-2003#2	240		
22-05-2003#3	373		
22-05-2003#4	127		
22-05-2003#5	360		
22-05-2003#6	367		
22-05-2003#7	83.3		
27-5-03#1	127		
27-5-03#3	317		
27-5-03#4	327		
14-3-05#1b	231.3		
14-3-05#2b	231.3		
14-3-05#4	175.0		
14-3-05#5	150.0		
14-3-05#6	218.8		
15-3-05#1	175.0		
8-04-05#2	87.5		
8-04-05#3	75.0		
8-04-05#4	343.8		
8-04-05#5	46.9		
9-07-03#2	263		
10-07-03#1	181		
10-07-03#2	178		
10-07-03#3	219		
10-07-03#4	131		
Mean Count SE	252 32 27		229 7 26.6
	p =	0.71	

Table 3.7 H-89 did not significantly affect the NMDA responses. The first NMDA responses from experiments where ATP and GTP were in the pipette solution (control) (n = 32) and the first NMDA response in the presence of intracellular H-89 (Table 3.6) are presented here. Both unpaired t-test and a randomization test show that H-89 did not induce a significant change in the NMDA responses ($p > 0.05$).

abundance of NR1, NR2A and NR2B subunits in the synaptosomal membrane fraction of striatal homogenates. Whole cell NMDA responses will include activation of synaptic, as well as extra synaptic NMDA receptors. Later this group (Dunah et al., 2004) showed further evidence that a non-receptor tyrosine kinase, Fyn, was responsible for this NMDA receptor trafficking change.

Thus intracellular lavendustin A (10 μM), a potent tyrosine kinase inhibitor (Onoda et al., 1989; Lu et al., 1999) was utilized to test if a tyrosine kinase is involved in D1 modulation of NMDA receptors in 14 neurons (Figure 3.7*A*, Table 3.8). Interestingly in the presence of intracellular lavendustin A, SKF-82958 did not induce a significant inhibition of NMDA responses (NMDA: 205 ± 77 pA, SKF-82958 + NMDA: 190 ± 53 pA, $p>0.05$) (Figure 3.7*B*), and the NMDA responses increased in 5 neurons in the presence of SKF-82958. D1 inhibition of the NMDA current was significantly reduced from 34.2 ± 12.3% (Figure 3.1*B*) to 1 ± 8.7 % ($p<0.05$) (Figure 3.7*C*). These results suggest tyrosine kinase activation is involved in D1 receptor inhibition of NMDA responses.

Surprisingly D1 receptor inhibition of NMDA receptor currents was not affected by another tyrosine kinase inhibitor, genistein (Figure 3.8A). In the presence of intracellular genistein (100 μM), SKF-82958 significantly reduced the NMDA receptor currents by 33.5 ± 3.6 % (NMDA: 348 ± 53 pA, SKF-82958 + NMDA: 231 ± 41 pA, $n = 6$, $p < 0.05$) (Figure 3.8B). Genistein is a less potent tyrosine kinase inhibitor than lavendustin A and may not have been able to compete effectively with intracellular ATP (1 mM) for its binding site.

Figure 3.7

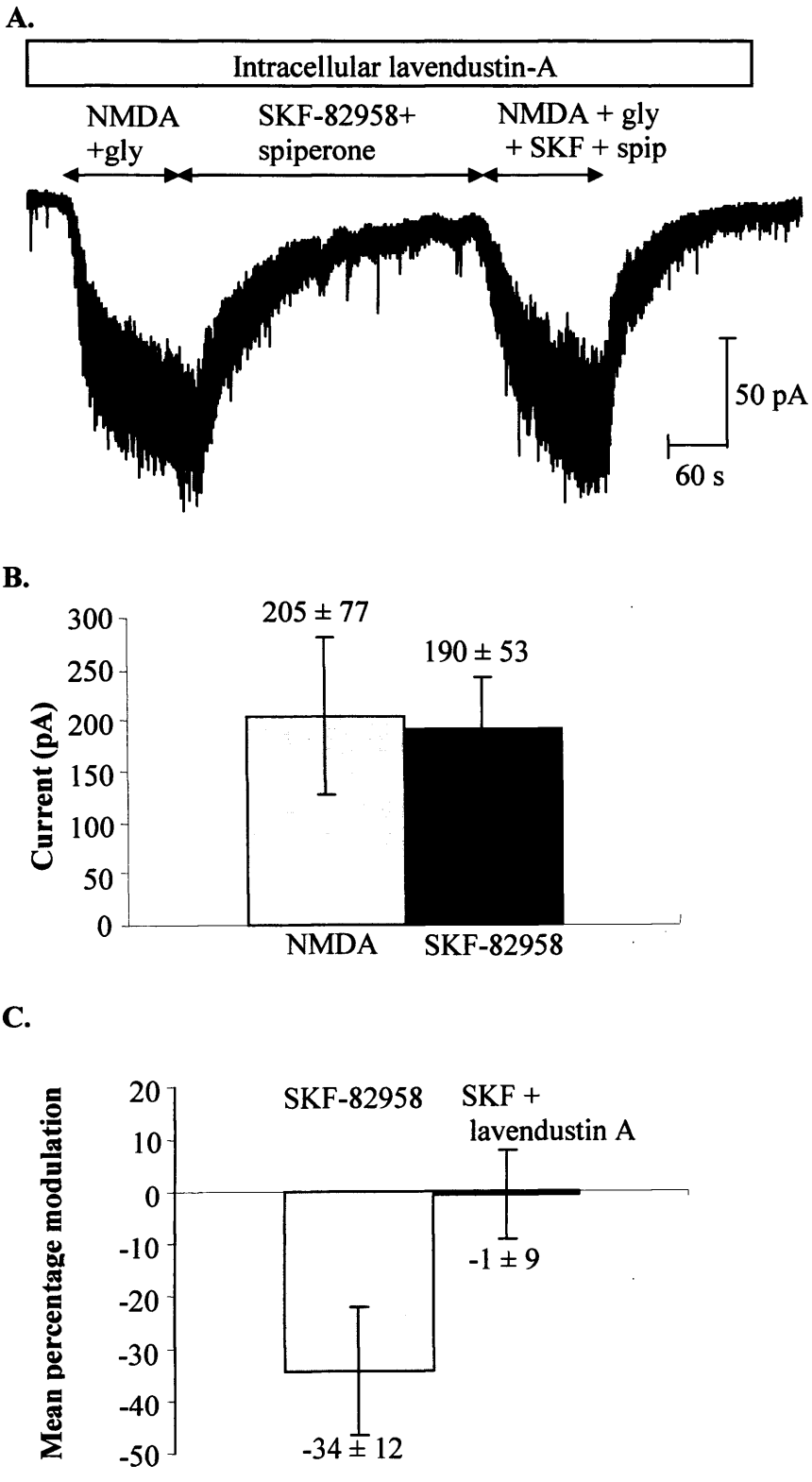
A.
Intracellular lavendustin-A
NMDA
+gly
SKF-82958+
spiperone
NMDA + gly
+ SKF + spip
50 pA
60 s
B.
205 ± 77
190 ± 53
Current (pA)
300
250
200
150
100
50
0
NMDA
SKF-82958
C.
Mean percentage modulation
20
10
0
-10
-20
-30
-40
-50
SKF-82958
SKF +
lavendustin A
-1 ± 9
-34 ± 12

Figure 3.7 D1 inhibition of NMDA responses is tyrosine kinase-dependent. A, whole cell current recording in the presence of intracellular lavendustin A (10 μM), ATP (1 mM) and GTP (1mM). NMDA (10 μM) and glycine (10 μM) were applied for 2 minutes, followed by 5 minutes SKF-82958 (20 nM) and spiperone (2 nM), and finally NMDA (10 μM), glycine (10 μM), SKF-82958 (20 nM) and spiperone (2 nM) for 2 minutes. The holding current was -5 pA prior to the control NMDA responses. **B,** The mean current (± SE) of the first NMDA response in the presence of intracellular lavendustin A (10 μM) compared to the second response in the presence of SKF-82958 and spiperone (n=14, $p>0.05$). **C,** mean percentage SKF-82958 inhibition (± SE) in experiments with only ATP and GTP in the pipette solution (Fig. 1*A*) compared to experiments in the presence of intracellular lavendustin A (unpaired t-test $p< 0.05$).

Cell number	I_{H1} (pA)	NMDA (pA)	I_{H2} (pA)	NMDA + SKF-82958 (pA)	% change	R_s (MΩ)	C_m (pF)
#1-24-11-04	-150	487.5	-200	300.0	-38.5	45.6	23.4
#2-24-11-04	-70	406.3	-130	350.0	-13.8	29.7	20.7
#3-24-11-04	-40	106.3	-52	68.8	-35.3	64.2	9.0
#1-25-11-04	-14	68.8	-40	75.0	9.1	43.8	11.1
#2-25-11-04	-25	75.0	-40	65.6	-12.5	33.9	18.2
#3-25-11-04	-5	96.9	-15	93.8	-3.2	27.9	10.8
#2-24-1-05_001a	-90	356.3	-83	306.3	-14.0	45.7	21.5
#3-24-1-05	-68	187.5	-65	125.0	-33.3	29.4	17.8
#1-25-1-05	-40	181.3	-110	281.3	55.2	29.8	34.0
#2-25-1-05	-200	181.3	-110	250.0	37.9	29.8	32.0
#3-25-1-05	-103	143.8	-90	181.3	26.1	38.2	15.0
#4-25-1-05	-40	125.0	-30	193.8	55.0	21.8	11.7
#1-27-1-05	-6	162.5	-50	118.8	-26.9	31.8	10.1
#3-28-1-05	-60	293.8	-120	250.0	-14.9	34.9	18.1
COUNT	14	14	14	14	14	14	14
MEAN	-65.1	205.1	-81.1	190.0	-0.7	36.2	18.1
SE	15.0	76.9	13.3	53.1	8.6	2.9	2.1

Table 3.8 Tyrosine kinases were involved in D1 inhibition of NMDA receptor activities. Lavendustin A (10 μM), an inhibitor of non-receptor tyrosine kinase, was applied in the pipette solution. Details of each whole cell recording from 14 neurons are illustrated, which include the holding currents (I_H), the steady state NMDA currents in the absence and in the presence of SKF-82958 and spiperone, the series resistance (R_s) and the capacitance (C_m) of each cell. Comparing the NMDA (10 μM) and glycine (10 μM) responses with NMDA, glycine, SKF-82958 (20 nM) and spiperone (2 nM) responses shows that in the presence of H-89, SKF-82958 did not produce a significant change in the NMDA responses ($p = 0.4$), and no significant difference was found between the holding currents prior (I_{H1}) and after (I_{H2}) the first NMDA responses ($p = 0.17$).

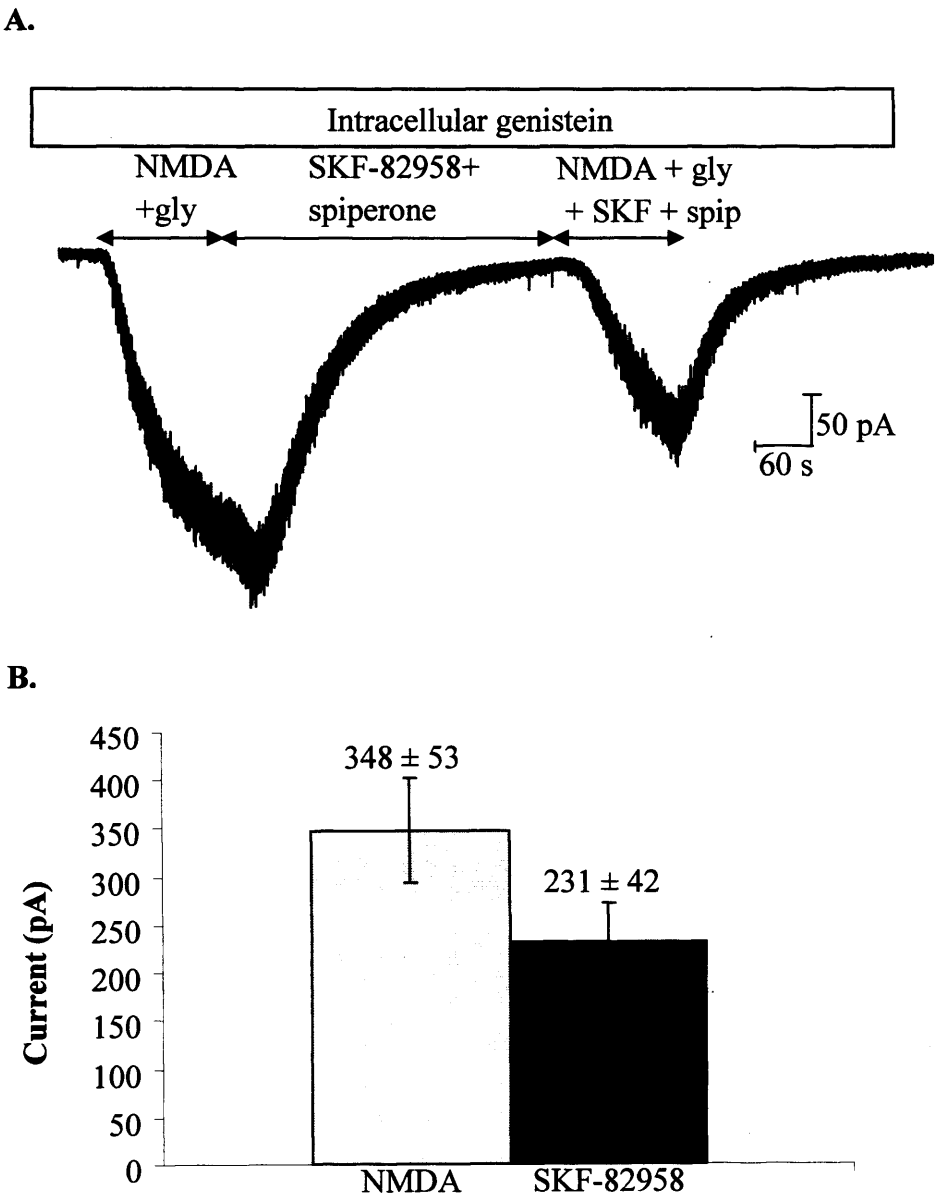

Figure 3.8 Intracellular genistein did not occlude D1 inhibition of NMDA receptor currents. A, whole cell current recording in the presence of intracellular geniestein (100 μM), ATP (1 mM) and GTP (1mM). NMDA (10 μM) and glycine (10 μM) were applied for 2 minutes, followed by 5 minutes SKF-82958 (20 nM) and spiperone (2 nM), and finally NMDA (10 μM), glycine (10 μM), SKF-82958 (20 nM) and spiperone (2 nM) for 2 minutes. The holding current was -55 pA prior to the control NMDA responses. **B,** The mean current (± SE) in the presence of intracellular genistein (100 μM) of the first NMDA response compared to the second response in the presence of SKF-82958 and spiperone (n=6, $p<0.05$).

Although both lavendustin A and genistein can inhibit the tyrosine protein kinase activity, they have been reported to be competitive inhibitors with respect to ATP (which has a K_A value of 2 μM for tyrosine kinases) (Akiyama et al., 1987; Onoda et al., 1989; Hsu et al., 1991). As ATP was always present in the pipette solution at a concentration of 1mM to maintain the energy level of the cell, the inhibitory capacity of both genistein and lavendustin A will be reduced. In this case the proportion of tyrosine kinase occupied by the tyrosine kinase inhibitor (P_{IR}) can be calculated with the Gaddum equation:

$$P_{IR} = \frac{[I]}{[I] + K_I\left(1 + \frac{[A]}{K_A}\right)}$$

Here, K_I and K_A are the dissociation equilibrium constants for tyrosine kinase binding of the tyrosine kinase inhibitor (lavendustin or genistein) and ATP respectively. K_I is 11 nM for lavendustin A and 2.6 μM for genistein. K_A is 2 μM for ATP. Therefore in the presence of 1 mM ATP, Lavendustin A (10 μM) is expected to occupy tyrosine kinases by 64.5%, and genistein 100μM will only occupy tyrosine kinases by 7%. Consequently the amount of lavendustin A in the experiment was sufficient to block the tyrosine kinase involved in D1 inhibition successfully, but the amount of genistein was inadequate.

In another 8 cells, I tested lavendustin B, an inactive analogue of lavendustin A. Intracellular lavendustin B (10 μM) did not affect the D1 inhibition induced by

SKF-82958 (NMDA: 370 ± 84 pA, SKF-82958 + NMDA: 221 ± 50 pA, n = 8, $p<0.05$) (Figure 3.9*A*). Intracellular lavendustin A did not significantly affect the size of control NMDA responses (control; 249 ± 36 pA, lavendustin A; 205 ± 77 pA, $p>0.05$) (Table 3.9) and the holding currents (control: -47 ± 7.1 pA, n = 32; lavendustin A: -65 ± 15 pA, n = 14, $p>0.05$). This experiment showed that lavendustin A probably blocked the D1 inhibition by its action on tyrosine kinase rather than some other action of lavendustin A.

In addition, lavendustin A was dissolved with 100 µl DMSO in 3.4 mM CsOH 900 µl, the same resulting concentration of DMSO and CsOH was applied in the pipette solution in a control experiment to test if DMSO and CsOH had any effect on D1 inhibition of NMDA receptor whole cell currents. There were 7 cells in this experiment. Under these conditions SKF-82958 significantly inhibited the NMDA second responses by 27.4 ± 8.4 % (NMDA: 395 ± 61 pA, SKF-82958 + NMDA: 287 ± 62 pA, $p<0.05$) (Figure 3.10). So neither DMSO nor CsOH affected the D1 inhibition.

3.2.4.2 Non-receptor tyrosine kinase inhibitor PP2

In order to specify the type of the tyrosine kinase that is involved in the D1 receptor modulation of NMDA receptors, a subtype-specific Src tyrosine kinase inhibitor was used. The Src family of protein tyrosine kinases is very likely to be involved because they have been reported to upregulate the activity of NMDA receptors by phosphorylation (Kohr and Seeburg., 1996; Zheng et al., 1998; Ali and Salter, 2001, Dunah et al., 2001, Dunnah et al 2004). Therefore, I decided to test if Src family

Figure 3.9

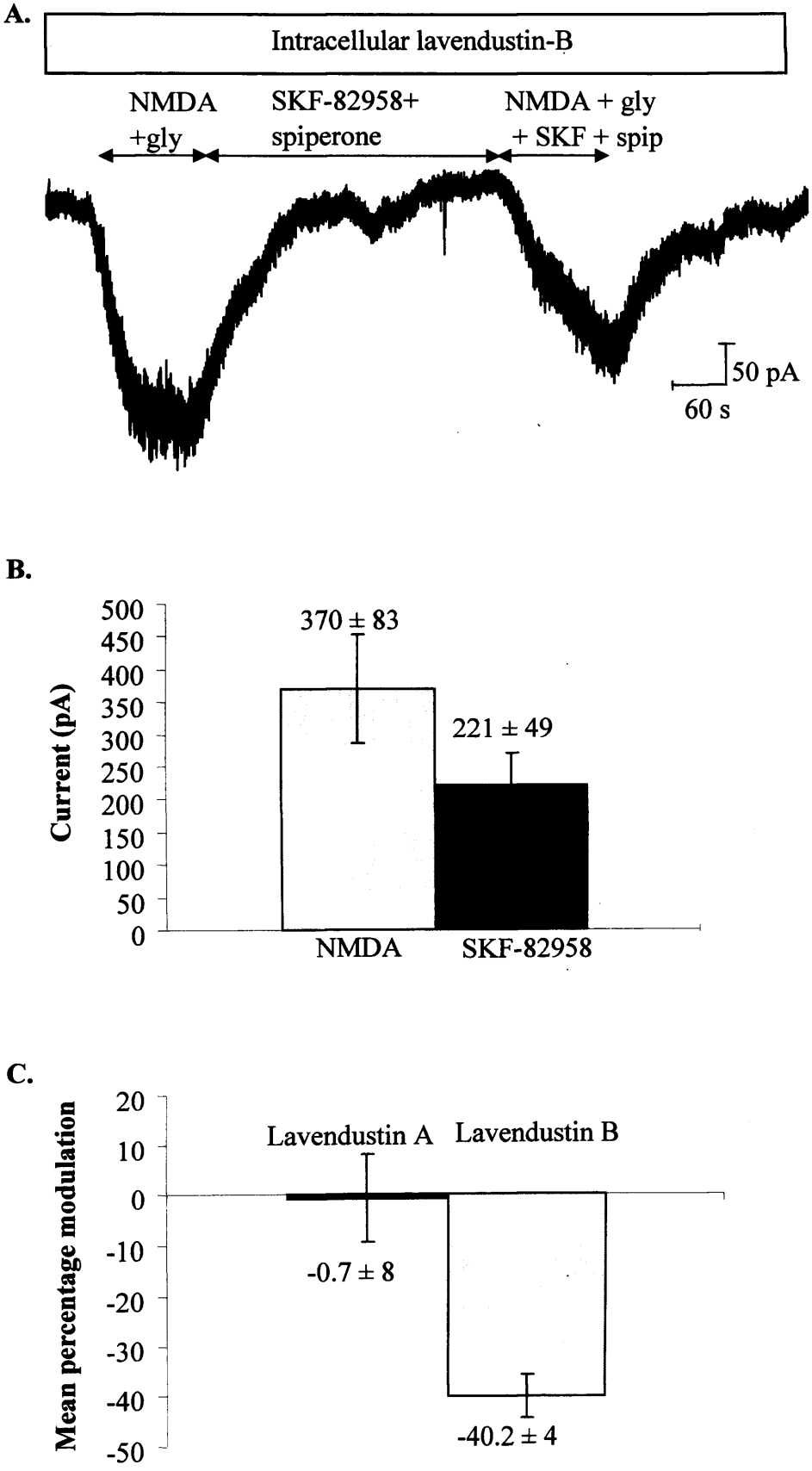
A.
Intracellular lavendustin-B
NMDA
+gly
SKF-82958+
spiperone
NMDA + gly
+ SKF + spip
50 pA
60 s
B.
Current (pA)
500
450
400
350
300
250
200
150
100
50
0
370 ± 83
221 ± 49
NMDA
SKF-82958
C.
Mean percentage modulation
20
10
0
-10
-20
-30
-40
-50
Lavendustin A
Lavendustin B
-0.7 ± 8
-40.2 ± 4

Figure 3.9 Lavendustin B, an inactive analogue of lavendustin A had no effect on D1 inhibition of NMDA receptor currents. A, whole cell current recording in the presence of intracellular lavendustin B (10 μM), ATP (1 mM) and GTP (1mM). NMDA (10 μM) and glycine (10 μM) were applied for 2 minutes, followed by 5 minutes SKF-82958 (20 nM) and spiperone (2 nM), and finally NMDA (10 μM), glycine (10 μM), SKF-82958 (20 nM) and spiperone (2 nM) for 2 minutes. The holding current was -67 pA prior to the control NMDA responses. **B,** The mean current (± SE) in the presence of intracellular lavendustin B (100 μM) of the first NMDA response compared to the second response in the presence of SKF-82958 and spiperone ($n = 8$, $p<0.05$). **C,** mean percentage SKF-82958 inhibition (± SE) in experiments with lavendustin A (Figure 3.7, $n = 14$) in the pipette solution compared to experiments in the presence of intracellular lavendustin B ($n = 8$, unpaired t-test $p< 0.05$).

cell number	Control NMDA response (pA)	Cell number	NMDA response in lavendustin A (pA)
04-02-05#4	725.00	#1-24-11-04	487.5
04-02-05#5	650.00	#2-24-11-04	406.3
10-02-05#1	156.25	#3-24-11-04	106.3
10-02-05#2	375.00	#1-25-11-04	68.8
10-02-05#6	300.00	#2-25-11-04	75.0
11-02-05#3	256.25	#3-25-11-04	96.9
11-02-05#5	400.00	#2-24-1-05_001a	356.3
22-05-2003#1	167	#3-24-1-05	187.5
22-05-2003#2	240	#1-25-1-05	181.3
22-05-2003#3	373	#2-25-1-05	181.3
22-05-2003#4	127	#3-25-1-05	143.8
22-05-2003#5	360	#4-25-1-05	125.0
22-05-2003#6	367	#1-27-1-05	162.5
22-05-2003#7	83.3	#3-28-1-05	293.8
27-5-03#1	127		
27-5-03#3	317		
27-5-03#4	327		
14-3-05#1b	231.3		
14-3-05#2b	231.3		
14-3-05#4	175.0		
14-3-05#5	150.0		
14-3-05#6	218.8		
15-3-05#1	175.0		
8-04-05#2	87.5		
8-04-05#3	75.0		
8-04-05#4	343.8		
8-04-05#5	46.9		
9-07-03#2	263		
10-07-03#1	181		
10-07-03#2	178		
10-07-03#3	219		
10-07-03#4	131		
Count	32		14
Mean	252		190.0
SE	27		53.1
	p =	0.30	

Table 3.9 Intracellular lavendustin A did not significantly affect the NMDA responses. The first NMDA responses from all the experiments where ATP and GTP were in the pipette solution (control) (n = 32) and the first NMDA response in the presence of intracellular lavendustin A (n = 14) (Table 3.9) are presented here. Both an unpaired t-test and a randomization test show that lavendustin A did not induce significant change in the NMDA responses (p = 0.30).

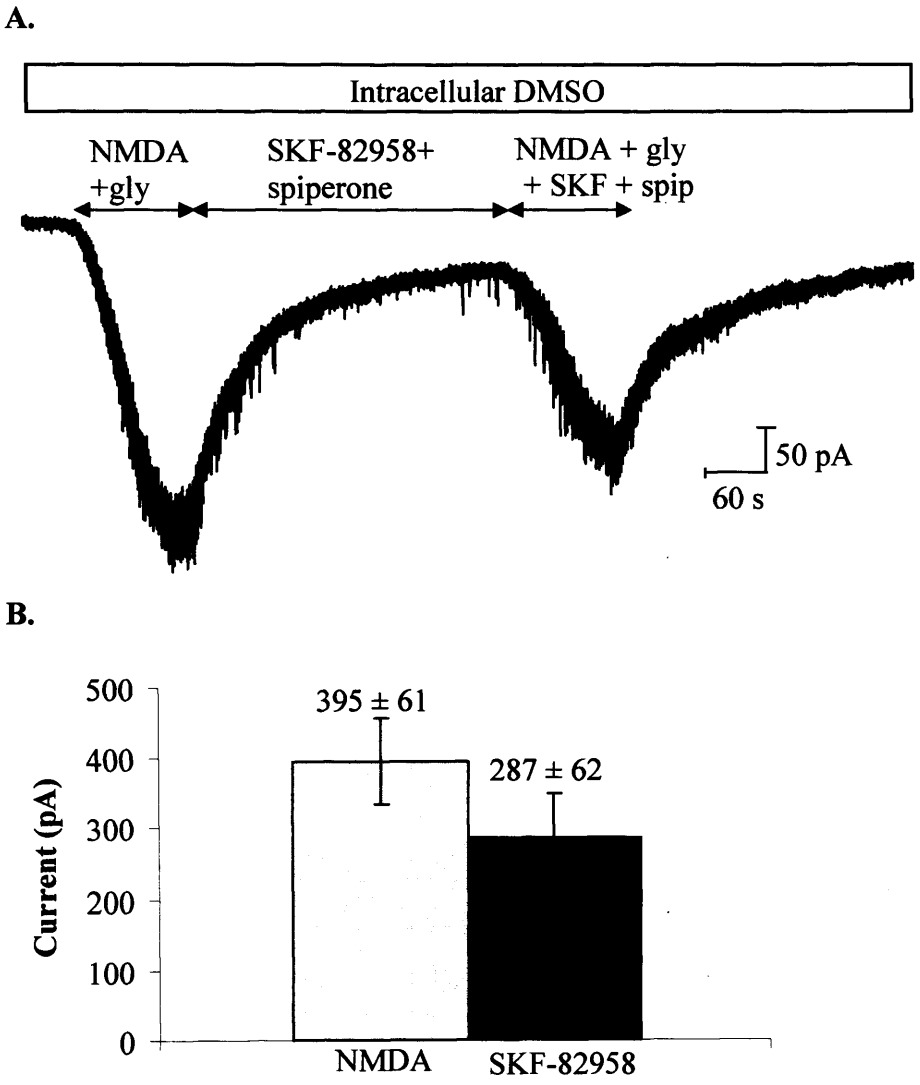

Figure 3.10 DMSO did not influence D1 inhibition of NMDA receptor currents. A. whole cell current recording in the presence of intracellular DMSO, ATP (1 mM) and GTP (1mM). NMDA (10 μM) and glycine (10 μM) were applied for 2 minutes, followed by 5 minutes SKF-82958 (20 nM) and spiperone (2 nM), and finally NMDA (10 μM), glycine (10 μM), SKF-82958 (20 nM) and spiperone (2 nM) for 2 minutes. The holding current was - 25 pA prior to the control NMDA responses. **B,** The mean current (± SE), in the presence of intracellular DMSO, of the first NMDA response is compared to the second response in the presence of SKF-82958 and spiperone ($n = 7$, $p<0.05$).

tyrosine kinases are involved in D1 inhibition. Thus inhibition of Src prior to SKF-82958 might be expected to occlude D1 inhibition.

PP2 is a potent Src family-selective tyrosine kinase inhibitor (Hanke et al., 1996) with a IC50 value of 4 to 5 nM, and 10 μM PP2 can block 80% of Src-family tyrosine kinase in the presence of 1 mM ATP. In the presence of intracellular PP2 (10 μM), SKF-82958 failed to decrease the NMDA responses significantly (NMDA: 282 ± 69 pA, SKF-82958 + NMDA: 262 ± 57 pA, $p>0.05$) (Figure 3.11, Table 3.10) and increased the NMDA response in 3 neurons. The D1 inhibition was reduced from 34.2 ± 12.3% (Figure 3.1*B*) to 1 ± 8.2 % ($P<0.05$) (Figure 3.11*C*). PP2 did not affect the holding currents (control: -47 ± 7.1 pA, n = 32; PP2: -46 ± 15 pA, n = 9, $p>0.05$). These results suggest that Src family non-receptor tyrosine kinases play an important role in D1 receptor inhibition of NMDA responses.

As tyrosine kinases have been shown to be involved in NMDA receptor distribution (Dunah et al., 2001, Dunah et al., 2004), I suspected there might be a change of NMDA receptor trafficking underlying this D1 inhibition.

3.2.5 Intracellular dynamin inhibitory peptide abolished D1 inhibition.

Dynamin plays an essential role in clathrin mediated endocytosis (Schimid, 1997) which has been shown to mediate endocytosis of $GABA_A$ receptors (Kittler et al., 2000), AMPA receptors (Carroll et al., 1999) and NMDA receptors (Nong et al., 2003). Here, intracellular dynamin inhibitory peptide (QVPSRPNRAP, 50 μM) was applied to prevent receptor endocytosis (Figure 3.12*A*) to investigate if NMDA receptor endocytosis is involved in D1 inhibition.

Figure 3.11

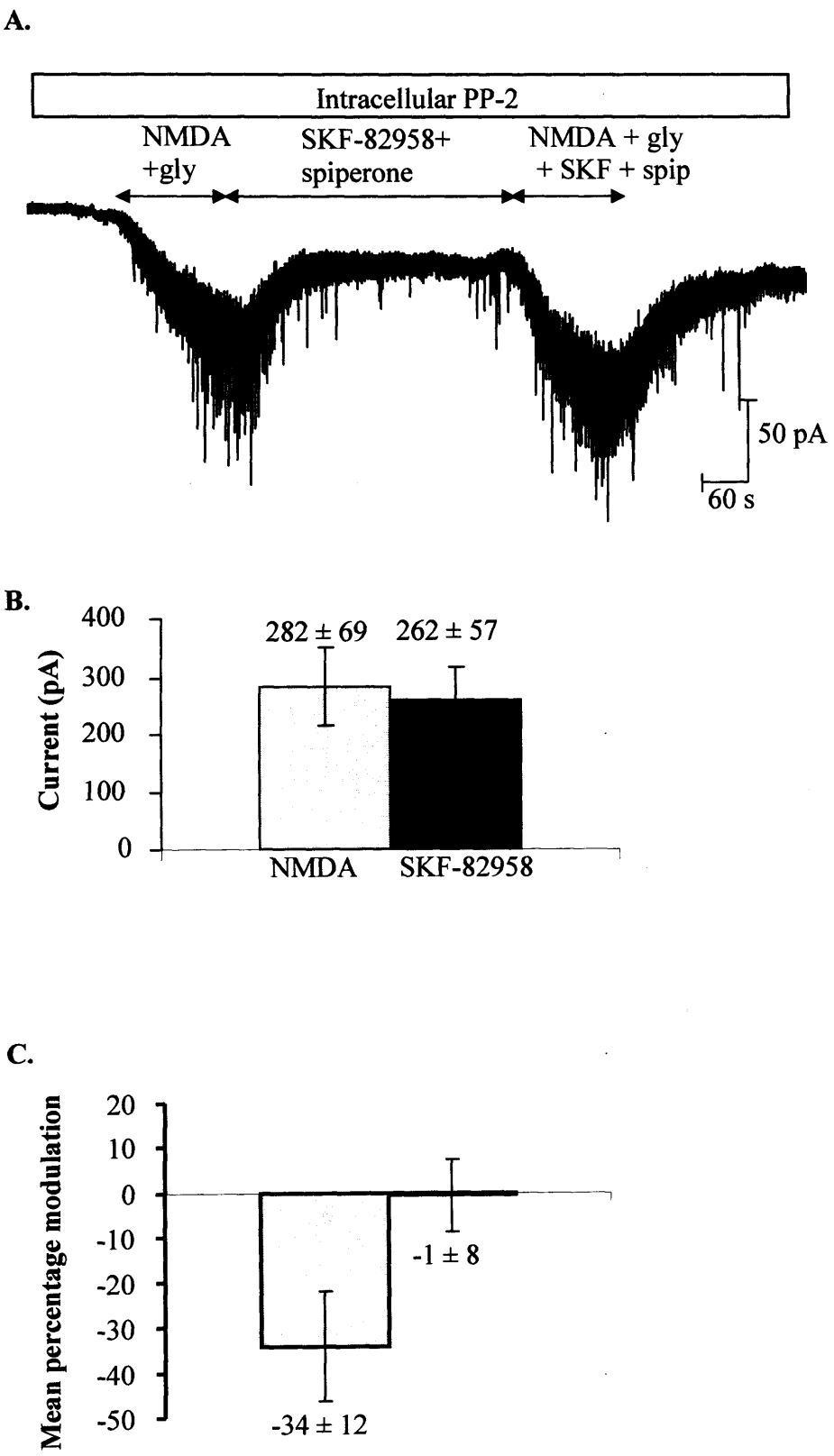
A.
Intracellular PP-2
NMDA
+gly
SKF-82958+
spiperone
NMDA + gly
+ SKF + spip
50 pA
60 s
B.
Current (pA)
400
300
200
100
0
282 ± 69
262 ± 57
NMDA
SKF-82958
C.
Mean percentage modulation
20
10
0
-10
-20
-30
-40
-50
-1 ± 8
-34 ± 12

Figure 3.11 PP2, a Src family-selective tyrosine kinase inhibitor, blocked D1 inhibition of NMDA responses. A, whole cell current recording in the presence of intracellular PP2 (10 μM), ATP (1 mM) and GTP (1mM). NMDA (10 μM) and glycine (10 μM) were applied for 2 minutes, followed by 5 minutes SKF-82958 (20 nM) and spiperone (2 nM), and finally NMDA (10 μM), glycine (10 μM), SKF-82958 (20 nM) and spiperone (2 nM) for 2 minutes. The holding current was -13 pA prior to the control NMDA responses. **B,** The mean current (± SE) in the presence of intracellular PP2 (10 μM) of the first NMDA response compared to the second response in the presence of SKF-82958 and spiperone (n = 9, $p>0.05$). **C,** mean percent SKF-82958 inhibition (± SE) in experiments with only ATP and GTP in the pipette solution (Fig. 1*A*) compared to experiments in the presence of intracellular PP2 (unpaired t-test $p< 0.05$).

Cell number	I_{H1} (pA)	NMDA (pA)	I_{H2} (pA)	NMDA + SKF-82958 (pA)	% change	R_s (MΩ)	C_m (pF)
16-11-05#3	-30	362.5	-100	250.0	-31.0	19.7	37.9
16-11-05#4	-40	225.0	-140	281.3	25.0	46.2	24.6
16-11-05#5	-7	193.8	-70	143.8	-25.8	35.4	14.4
16-11-05#6	-13	71.9	-40	68.8	-4.3	24.9	17.6
16-11-05#7	-60	145.0	-140	143.8	-0.9	19.3	33.4
17-11-05#2	-50	487.5	-235	462.5	-5.1	47.9	25.9
17-11-05#3	-160	712.5	-249	600.0	-15.8	26.1	45.9
17-11-05#7	-40	106.3	-70	156.3	47.1	38.2	17.8
17-11-05#9	-17	237.5	-70	250.0	5.3	40.8	20.4
Count	9.0	9.0	9.0	9.0	9.0	9.0	9.0
Mean	-46.3	282.4	-134.9	261.8	-0.6	33.2	26.4
SE	15.4	68.8	28.1	56.7	8.2	3.7	3.5

Table 3.10 Intracellular of the Src family-selective inhibitor, PP2 (10 μM) abolished SKF-82958 induced NMDA receptor current inhibition. Details of each whole cell recording from 9 neurons are illustrated, which include the holding currents (I_H), the steady state NMDA currents in the absence and in the presence of SKF-82958 and spiperone, the series resistance (R_s) and the capacitance (C_m) of each cell. Comparing the NMDA (10 μM) and glycine (10 μM) responses with NMDA, glycine, SKF-82958 (20 nM) and spiperone (2 nM) responses shows that, in the presence of PP2, SKF-82958 failed to produce a significant change in the NMDA responses ($p = 0.3$). The holding current prior to the NMDA response in the presence of SKF-82958 (I_{H2}) is not significantly greater than prior to the control NMDA response (I_{H1}) ($p = 0.02$)

D1 inhibition of NMDA responses was effectively blocked by intracellular dynamin inhibitory peptide. There was no significant difference between the mean current of NMDA responses in the absence and in the presence of SKF-82958 (NMDA: 425 ± 89 pA, NMDA + SKF-82958: 409 ± 76 pA, n= 9, p> 0.05) (Figure 3.12*B*, Table 3.11), and the NMDA responses in the presence of SKF-82958 increased in 4 neurons. The average percentage inhibition decreased from 34.3 ± 12.3% (Figure 3.1*B*) to -1.1 ± 8.2 % (Figure 3.12*C*). These results suggested an essential role of dynamin in D1 inhibition of NMDA receptor whole cell currents.

In the presence of dynamin inhibitory peptide, NMDA responses were significantly increased compared to all other control NMDA responses where only ATP and GTP was present in the pipette solution. Control currents averaged 251 ± 27 pA (n = 32) and dynamin control currents averaged 497 ± 62 pA (n = 18) (Figure 3.13C, Table 3.12). However dynamin inhibitory peptide did not affect the holding currents (Control: -47 ± 7 pA, n = 32; Dynamin inhibitory peptide:-32 ± 6, n = 18, p>0.05). In nine dynamin control experiments where two successive NMDA responses were evoked in cells dialysed with dynamin inhibitory peptide, without application of SKF-82958 (Figure 3.12A, there was no significant difference between the first and second NMDA responses (first response 569 ± 86pA; second response: 526 ± 93pA) (Figure 3.13B) suggesting dynamin independent processes involving the NMDA receptors (that result in an approximately 2-fold increase in current size) had reached a steady-state within the first few minutes of whole-cell recording. If we assume that dynamin-dependent receptor internalization is the dominant NMDA receptor internalization mechanism, these results suggest that approximately 50% of NMDA receptors are located on the cell surface at any one time. Furthermore, since the

Figure 3.12

A.

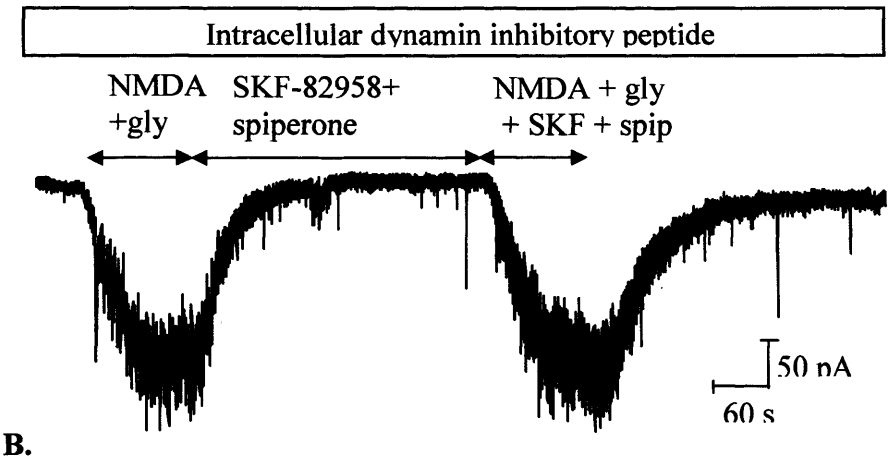

B.

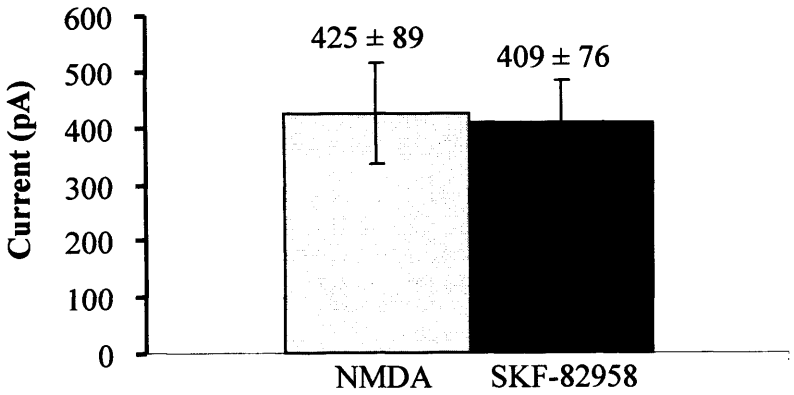

C.

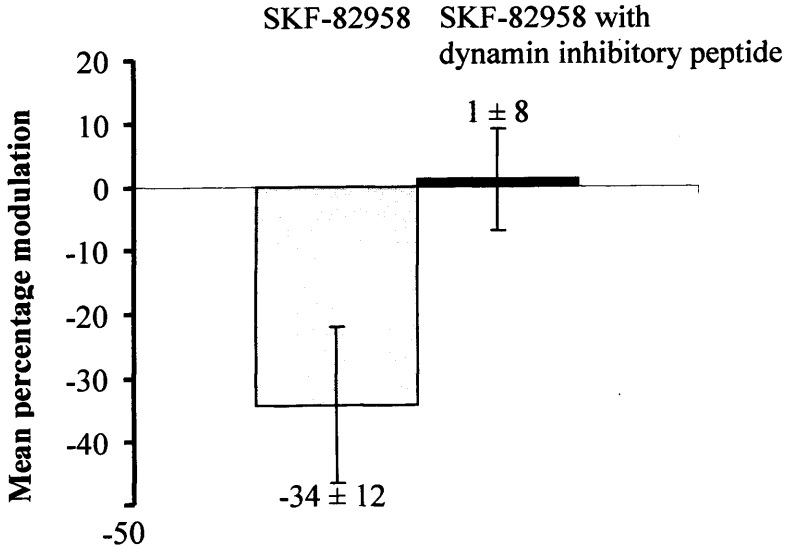

Figure 3.12 Intracellular dynamin inhibitory peptide (50 μM) abolishes D1 inhibition of whole cell NMDA receptor currents. A, Response to NMDA (10 μM) and glycine (10 μM) applied for 2 minutes, followed by 5 mins SKF-82958 (20 nM) and spiperone (2 nM), and finally NMDA (10 μM), glycine (10 μM), SKF-82958 (20 nM) and spiperone (2 nM) for 2 minutes. The holding current was - 30 pA prior to the control NMDA responses. **B,** Mean current (± SE) in the presence of dynamin inhibitory peptide of the first NMDA response compared to the second response in the presence of SKF-82958 and spiperone ($n = 9$, $p > 0.05$). **C,** mean percent SKF-82958 inhibition (± SE) in the experiments with only ATP and GTP in the pipette solution (Figure 3.1) compared to the experiments in the presence of intracellular dynamin inhibitory peptide (unpaired t-test $p< 0.05$).

Cell number	I_{H1} (pA)	NMDA (pA)	I_{H2} (pA)	NMDA + SKF-82958 (pA)	% change	R_s (MΩ)	C_m (pF)
16-06-05#2	-60	378	-70	577.8	52.9	24.3	24.7
16-06-05#3	-60	1000	-470	861	-13.9	21.3	41.8
16-06-05#4	-20	450	-90	411	-8.6	22.7	22.8
16-06-05#5	-12	257	-180	322.2	25.6	43.0	14.00
17-06-05#1	-30	233	-28	233	0.0	42.0	10.3
17-06-05#3	-40	522	-70	433	-17.0	29.4	11.2
17-06-05#4	-12	77.8	-25	83	7.1	36.3	11.3
17-06-05#6b	-40	322	-40	244.4	-24.1	28.6	12.6
17-06-05#7	-15	589	-50	517	-12.3	32.4	15.8
Count	9	9	9	9	9	9	9
Mean	-32.1	425	-113.7	409	-3.8	31.1	18.3
SE	6.4	88.7	47.2	76.1	8.2	2.7	3.4

Table 3.11 Intracellular dynamin inhibitory peptide (50 μM) blocked NMDA receptor current inhibtion induced by SKF-82958. Details of each whole cell recording from 9 neurons are illustrated, which include the holding currents (I_H), the steady state NMDA currents in the absence and in the presence of SKF-82958 and spiperone, the series resistance (R_s) and the capacitance (C_m) of each cell. Comparing the NMDA (10 μM) and glycine (10 μM) responses with NMDA, glycine, SKF-82958 (20 nM) and spiperone (2 nM) responses shows that, in the presence of dynamin inhibitory peptide, SKF-82958 failed to produce significant changes in the NMDA responses ($p = 0.1$). There is no significant difference between the holding currents prior to the NMDA response in the presence of SKF-82958 (I_{H2}) and the holding currents prior to the control NMDA response (I_{H1}) ($p = 0.11$)

Figure 3.13

A.

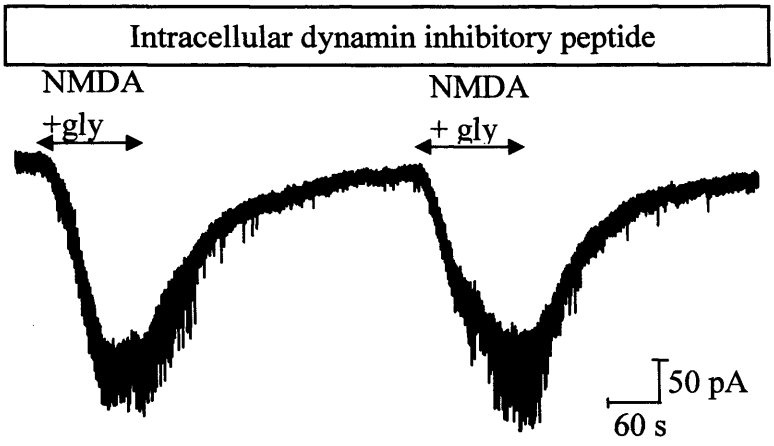

B.

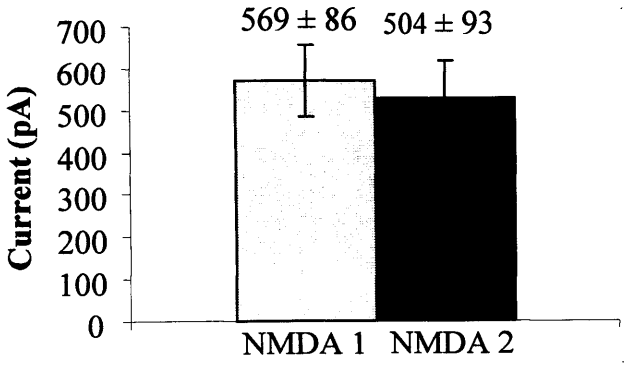

C.

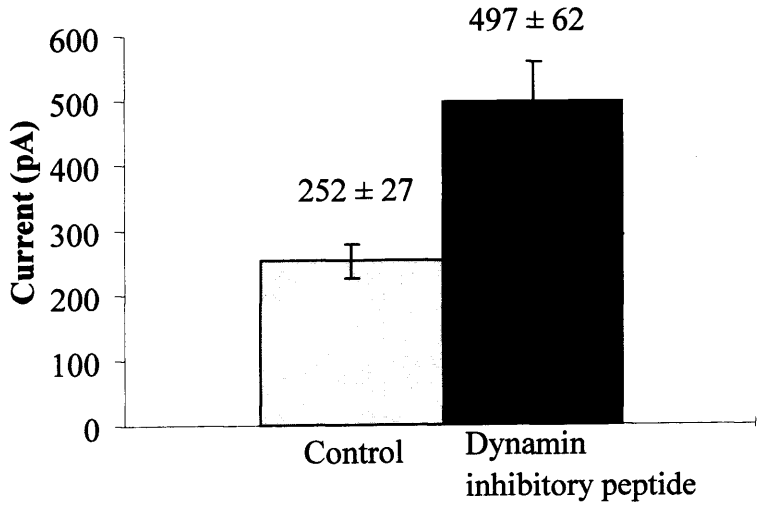

Figure 3.13 Intracellular dynamin inhibitory peptide control experiments. A, The two consecutive NMDA responses in the presence of intracellular dynamin inhibitory peptide (50 μM), ATP (1 mM) and GTP (1mM). NMDA (10 μM) and glycine (10 μM) were applied for 2 minutes, followed by 5 minutes of control recording solution, and finally NMDA (10 μM), glycine (10 μM) for 2 minutes. The holding current was -110 pA prior to the control NMDA responses. **B,** The mean current (± SE) of the first NMDA response compared to the second NMDA response ($n = 9$, $P > 0.05$). **C,** The mean current of the first NMDA response from all experiments where dynamin inhibitory peptide was present ($n = 18$) compared to the first NMDA response (control) averaged from all the experiments where only ATP and GTP were in the pipette solution ($n = 32$, $p < 0.05$).

cell number	Control NMDA response (pA)	Cell number	NMDA response in dynamin inhibitory peptide (pA)
04-02-05#4	725.00	16-06-05#2	378
04-02-05#5	650.00	16-06-05#3	1000
10-02-05#1	156.25	16-06-05#4	450
10-02-05#2	375.00	16-06-05#5	257
10-02-05#6	300.00	17-06-05#1	233
11-02-05#3	256.25	17-06-05#3	522
11-02-05#5	400.00	17-06-05#4	77.8
22-05-2003#1	167	17-06-05#6b	322
22-05-2003#2	240	17-06-05#7	589
22-05-2003#3	373	22-06-05#1b	344
22-05-2003#4	127	22-06-05#4	678
22-05-2003#5	360	22-06-05#5	300
22-05-2003#6	367	24-06-05#1	239
22-05-2003#7	83.3	24-06-05#2	789
27-5-03#1	127	24-06-05#3	450
27-5-03#3	317	24-06-05#4	972.2
27-5-03#4	327	24-06-05#5	522
14-3-05#1b	231.3	24-06-05#6	822
14-3-05#2b	231.3		
14-3-05#4	175.0		
14-3-05#5	150.0		
14-3-05#6	218.8		
15-3-05#1	175.0		
8-04-05#2	87.5		
8-04-05#3	75.0		
8-04-05#4	343.8		
8-04-05#5	46.9		
9-07-03#2	263		
10-07-03#1	181		
10-07-03#2	178		
10-07-03#3	219		
10-07-03#4	131		
Count Mean SE	32 252 27		18 497 62
	p =	0.002	

Table 3.12 Intracellular dynamin inhibitory peptide significantly enhanced the NMDA responses. Details of the first NMDA responses from all experiments with ATP and GTP in the pipette solution (control) (n = 32) and the first NMDA response in the presence of intracellular dynamin inhibitory peptide (n = 18) are presented here. Both unpaired t-test and a randomization test show that the first NMDA responses in the presence of dynamin inhibitory peptide were remarkably increased when compared with the control NMDA responses (p = 0.002).

NMDA current in the presence of dynamin inhibition was stable within 5 minutes of beginning whole-cell recording, these results suggest an estimate of the lifetime of a surface receptor of around 1.0 minute (given exponential processes normally require around 5 time constants for establishment of a new steady-state).

The NMDA whole cell current may be described by the equation:

$$I_{NMDA} = N \cdot P_{open} \cdot i$$

Where N is receptor number, P_{open} is receptor open probability and i is single channel amplitude. At -60 mV, weighted mean single channel current was 2.12pA (chapter 4). The receptor open probability in these experiments can be estimated from the receptor agonist occupancy P_{AR} (assuming an EC_{50} for NMDA of 20 μM) and a maximal single channel open probability of 0.2 (Gibb & Colquhoun, 1992; Rycroft & Gibb, 2002), so $P_{open} = 0.067$. Then our average control response of 250 pA at -60 mV corresponds to a total of 1750 NMDA receptors on the cell surface and this increases to 3500 receptors in the presence of the dynamin inhibitory peptide.

In another control experiment, a myristoylated scrambled dynamin inhibitory peptide was applied intracellularly in 9 neurons to test if the D1 inhibition was dependent on the structure of the dynamin inhibitory peptide used in the earlier experiments rather than receptor endocytosis. In the presence of the scrambled dynamin inhibitory peptide, SKF-82958 significantly reduced the mean NMDA responses by 25 ± 4% (NMDA: 168 ± 31 pA, SKF-82958 + NMDA: 127 ± 27 pA, n = 9, $p<0.5$) (Figure 3.14, Table 3.13), and there was no significant difference when comparing the first NMDA responses (control) in this experiment with the control NMDA responses where only ATP and GTP were in the

Figure 3.14

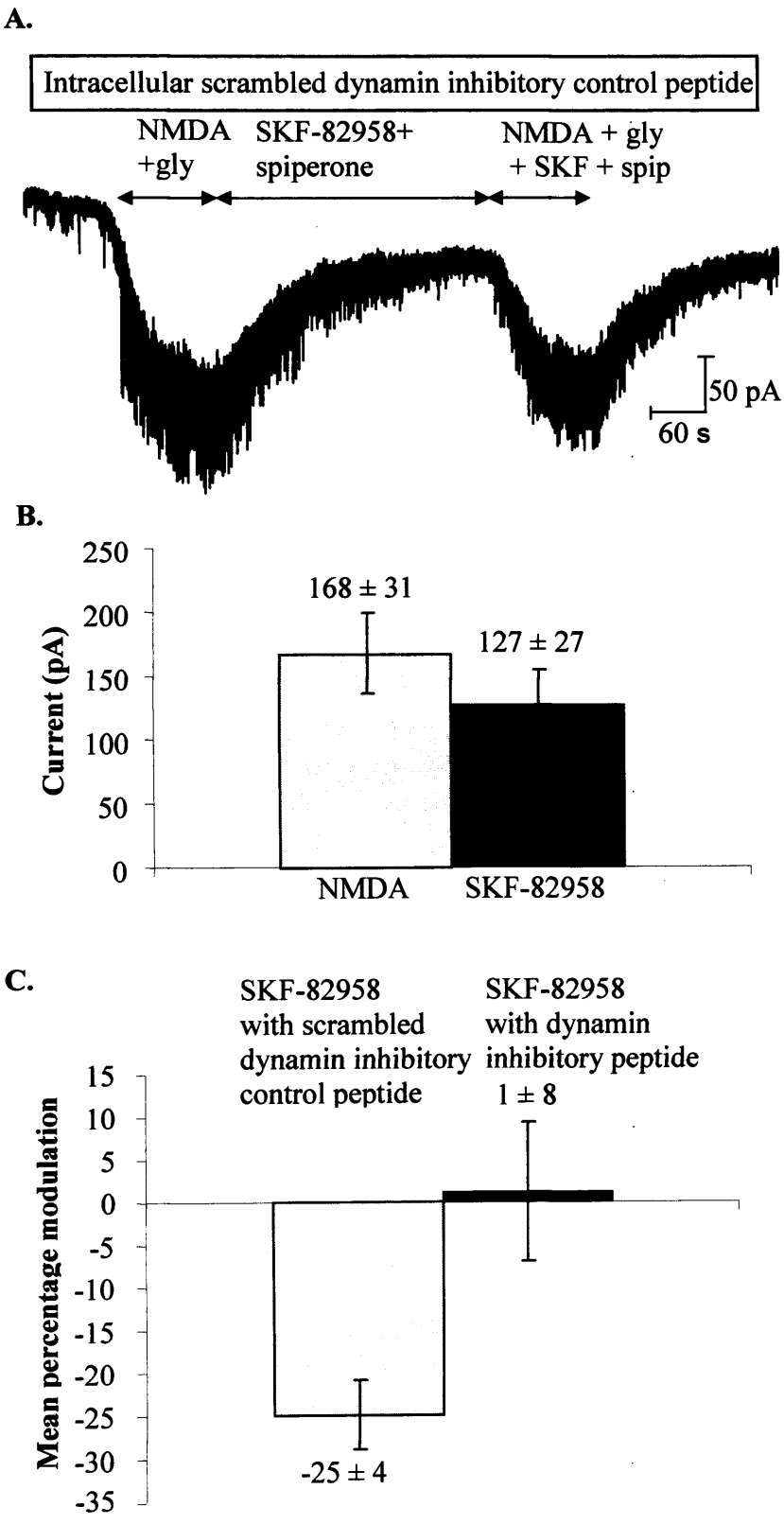
A.
Intracellular scrambled dynamin inhibitory control peptide
NMDA +gly
SKF-82958+ spiperone
NMDA + gly + SKF + spip
50 pA
60 s
B.
Current (pA)
250
200
150
100
50
0
168 ± 31
127 ± 27
NMDA
SKF-82958
C.
SKF-82958 with scrambled dynamin inhibitory control peptide
SKF-82958 with dynamin inhibitory peptide
Mean percentage modulation
15
10
5
0
-5
-10
-15
-20
-25
-30
-35
1 ± 8
-25 ± 4

Figure 3.14 Intracellular myristoylated scrambled dynamin inhibitory peptide (50 μM) did not affect SKF-82958 induced D1 inhibition of NMDA responses. A, Response to NMDA (10 μM) and glycine (10 μM) applied for 2 minutes, followed by 5 mins SKF-82958 (20 nM) and spiperone (2 nM), and finally NMDA (10 μM), glycine (10 μM), SKF-82958 (20 nM) and spiperone (2 nM) for 2 minutes. The holding current was -40 pA prior to the control NMDA responses. **B,** Mean current (± SE) in the presence of myristoylated dynamin inhibitory peptide of the first NMDA response compared to the second response in the presence of SKF-82958 and spiperone ($n = 8$, $p < 0.05$). **C,** mean percent SKF-82958 inhibition (± SE) in the experiments with dynamin inhibitory peptide in the pipette solution (Figure 3.18) compared to the experiments in the presence of intracellular myristoylated scrambled dynamin inhibitory peptide (unpaired t-test $p< 0.05$).

Cell number	I_{H1} (pA)	NMDA (pA)	I_{H2} (pA)	NMDA + SKF-82958 (pA)	% change	R_s (MΩ)	C_m (pF)
21-11-05#3	-30	350.0	-70	237.5	-32.1	18.7	17.0
21-11-05#5	-10	37.5	-10	31.3	-16.7	63.9	5.2
21-11-05#7	-250	200.0	-400	168.8	-15.6	30.0	18.0
21-11-05#8	-13	171.0	-35	131.3	-23.2	12.0	13.4
21-11-05#9	-14	150.0	-60	93.8	-37.5	29.1	13.7
22-11-05#1	-40	50.0	-46	31.3	-37.5	39.6	10.1
22-11-05#2	-66	231.3	-85	218.8	-5.4	13.7	21.7
22-11-05#4	-40	187.5	-80	131.3	-30.0	12.8	15.6
22-11-05#5	-50	134.4	-80	100.0	-25.6	25.6	15.8
count	9.0	9.0	9.0	9.0	9.0	9.0	9.0
Mean	-57.0	168.0	-96.2	127.1	-24.9	27.3	14.5
SE	24.9	31.4	38.8	27.3	4.1	6.3	1.8

Table 3.13 Myristoylated scrambled dynamin inhibitory peptide, did not affect D1 inhibition of NMDA receptor currents. Details of each whole cell recording from ten neurons are shown, which include the holding currents (I_H), the steady state NMDA currents in the absence and in the presence of SKF-82958 and spiperone, the series resistance (R_s) and the capacitance (C_m) of each cell. Comparison of the two NMDA responses with intracellular scrambled inhibitory dynamin peptide (50 μM) shows that in the presence of SKF-82958 and spiperone the NMDA responses were significantly smaller ($p = 0.021$) by both paired t-test and randomization test. The holding current prior to the NMDA response in the presence of SKF-82958 (I_{H2}) is significantly greater than prior to the control NMDA response (I_{H1}) ($p = 0.03$)

Table 3.14

cell number	Control NMDA response (pA)	Cell number	NMDA response in myristoylated dynamin inhibitory peptide (pA)
04-02-05#4	725.00	21-11-05#3	350.0
04-02-05#5	650.00	21-11-05#5	37.5
10-02-05#1	156.25	21-11-05#7	200.0
10-02-05#2	375.00	21-11-05#8	171.0
10-02-05#6	300.00	21-11-05#9	150.0
11-02-05#3	256.25	22-11-05#1	50.0
11-02-05#5	400.00	22-11-05#2	231.3
22-05-2003#1	167	22-11-05#4	187.5
22-05-2003#2	240	22-11-05#5	134.4
22-05-2003#3	373		
22-05-2003#4	127		
22-05-2003#5	360		
22-05-2003#6	367		
22-05-2003#7	83.3		
27-5-03#1	127		
27-5-03#3	317		
27-5-03#4	327		
14-3-05#1b	231.3		
14-3-05#2b	231.3		
14-3-05#4	175.0		
14-3-05#5	150.0		
14-3-05#6	218.8		
15-3-05#1	175.0		
8-04-05#2	87.5		
8-04-05#3	75.0		
8-04-05#4	343.8		
8-04-05#5	46.9		
9-07-03#2	263		
10-07-03#1	181		
10-07-03#2	178		
10-07-03#3	219		
10-07-03#4	131		
Count Mean SE	32 252 27 p =	 0.06	9 168 31.4

Table 3.14 Intracellular myristoylated scrambled dynamin inhibitory peptide did not significantly affect the NMDA responses although there was a clear tendency for the response to decrease. The first NMDA responses from all the experiments where ATP and GTP were in the pipette solution (control) (n = 32) and the first NMDA response in the presence of intracellular myristoylated dynamin inhibitory peptide (Table 3.14) are presented here. Both unpaired t-test and a randomization test show that myristoylated scrambled dynamin inhibitory peptide did not induce a significant change in NMDA response.

pipette solution (Table 3.14). However, there is great contrast between the control NMDA responses in the presence of myristoylated dynamin inhibitory peptide (168 ± 31 pA) and in the presence of dynamin inhibitory peptide (497 ± 62, n = 18,) (p = 0.0001). Therefore these results demonstrated that the structure of the dynamin inhibitory peptide was not involved in the D1 modulation of NMDA receptors.

3.2.6 In 3 week old rats D1 receptor activation did not significantly reduce the NMDA receptor currents in striatal medium spiny neurons.

Considering most experiments showing that D1 receptor activation enhances the NMDA receptor responses, have been made in adult rat (Blank et al., 1997; Cepeda et al., 1998a; Flores-Hernandez et al., 2002), it is likely that D1 receptor modulation of NMDA receptors changes with development. Therefore, I tested D1 modulation in 9 neurons in 3-week old rats using the same procedures as in 7-day old rats.

Figure 3.15 shows that the D1 receptor agonist, SKF-82958, did not decrease the NMDA whole-cell current in 3 week old rats. Figure 3.15*A* illustrates a current trace from a whole-cell recording in these experiments. Figure 3.15*B* shows the comparison of the mean maximum currents, averaged from the 9 neurons in this experiment between the NMDA responses in the absence and in the presence of SKF-82958 and spiperone. D1 receptor activation decreased NMDA receptor currents in 6 neurons and increased NMDA receptor currents in 3 neurons (Table.3.15). The results indicated that dopamine D1 receptor activation had inconsistent effects on the NMDA receptor whole-cell currents in striatal medium spiny neruons in 3 week-old rats.

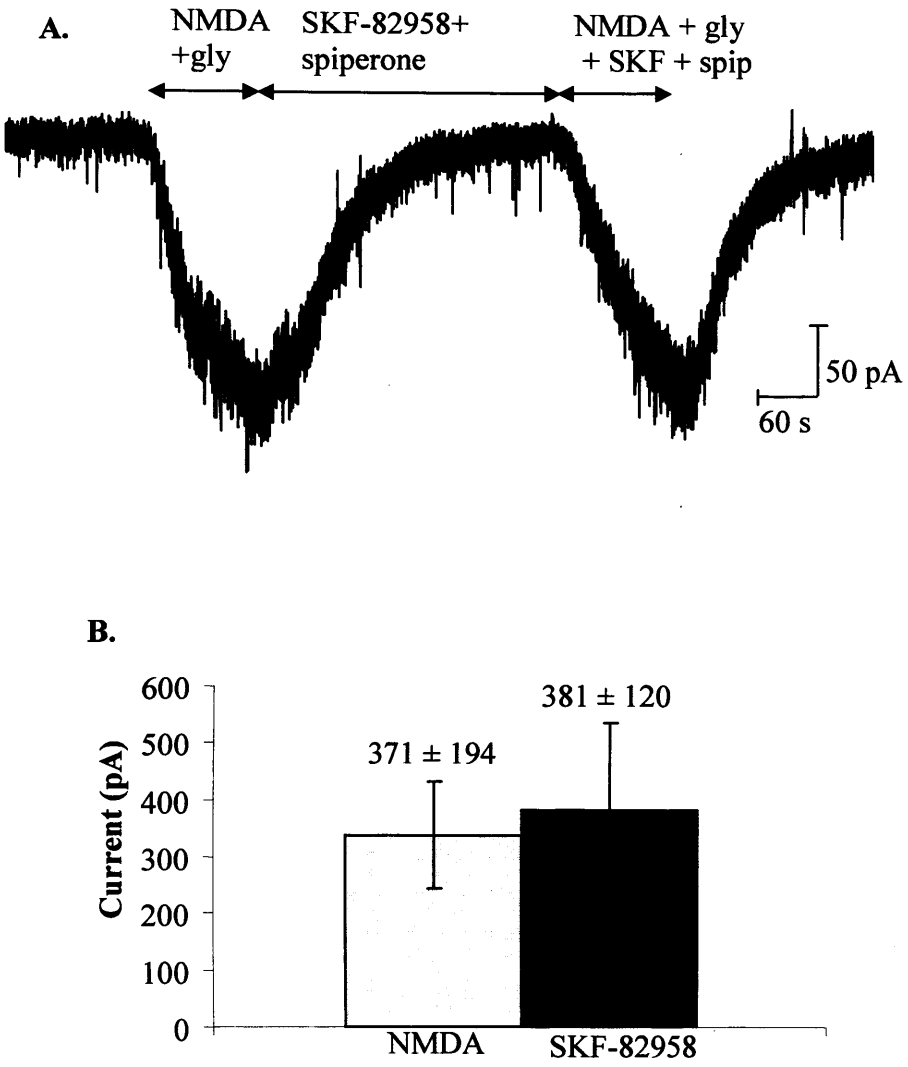

Figure 3.15 D1 receptor activation had inconsistent effects on the whole cell NMDA receptor currents recorded from 3 week-old rat striatal neurons. A, Response to NMDA (10 μM) and glycine (10 μM) applied for 2 minutes, followed by 5 mins SKF-82958 (20 nM) and spiperone (2 nM), and finally NMDA (10 μM), glycine (10 μM), SKF-82958 (20 nM) and spiperone (2 nM) for 2 minutes. The holding current was -40 pA prior to the control NMDA responses. **B**, Mean current (± SE) of the first NMDA response compared to the second response in the presence of SKF-82958 and spiperone ($n = 9$, $p > 0.05$).

Cell number	I_{H1} (pA)	NMDA (pA)	I_{H2} (pA)	NMDA + SKF-82958 (pA)	% change	R_s (MΩ)	C_m (pF)
11-05-05#1c	-40	182.1	-60	178.6	-2.0	50.3	12.70
16-05-05#1	-90	478.6	-100	1178.6	146.3	43.6	41.40
16-05-05#2	-40	385.7	-140	342.9	-11.1	45	30.40
18-05-05#1	-60	121.4	-35	92.9	-23.5	56.41	13.54
18-05-05#2b	-260	225.0	-200	82.1	-63.5	36	15.00
20-05-05#1	-200	346.4	-140	250.0	-27.8	24.6	42.90
23-05-05#3	-180	858.8	-340	752.9	-12.3	25	29.10
1-06-05#1	-80	339.3	-95	359.3	5.9	41.0	18.0
1-06-05#2	-10	103.6	-20	196.4	89.6	27.0	22.6
Count	9	9	9	9	9	9	9
Mean	-106.7	337.9	-125.6	381.5	11.37	38.8	25.1
SE	28.6	93.8	32.7	120.2	25.4	4.6	4.9

Table 3.15 D1 receptor activation did not affect whole-cell NMDA receptor currents in striatal neurons from 3 week old rats. Details of each whole cell recording from 9 neurons are illustrated, which include the holding currents (I_H), the steady state NMDA currents (10 μM NMDA and 10 μM glycine) in the absence and in the presence of SKF-82958 (20 nM) and spiperone (2 nM), the series resistance (R_s) and the capacitance (C_m) of each cell. ATP (1 mM) and GTP (1 mM) were in the pipette solution and TTX (100 nM) was in the bath solution. Paired t-test and a randomization test did not show significant difference for NMDA responses in the presence of SKF-82958 ($p = 0.6$). There is no significant difference between the holding current prior to the NMDA response in the presence of SKF-82958 (I_{H2}) and the holding currents prior to the control NMDA response (I_{H1}) ($p = 0.45$)

3.3 Discussion

Dopamine modulation of NMDA receptors in the striatum is crucial not only to the efficacy of synaptic transmission in the cortico-striatal pathway (Calabresi et al., 2000c; Centonze et al., 2003) but may also influence excitotoxicity in some neuronal pathologies. For example NMDA receptor-dependent long-term potentiation (LTP) and long-term depression (LTD), have been described in several brain areas including the striatum (Calabresi et al., 1992; Charpier et al., 1997) and NMDA receptor mediated excitotoxicity contributes to the death of striatal neurons under some pathological conditions (Koroshetz et al., 1990; Cepeda et al., 1998b; Li et al., 2003 and Zeron et al., 2002). In this chapter I have shown that dopamine D1 receptor activation attenuates NMDA receptor currents in striatal medium spiny neurons of 7 day old rats. The experimental data suggest this is a G protein-independent, non-receptor tyrosine kinase-mediated mechanism involving NMDA receptor trafficking.

3.3.1 G protein-independent NMDA receptor inhibition

In whole cell recordings, D1 receptor activation by SKF-82958 significantly decreased NMDA receptor currents in striatal medium spiny neurons. This result is not consistent with the hypothesis of the classical adenylate cyclase pathway involving G_S G protein stimulation, where D1 activation has been shown to enhance NMDA responses via the adenylate cyclase – protein kinase-A and DARPP-32 (Dopamine and cyclic adenosine 3',5'-monophosphate-regulated PhosphoProtein, 32 kDa) cascade (Levine et al., 1996; Blank et al., 1997; Flores-Hernandez et al., 2002). In our experiments D1 inhibition of

NMDA receptor currents could not be abolished by intracellular application of either GDP-β–S (an inhibitor of G protein function) or occluded by GTP-γ–S (an irreversible activator of G proteins), which strongly suggests that D1 receptor activation attenuates NMDA receptor currents by a G protein-independent mechanism. In addition, the PKA inhibitor H-89 did not affect D1 inhibition.

3.3.3 Non-receptor tyrosine kinase is required for D1 inhibition of NMDA receptors

The Src family of protein tyrosine kinases, which consists of Src, Fyn, Lyn, Lck and Yes (Ali and Salter 2001), has been reported to upregulate the activity of NMDA receptors by phosphorylation (Kohr and Seeburg., 1996; Zheng et al., 1998; Ali and Salter, 2001). In recombinant NMDA receptors, Kohr and Seeburg (1996) showed that Src potentiated whole cell currents in Xenopus oocytes mediated by NR1/NR2A but not by NR1/NR2B. Salter (1998) suggested there might be an additional possibility that phosphorylation of NR2B subunits by tyrosine kinase does not affect channel gating but rather affects another function such as receptor trafficking.

G protein-coupled receptors have been reported to potentiate NMDA receptor function (Lu et al., 1999) and trafficking (Dunah & Standaert, 2001) by the activation of Src. Heuss et al. (1999) have proposed that a Src-family tyrosine kinase mediates the metabotropic glutamate receptor (mGluR) EPSC by associating with the receptor either directly or via an adaptor protein. Furthermore Benquet et al. (2002) demonstrated that the activation of mGluR1 potentiates the NMDA current via a G protein-independent

mechanism involving Src kinase activation. In terms of D1 receptor modulation, Dunah et al. (2004) showed that deletion of the gene for the protein tyrosine kinase Fyn, inhibits dopamine D1 receptor-induced enhancement of the abundance of NR1, NR2A and NR2B subunits in the synaptosomal membrane fraction and demonstrated that Fyn and tyrosine phosphorylation is required for D1-dependent redistribution of NMDA receptor protein.

In this study intracellular application of lavendustin A, an inhibitor of non-receptor protein tyrosine kinases, blocked D1 inhibition of NMDA receptor currents, while lavendustin B, an inactive analog of lavendustin A, had no effect. These results indicate D1 inhibition of NMDA currents requires tyrosine kinase activation. Moreover, the Src family-selective tyrosine kinase inhibitor, PP2 occluded the effect of SKF-82958 on NMDA responses suggesting that the Src family tyrosine kinases are responsible for D1 inhibition of NMDA receptors in striatal medium spiny neurons.

3.3.4 Dynamin-dependent D1 inhibition

In this study, D1 inhibition of NMDA responses was blocked by intracellular application of a dynamin inhibitory peptide. The dynamin inhibitory peptide also produced an approximate doubling of the average response to 10 μM NMDA. These results support the concept that normally there is constitutive turn over of NMDA receptors in the cell membrane (Roche et al., 2001; Wenthold et al., 2003; Lavezzari et al., 2004) and my results suggest this turn over is rapid with receptors spending on average 1 minute or less on the cell surface. Inhibition of receptor internalization results in an accumulation of receptors on the cell surface and occlusion of D1 inhibition suggesting that dynamin-

dependent internalization is essential in order to be able to observe D1-dependent inhibition.

3.3.5 Summary

In summary, it is clear that the D1 receptor inhibition of NMDA receptors in my experiments is not mediated by the classical G protein-dependent pathways but instead involves tyrosine kinase activation and dynamin dependent receptor internalization.

Chapter 4

NMDA receptor properties in 7-day-old rat striatal neurons

4.1 NMDA receptors do not contain NR2A subunits in striatal medium spiny neurons of 7 day old rats

The D1 inhibition of NMDA receptor whole-cell currents shown in chapter 3 is in agreement with those of Lee et al (2002). They claimed D1 inhibition was induced by direct protein–protein interactions between the C-terminus of the D1 receptor (D1-t3) and the C-terminus of the NR2A subunit. I therefore tested for the presence of functional NR2A-containing receptors using $ZnCl_2$ (Paoletti et al. 1997) or for the presence of tonic Zn inhibition using the Zn chelating agent TPEN (Figure 4.1*A*).

Three consecutive NMDA responses were evoked in these experiments, and $ZnCl_2$ (100 nM) and TPEN (1μM) were applied together with NMDA respectively in the second and third NMDA responses (Figure 4.1*A*). There was no significant difference among these three NMDA responses (control: 194 ± 20 pA, $ZnCl_2$: 198 ± 15 pA, TPEN: 181 ± 11 pA, $n = 5$ cells) (Figure 4.1*B*, Table 4.1).

These results suggested an absence of functional NR2A receptors in 7 day old rat striatum. Similarly, protein immunohistochemistry (Portera-Cailliau et al., 1996) and *in situ* mRNA hybridization (Monyer et al., 1994) show a lack of NR2A expression in 7 day old rat striatum.

A.

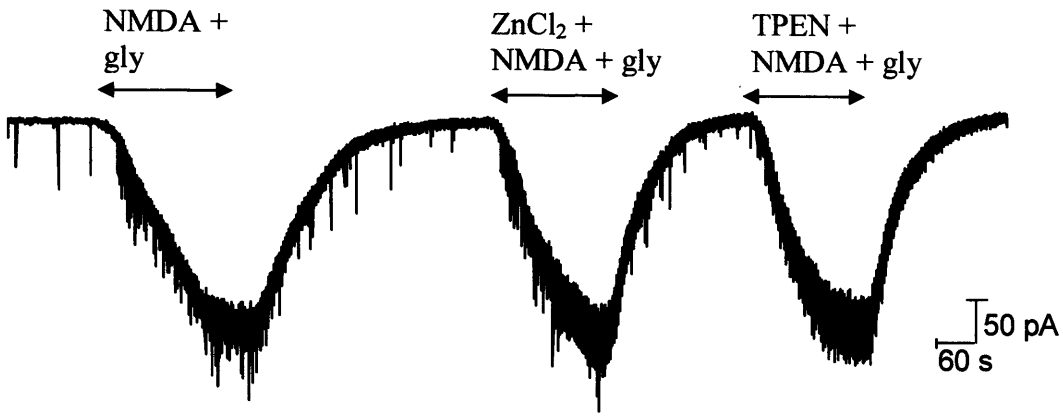

B.

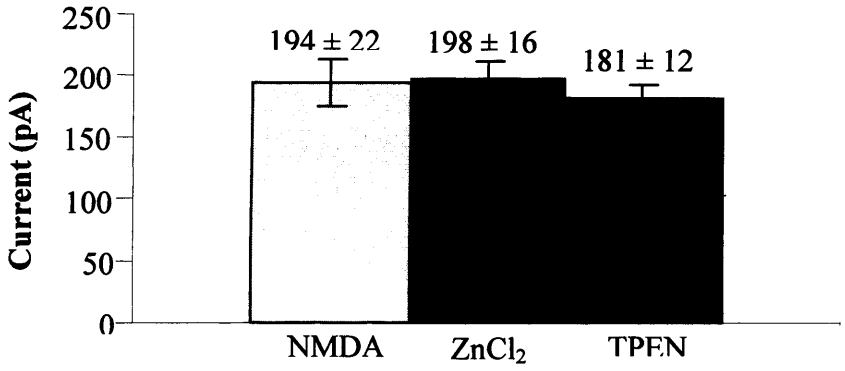

Figure 4.1 Absence of functional NR2A containing NMDA receptors in striatal neurons. A, whole cell recording from striatal medium spiny neuron in the presence of TTX (100 nM), intracellular ATP (1 mM) and GTP (1 mM). A control response to NMDA (10 μM) and glycine (10 μM) is followed by a second response in the presence of $ZnCl_2$ (100 nM), and finally TPEN (1 μM), NMDA and glycine were applied. The holding current was -15 pA prior to the control NMDA responses. B, The mean current (± SE) of the first NMDA response compared to the NMDA responses in the presence of $ZnCl_2$ (100 nM) or in the presence of TPEN (1 μM) were not significantly different from one another (n=5, $p>0.05$).

Cell number.	NMDA (pA)	$ZnCl_2$ (pA)	TPEN (pA)	Percentage change of $ZnCl_2$ and NMDA	Percentage change of TPEN and $ZnCl_2$	Percentage change of TPEN and NMDA	R (MΩ)	C_m (pF)
9-07-03#2	263	181	156	-31.0	-13.8	-40.5	42.3	14.6
10-07-03#1	181	206	206	13.8	0.0	13.8	23.1	21.8
10-07-03#2	178	150	150	-15.8	0.0	-15.8	41.0	12.5
10-07-03#3	219	250	206	14.3	-17.5	-5.7	45.5	16.5
10-07-03#4	131	200	188	52.4	-6.25	42.9	49.2	16.1
COUNT	5	5	5	5	5	5	5	5
MEAN	194	198	181	1.61	-8.23	-6.75	40.2	16.3
SE	19.7	14.6	10.8	12.8	3.2	12.6	4.03	1.38
	Paired t-test for $ZnCl_2$ and NMDA, p =0.456 Paired t-test for $ZnCl_2$and TPEN, p =0.307 Paired t-test for NMDA and TPEN, p=0.223							

Table 4.1 No evidence for functional NR2A subunit containing NMDA receptors was found in these experiments. Details of each whole-cell recording from five neurons are given. Comparison of the NMDA (10 μM) and glycine (10 μM) induced NMDA responses with NMDA responses in the presence of ZnCl2 (100 nM) and with NMDA responses in the presence of TPEN (1 μM) shows that there is no significant effect of $ZnCl_2$ or TPEN on the NMDA response. (P=0.46, 0.31, 0.22)

Thus NR2A subunits may not be involved in D1 inhibition of striatal NMDA receptors at this stage of development, and the direct protein-protein interaction between the D1 receptor and NR2A C-terminus described by Lee et al. may not be the reason for D1 inhibition in my experiments.

4.2 D1 inhibition is not evident in single-channel recordings

In order to investigate whether D1 inhibition of NMDA receptors could be observed in isolated membrane patches or whether the D1 agonist, SKF-82958, has any direct effects on NMDA receptor, I made 21 outside-out patch-clamp recordings from medium spiny neurons of different striatal slices from 7 day old rats. In these experiments GDP-β-S (0.5 mM) and ATP (1 mM) were present in the pipette solution and TTX (100 nM) was applied in the recording solution. Single channel openings were evoked by NMDA (1 μM) and glycine (10 μM) at -60 mV, and were recorded for 2 minutes both in the absence of SKF-82958 (20 nM) and spiperone (2 nM) (control) and in the presence of them. Furthermore, in control experiments NMDA receptor single channel openings were identified by block with 7-chlorokynurenic acid (100 μM), a glycine site NMDA receptor antagonist (Kemp et al., 1988). Figure 4.2 illustrates continuous recordings, each 5 seconds in duration, from a patch in control and then in the presence of 20 nM SKF-82958. Examination of individual single channel recordings illustrates that SKF-82958 produced no obvious changes in NMDA channel behaviour.

Figure 4.2

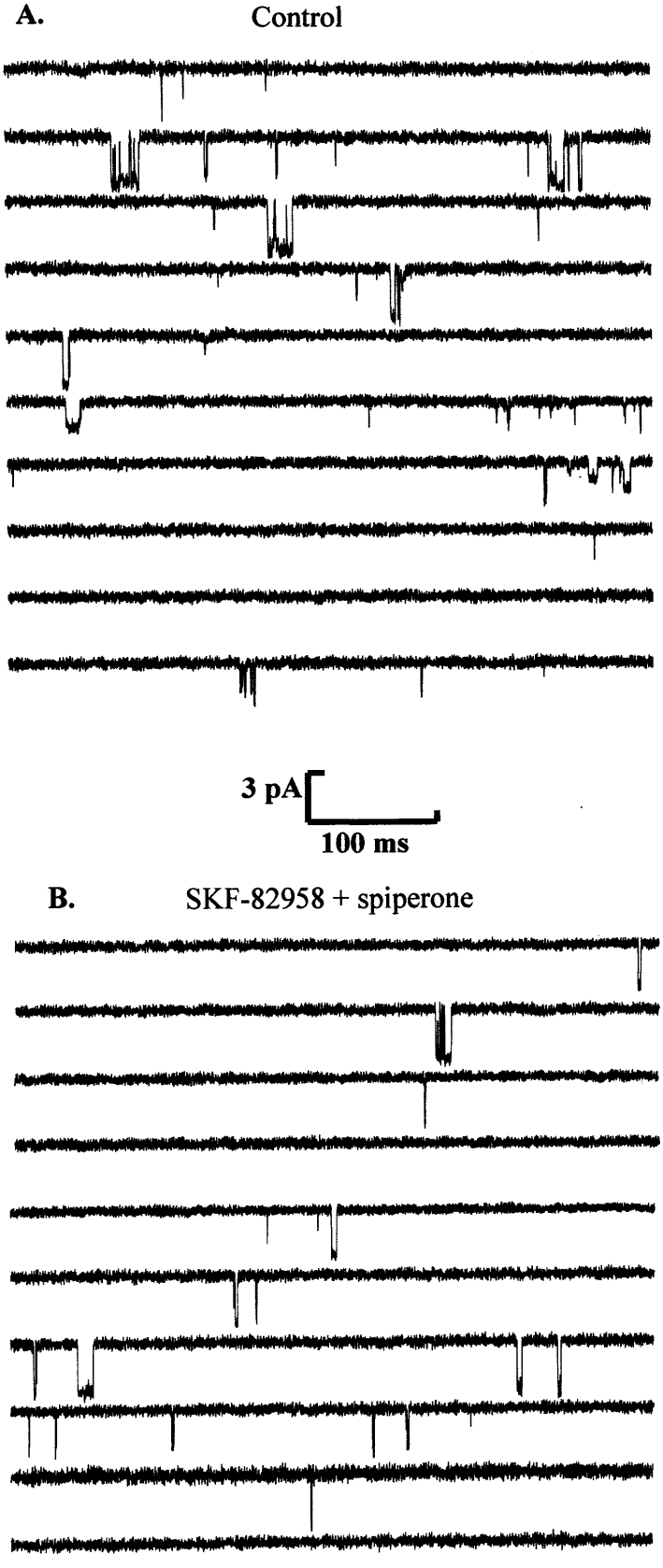

Figure 4.2 Single channel activity mediated by NMDA receptors in (A) control and (B) 20 nM SKF-82958 and 2 nM spiperone treated outside-out patches. Downward deflections in the baseline indicate single channel openings in the presence of 1.0 μM NMDA and 10 μM glycine. Both A and B show 5 seconds of continuous recording at a holding potential of –60 mV from the same patch. Currents were low-pass filtered at 2 kHz and digitized at 20 kHz.

4.2.1 Stability plots

As illustrated in Figure 4.3 the presence of 20 nM SKF-82958 applied to outside-out patches did not change the long-term stability of NMDA channel amplitude or kinetic behavior, such as mean shut time (control: 167 ± 37 ms, SKF-82958: 160 ± 46 ms), mean open time (control: 2.74 ± 0.39, SKF-82958: 3.34 ± 0.5), and open probability (control: 0.043 ± 0.01, SKF-82958: 0.058 ± 0.02).

4.2.2 Distribution of single channel amplitude

Single NMDA channel amplitude distributions were fitted with the sum of three Gaussian components (Figure 4.4). Only the amplitude of channel openings longer than twice the filter rise-time (T_r= 332 μs) were included in the distributions as these openings last long enough for the channel amplitude to reach at least 98% at its final value of the filter setting used in these experiments (Bessel, 2 kHz, -3dB). In the presence of SKF-82958 and spiperone the single channel amplitude distributions were not significantly different to control data. Mean values (and relative areas) for these three components were 1.1 ± 0.1 pA (18 ± 4%), 1.9 ± 0.1 pA (48 ± 7%), 3.05 ± 0.2 pA (33 ± 7%) for control and 1.1 ± 0.1 pA (23 ± 4%), 1.9 ± 0.1 pA (45 ± 7%), 2.9 ± 0.1 pA (34 ± 7%) in the presence of SKF-82958. Weighted single channel current amplitude

Single-channel amplitude measurements gave a main chord conductance of 50.8 ± 3 pS and two subconductances 31.6 ± 1.5 pS of and 17.5 ± 0.9 pS for control patches. For SKF-82958 treated patches the main conductance was 47.9 ± 2.5 pS, and two subconductances were 31.5 ± 1.6 pS, 18.7 ± 1.0 pS.

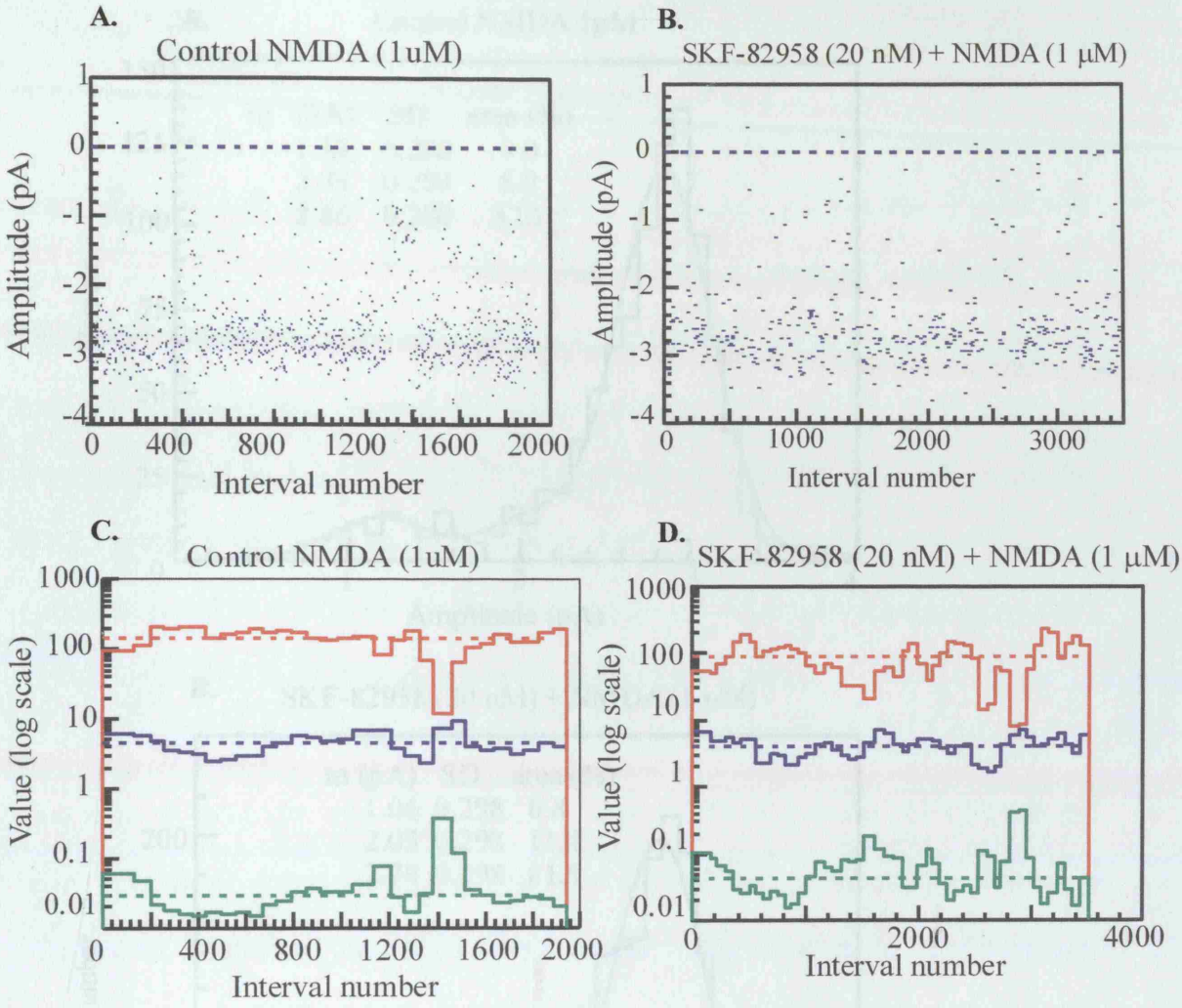

Figure 4.3 Stability plot analysis of NMDA receptor single-channel amplitudes, shut times, open times, and P_{open} for control (A, C) and SKF-82958 with spiperone (B, D). Amplitude stability plots contain 1951 (A) and 1895 (B) amplitudes longer than two filter rise times, observed during recordings of 120 seconds. Kinetic stability plots (C, D) show a running average of shut times (top), open times (middle), and Popen (bottom). Bins show a running average of 100 or 150 consecutive open or shut time intervals with an overlap of 50 or 75 events plotted against the interval number at the center of the averaged values. Horizontal dashed lines represent the average values for the whole recording. In these examples, the overall mean shut time, mean open time, and Popen were 130 msec, 4.49 msec, and 0.03 for control and 90 msec, 3.48 msec, and 0.043 for 20 nM SKF-82958 and 2 nM spiperone, respectively.

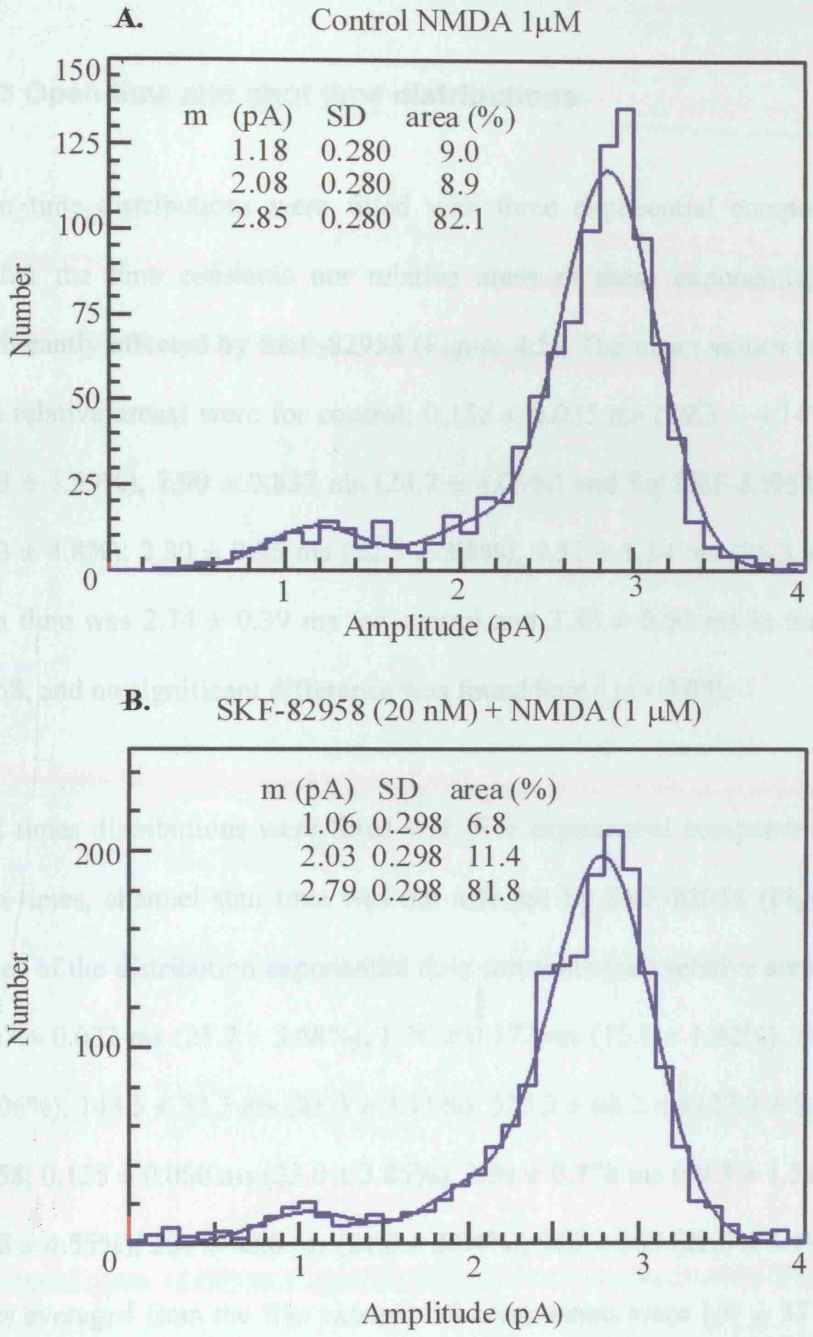

Figure 4.4 Amplitude histograms from A, control and B, in the presence of SKF-82958 (20nM) and spiperone (2 nM). Distributions of channel amplitudes were fitted with the sum of three Gaussian components for amplitudes of openings longer then two filter rise-times (332 μs). Mean amplitude, standard deviation and relative area for each Gaussian component are inset.

4.2.3 Open time and shut time distributions

Open time distributions were fitted with three exponential components (Figure 4.5). Neither the time constants nor relative areas of these exponential components were significantly affected by SKF-82958 (Figure 4.5). The mean values of the time constants (and relative areas) were for control; 0.155 ± 0.035 ms (39.3 ± 4.14%), 1.53 ± 0.22 ms (29.3 ± 3.59%), 7.90 ± 0.837 ms (28.7 ± 4.05%) and for SKF-82958; 0.223 ± 0.061 ms (41.3 ± 4.8%), 2.30 ± 0.35 ms (32.5 ± 3.8%), 9.57 ± 1.14 ms (26.3 ± 3.5 %). The mean open time was 2.74 ± 0.39 ms for control and 3.36 ± 0.50 ms in the presence of SKF-82958, and no significant difference was found here ($p > 0.05$).

Shut times distributions were fitted with five exponential components. As with channel open times, channel shut time was not affected by SKF-82958 (Figure 4.6). The mean values of the distribution exponential time constants (and relative areas) were for control; 0.167 ± 0.032 ms (21.7 ± 3.68%), 1.26 ± 0.172 ms (15.1 ± 1.82%), 14.3 ± 3.58 ms (15.3 ± 2.06%), 143.5 ± 34.3 ms (21.3 ± 3.11%), 523.2 ± 68.2 ms (27.3 ± 5.44%) and for SKF-82958; 0.125 ± 0.050 ms (23.0 ± 3.86%), 2.94 ± 0.778 ms (19.3 ± 1.51%), 22.7 ± 5.65 ms (18.8 ± 4.55%), 201 ± 62.6 ms (21.6 ± 3.04%), 963 ± 367 (22.0 ± 4.19%). The mean shut times averaged from the five exponential componnets were 167 ± 37 ms for control and 160 ± 46 ms in the presence of SKF-82958. Although the mean value for channel shut times was not significantly different in SKF-82958 ($p = 0.85$), the time constants of the second and third exponential component were significantly longer in SKF-82958.

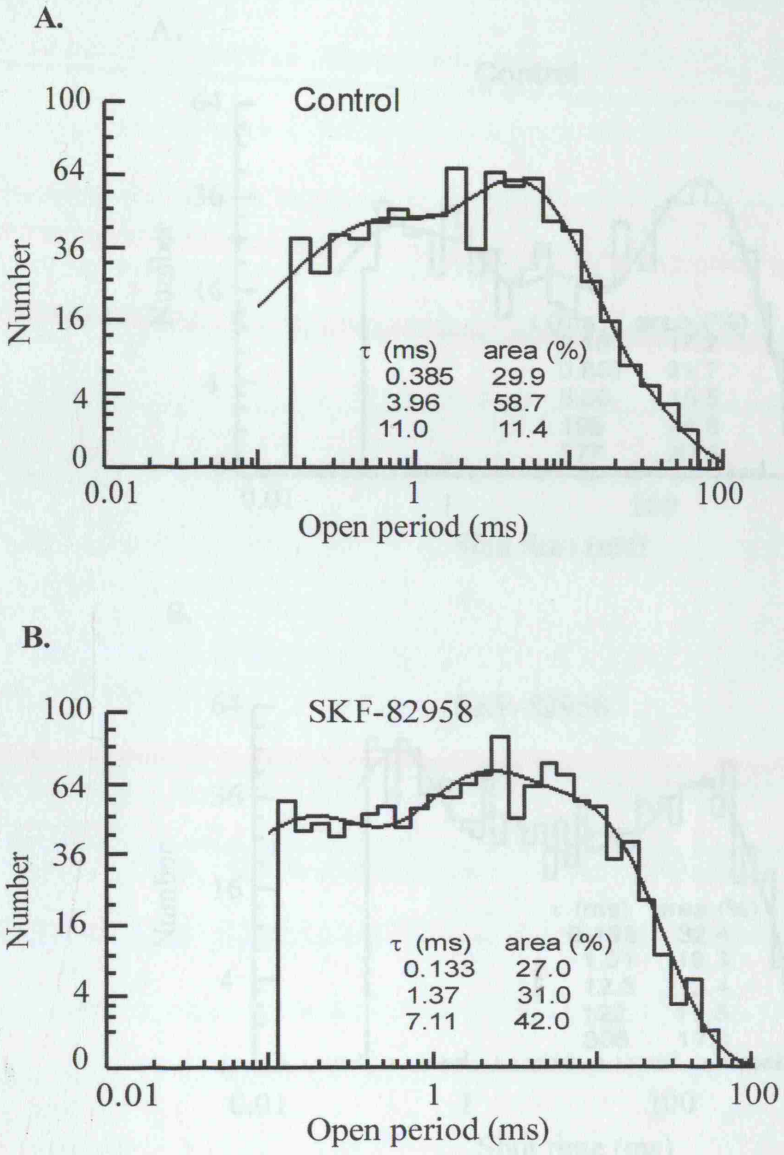

Figure 4.5 Lack of effect of 20nM SKF-82958 on channel open times. Distributions of open times ranging from 0.15 to 100 ms (A) and 0.12 to 100 ms (B) were fitted with a mixture of three exponential components (time constants and associated areas are inset). Predicted mean open times were 3.69 ms for control (A) and 3.45 ms in SKF-82958 (B). From all patches the average mean open time was 2.74 ± 0.39 ms in control and 3.36 ± 0.50 ms in the presence of SKF-82958 (n = 21, p = 0.19).

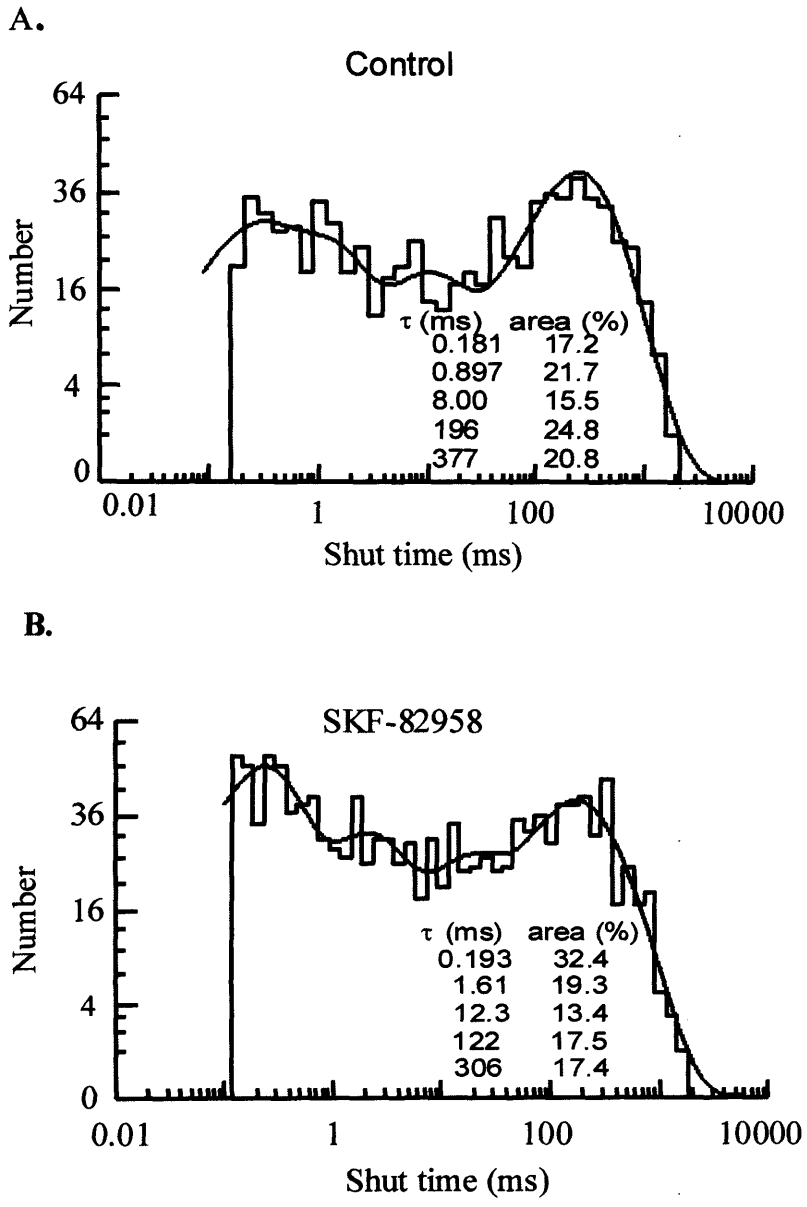

Figure 4.6 SKF-82958 did not induce any significant effect in the NMDA channel closed times. Distributions of shut time intervals ranging from 0.15 to 10,000 ms (A) and 0.12 to 10,000 ms (B) were fitted with a mixture of five exponential components (time constants and associated areas are inset). The predicted mean shut times were 129 ms for control (A) and 76.6 ms for SKF-82958 (B). From all patches the average mean shut time in control was 167 ± 37 ms for control and 160 ± 46 ms in the presence of SKF-82958 (n = 21, p = 0.85)

These results gave an open probability of 0.043 ± 0.01 for control and 0.058 ± 0.02 in the presence of SKF-82958. Therefore SKF-82958 did not significantly change the NMDA receptor single channel properties in outside out patches. In other words, D1 receptor inhibition of NMDA receptors cannot be observed in isolated membrane patches. This may be because some essential factor is lost when making an outside-out patch. However since whole-cell currents are determined by the single channel conductance, open probability and the number of channels, these results suggest that D1 inhibition of NMDA responses in whole-cell recordings may be due to a change in the number of surface NMDA receptors, suggesting an effect on NMDA receptor trafficking.

4.3 Discussion

4.3.1 The absence of functional NR2A containing NMDA receptors

Lee et al. (2002) identified direct protein – protein interactions between the C-terminus of the D1 receptor (D1-t3) and the C-terminus of the NR2A subunit which led to inhibition of NMDA receptor currents. However, their results also showed that the carboxyl tail of NR2B could not form a complex with the D1 receptor directly. Interestingly, in our experiments we could not find evidence for the presence of functional NR2A subunits in the striatum of 7 day old rats using either the zinc chelating agent TPEN to unmask any tonic zinc inhibition of NR2A receptors or addition of zinc to cause inhibition of NR2A receptors (Paoletti et al., 1997). These results are consistent with the absence of NR2A mRNA (Monyer et al., 1994) or protein (Portera-Cailliau et al., 1996) from the striatum of 7 day old rats. At postnatal day 7 there is a strong expression of the NR2B mRNA (Monyer et al., 1994) and protein (Portera-Cailliau et al., 1996) in the striatum (Wenzel et

al., 1997; Standaert et al., 1994). These results suggest NR2A subunits are not involved in the D1 inhibition of striatal NMDA receptors observed in this study and therefore, a mechanism other than a direct interaction between dopamine and NMDA receptors may predominate.

4.3.2 D1 receptor activation does not change NMDA receptor single channel activity in isolated membrane patches

D1 receptor inhibition of NMDA receptors could not be observed in outside-out membrane patches from the cell body; application of SKF-82958 did not change the single channel conductance, mean open time, mean shut time or open probability in 21 outside-out patch-clamp recordings. Whole-cell currents are determined by the channel conductance, the open probability and the channel number. Therefore I hypothesized that D1 inhibition of NMDA responses in whole-cell recordings may be mediated by a change in surface receptor number caused by NMDA receptor trafficking, although there is also the possibility that D1 receptors are not co-localized with NMDA receptors in the somatic membrane patches used for these single channel recordings or that some essential factor is lost when making an outside-out patch. In addition, this hypothesis is supported by the dynamin inhibitory peptide experiments shown in chapter 3 where D1 inhibition could not be observed after the blockade of receptors endocytosis. Likewise, Lee et al (2002) also found that D1 receptor activation decreased the number of NMDA receptors expressed on the cell surface.

Chapter 5
Dopamine D2 receptor inhibition of NMDA receptors in medium spiny neurons

5.1 Introduction

The D2 class of dopamine receptors (D2, D3 and D4) has been shown to inhibit NMDA receptor activity in some regions of the central nervous system (Kotecha *et al.*, 2002; Wang et al., 2003). In the hippocampus Kotecha et al. (2000) suggested that activation of D2/D4 receptors decreased NMDA responses and excitatory NMDAR-mediated synaptic transmission via the transactivation of PDGFRs (PDGFR: platelet-derived growth factor receptor), and the mechanisms depended upon stimulation of PLC (phospholipase C) and an increase in intracellular calcium. In prefrontal cortex the D4 receptor has also been shown to reduce both NMDA-evoked currents in dissociated neurons and NMDA receptor-mediated EPSCs in slices (Wang et al., 2003). They suggested that this D4 modulation of NMDA receptor currents and EPSCs is mediated by a signaling cascade involving the inhibition of PKA and the subsequent activation of PP1.

However, few studies have reported D2-like receptor modulation of NMDA receptors in the striatum, and Cepeda et al. (1998a) showed that D2 receptor activation produced inconsistent effects on NMDA evoked inward currents in neostriatal neurons. In this study, I used whole cell recordings to investigate D2 family receptor regulation of NMDA receptors in striatal medium spiny neurons of 7 day old rats.

5.2 Results

Experiments were carried out upon medium spiny neurons in striatal brain slices from 7 day old rats. Medium spiny neurons were voltage clamped at -60mV in the presence of TTX (100nM) to block voltage-gated Na^+ currents. ATP (1 mM) and GTP (1mM) were in the pipette solution unless otherwise specified. Quinpirole (40 nM or 1 μM), a selective D2 class receptor agonist, was used to activate D2 family receptors in the persence of SCH-23390, a D1 class receptor antagonist.

5.2.1 D2 receptor activation reduced NMDA receptor currents

Although the D2 receptor agonist, quinpirole (40 nM) produced an apparent decrease of the NMDA whole-cell current, this was not statistically significant (Figure 5.1). Figure 5.1*A* illustrates a current trace from a whole-cell recording in this experiment, where the first NMDA response was evoked by a 2 minute application of NMDA (10 μM) and glycine (10 μM) followed by a 5 minute application of quinpirole (40 nM) and SCH-23390 (10 nM) in the absence of NMDA and glycine then a further another 2 minutes in the presence of NMDA and glycine. SCH-23390, a D1 family antagonist, was used to rule out the possibility of D1 receptor activation during the NMDA responses. ATP (1 mM) and GTP (1 mM) were applied to the intracellular solution. Figure 5.1*B* shows a comparison of the mean maximum NMDA currents in the absence and in the presence of quinpirole and SCH-23390, averaged from the seven neurons in this experiment (Table 5.1). Five neurons showed a decrease in the NMDA responses, and two neurons showed

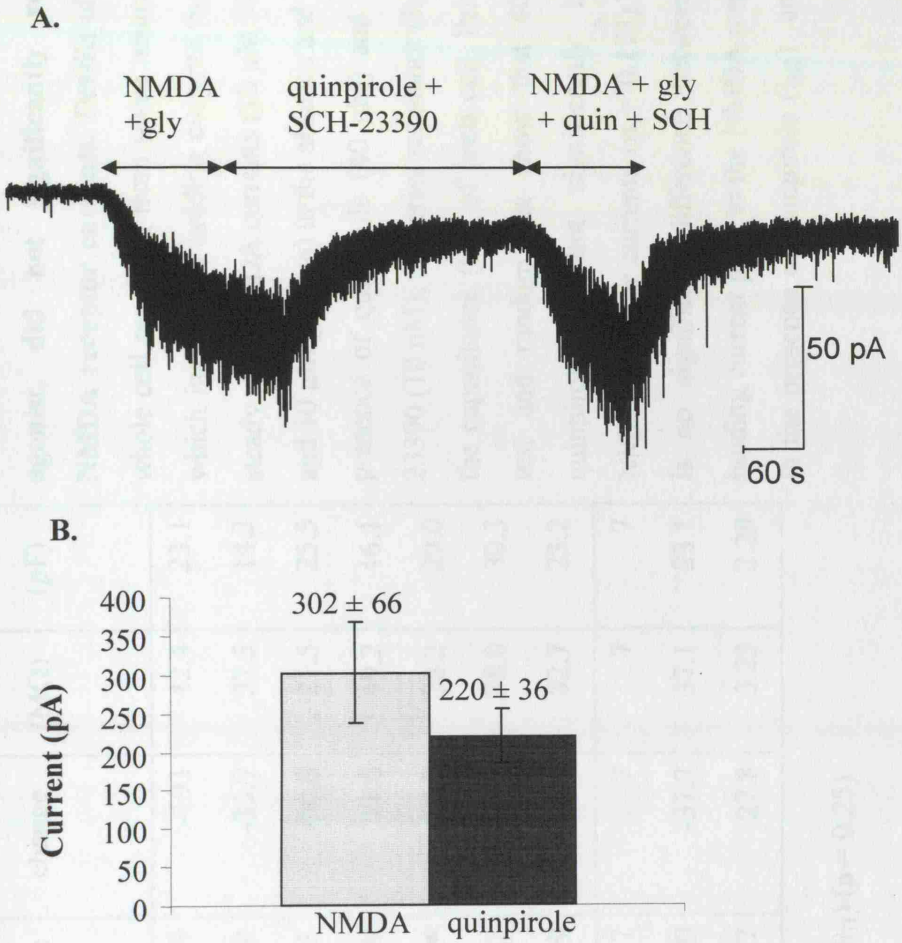

Figure 5.1 The D2 receptor agonist, quinpirole (40 nM) reduced the whole cell NMDA receptor currents recorded from 7 day-old rat striatal neurons voltage clamped at -60mV but this reduction was not statistically significant. A, Response to NMDA (10 μM) and glycine (10 μM) applied for 2 minutes, followed by 5 minutes quinpirole (40 nM) and SCH-23390 (10 nM), and finally NMDA (10 μM), glycine (10 μM), quinpirole (40 nM) and SCH-23390 (10 nM) for 2 minutes. Brief downward deflections of the current trace show occasional miniature synaptic currents. The holding current was -20 pA prior to the control NMDA responses. **B,** Mean current (± SE) of the first NMDA response was not significantly different from the second response in the presence of quinpirole and SCH-23390 ($n = 7$, $p > 0.05$).

Cell number	I_{H1} (pA)	NMDA (pA)	I_{H2} (pA)	NMDA + quinpirole (pA)	% change	R_s (MΩ)	C_m (pF)
29/5/03#1	-70	526	-250	179	-193	42.4	23.1
29/5/03#2	-20	45.5	-31	34.0	-33.9	37.5	14.2
29/5/03#3	-76	346	-150	231	-50.0	21.5	25.5
15/7/03#1	-6	238	-4	269	11.6	49.2	16.1
16/7/03#2	-120	475	-60	325	-46.2	38.2	29.0
16/7/03#3	-150	350	-170	281	-24.6	38.0	30.3
22/7/03#2b	-90	138	-120	219	37.1	32.7	23.2
Count	7	7	7	7	7	7	7
Mean	-76.0	302	-112.1	220	-37.7	37.1	23.1
SE	19.3	65.7	32.7	35.7	27.8	3.23	2.29

holding currents prior to the control NMDA response (I_{H1}) ($p = 0.25$)

Table 5.1 40 nM quinpirole, a D2 receptor agonist, did not significantly reduce NMDA receptor currents. Details of each whole cell recording from seven neurons in, which include the holding currents (I_H), the steady state NMDA currents (10 μM NMDA and 10 μM glycine) in the absence and in the presence of quinpirole (40 nM) and SCH-23390 (10 nM), the series resistance (R_s) and the capacitance (C_m) of each cell. Paired t-test and random test show that 40 nM quinpirole did not significantly inhibit NMDA receptor currents ($p = 0.173$).There is no significant difference between the holding current prior to the NMDA response in the presence of quinpirole (I_{H2}) and the

an increase. On average the NMDA receptor currents decreased from 302 ± 66 pA to 220 ± 36 pA (mean ± SE, n= 7 neurons) (Table 5.1); however, there is no significant difference statistically ($p>0.05$). The results indicated that dopamine D2 receptor activation did not reduce the NMDA receptor whole-cell currents significantly in striatal medium spiny neurons in 7 day-old rats.

G proteins have been shown to be required for D2 receptor family modulation of NMDA receptors (Kotecha et al., 2002). In order to test if G proteins were involved in a possible D2 modulation of NMDA receptor, intracellular GTP (1mM) was substituted with a general G protein inhibitor, GDP-β-S (0.5 mM). There were nine cells in this experiment. In the presence of intracellular GDP-β-S, quinpirole inhibited the NMDA responses in five neurons and enhanced the NMDA responses in four neurons (Table. 4.2). Consequently no significant difference was found between the NMDA responses in the absence and in the presence of quinpirole and SCH-23390 (NMDA: 258 ± 61 pA, quinpirole + NMDA: 230 ± 46 pA) ($n = 9$, $p > 0.05$). However, it is difficult to draw a firm conclusion on the role of G proteins at this stage because the D2 receptor agonist, quinpirole, did not produce a convincing effect on the NMDA receptor currents.

5.2.2 Quinpirole 1 μM inhibited the NMDA receptor current significantly

A higher concentration of quinpirole (1 μM) was tested in six neurons (Figure. 4.2). The experiment was executed using the same procedure as in the 40 nM quinpirole experiments

Cell number	I_{H1} (pA)	NMDA (pA)	I_{H2} (pA)	NMDA + quinpirole (pA)	% change	R_s (MΩ)	C_m (pF)
180603#2	-22	450	-70	256	-43.1	32.1	16.4
180603#3	-54	450	-150	213	-52.8	17.4	27.9
190603#2b	-67	62.5	-60	325	420	30.8	28.3
190603#4	-155	513	-200	500	-2.44	19.8	30.1
190603#5	-100	119	-200	150	26.3	38.5	12
190603#7	-115	331	-110	269	-18.9	18.5	19.3
220703#2	-80	125	-14	75.0	-40.0	49.5	10.2
220703#3	-15	238	-68	244	2.63	25	19.8
230703#1	-31	37.5	-32	37.5	0	27.9	6.7
COUNT	9	9	9	9	9	9	9
MEAN	-71.0	258	-100.4	230	-11.0	28.8	19.0
SE	15.5	61.0	23.0	46.0	49.2	3.5	2.8

Table 5.2 In the presence of GDP-β-S, a G proteins inhibitor, 40 nM quinpirole failed to modulate the NMDA receptor currents. Details of each whole cell recording from nine neurons are illustrated, which include the steady state NMDA currents (10 μM NMDA and 10 μM glycine) in the absence and in the presence of quinpirole (40 nM) and SCH-23390 (10 nM), the series resistance (R_s) and the capacitance (C_m) of each cell. Paired t-test and randomization test showed that 40 nM quinpirole did not significantly inhibit NMDA receptor currents in the presence of intracellular GDP-β–S (0.5 mM) ($p = 0.57$). There is no significant difference between the holding current prior to the NMDA response in the presence of quinpirole (I_{H2}) and the holding currents prior to the control NMDA response (I_{H1}) ($p = 0.14$)

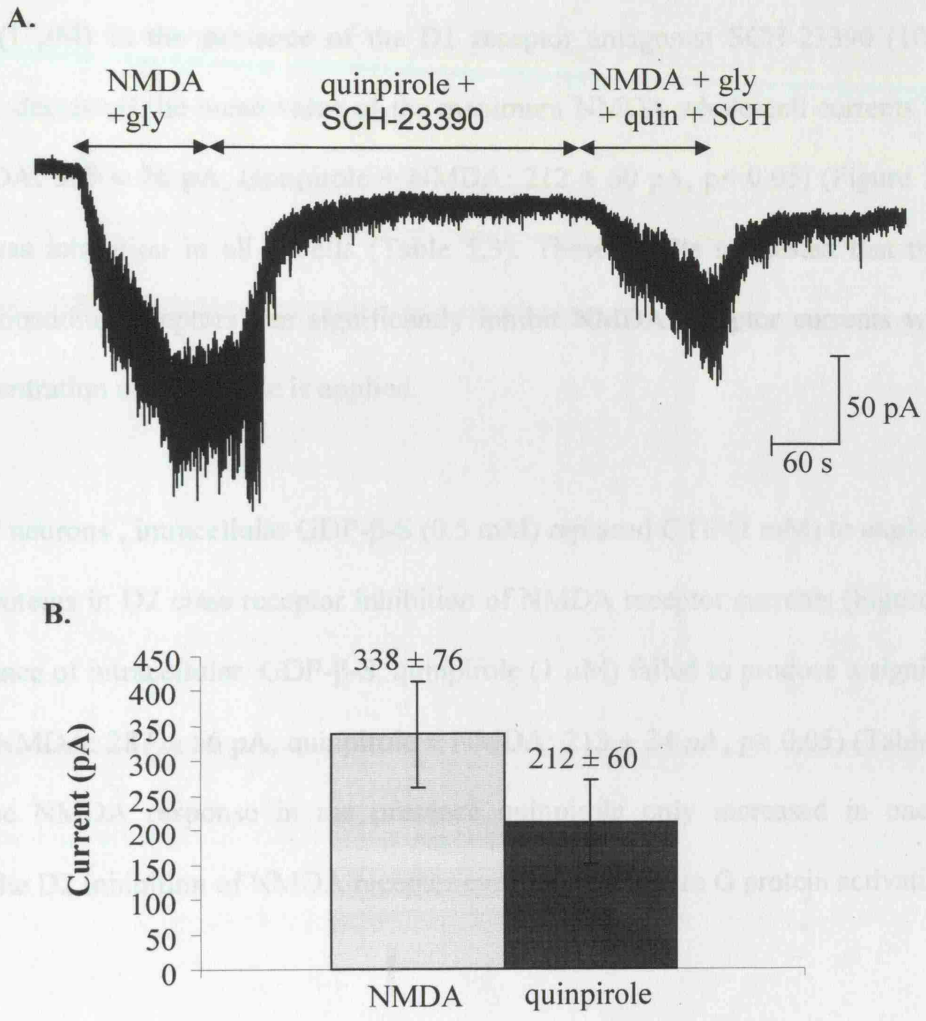

Figure 5.2 Quinpirole (1 μM) inhibited whole cell NMDA receptor currents significantly. **A,** Response to NMDA (10 μM) and glycine (10 μM) applied for 2 minutes, followed by 5 mins quinpirole (1 μM) and SCH-23390 (10 nM), and finally NMDA (10 μM), glycine (10 μM), quinpirole (1 μM) and SCH-23390 (10 nM) for 2 minutes. The holding current was -8 pA prior to the control NMDA responses. **B,** Mean current (± SE) of the first NMDA response compared with the second response in the presence of quinpirole and SCH-23390 ($n = 6$, $p < 0.05$).

(Figure 5.2*A*), and ATP (1 mM) and GTP (1 mM) were applied to the intracellular solution. Quinpirole (1 μM) in the presence of the D1 receptor antagonist SCH-23390 (10 nM) significantly decreased the mean value of the maximum NMDA whole-cell currents by 37 ± 7% (NMDA: 339 ± 76 pA, quinpirole + NMDA: 212 ± 60 pA, $p< 0.05$) (Figure 5.2*B*), and there was inhibition in all 6 cells (Table 5.3). These results suggested that the D2 family of dopamine receptors can significantly inhibit NMDA receptor currents when a higher concentration of quinpirole is applied.

In another 7 neurons , intracellular GDP-β-S (0.5 mM) replaced GTP (1 mM) to explore the role of G proteins in D2 class receptor inhibition of NMDA receptor currents (Figure 5.3). In the precence of intracellular GDP-β-S, quinpirole (1 μM) failed to produce a significant inhibition (NMDA: 287 ± 56 pA, quinpirole + NMDA: 213 ± 34 pA, $p> 0.05$) (Table 5.4), although the NMDA response in the presence quinpirole only increased in one cell. Therefore, the D2 inhibition of NMDA receptor currents did require G protein activation.

5.2.3 D2 receptor activation reduced the high-voltage activated calcium channels.

D2 class dopamine receptors have been reported to inhibit the L-type calcium currents in medium spiny neurons of the striatum via G protein activation (Hernandez-Lopez et al., 2000, Olson et al., 2005). As a control experiment to confirm D2 receptor activation, Ba^{2+} currents through Ca^{2+} channels were tested both in the absence (control) and in the presence of quinpirole at a concentration of 40 nM or 1 μM. Neurons were voltage clamped at -80 mV. Whole cell Ba^{2+} (5 mM) currents through Ca^{2+} channels were elicited by 100 ms

Cell number	I_{H2} (pA)	NMDA (pA)	I_{H2} (pA)	NMDA + quinpirole (pA)	% change	R_s (MΩ)	C_m (pF)
#1-26-8-04	-53	368.8	-65	256.3	-30.5	30.8	18.9
#2-26-8-04	-20	362.5	-30	150.0	-58.6	33.4	14
#3-26-8-04	-12	543.8	-120	281.3	-48.3	28.2	26.2
#4-26-8-04	-6	118.8	-15	78.1	-34.3	29.6	16.4
#1-27-8-04	-8	118.8	-27	56.3	-52.6	28.3	9
#2-27-8-04	-30	518.8	-85	450.0	-13.3	35	28.5
Count		6		6	6	6	6
Mean	-21.5	338.6	-57.0	212.0	-37.4	30.9	18.8
SE	7.3	75.9	16.5	60.4	6.9	1.1	3.0

Table 5.3 1 μM quinpirole significantly reduced NMDA receptor currents. Details of each whole cell recording from six neurons are illustrated, which include the holding currents (I_H), the steady state NMDA currents (10 μM NMDA and 10 μM glycine) in the absence and in the presence of quinpirole (1 μM) and SCH-23390 (10 nM), the series resistance (R_s) and the capacitance (C_m) of each cell. A paired t-test and a randomization test showed that NMDA currents were remarkably inhibited by 1 μM quinpirole ($p = 0.018$). There is no significant difference between the holding current prior to the NMDA response in the presence of quinpirole (I_{H2}) and the holding currents prior to the control NMDA response (I_{H1}) ($p = 0.08$)

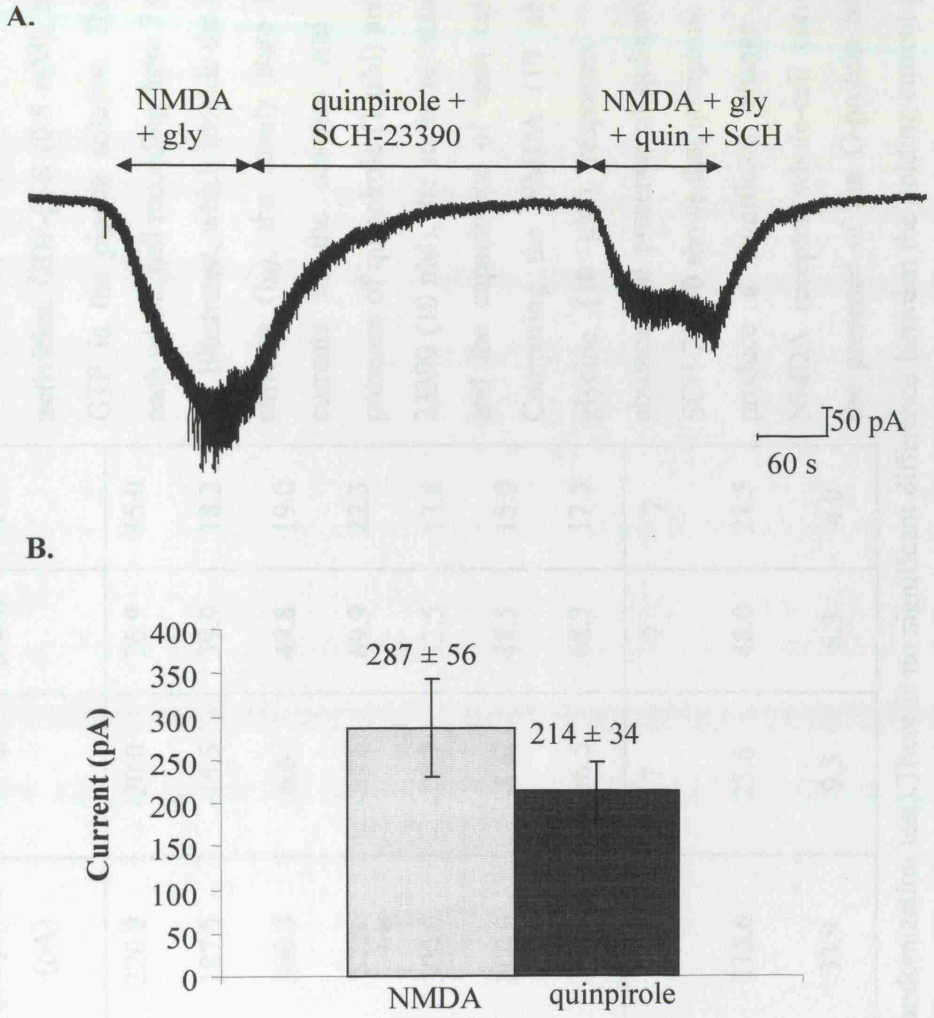

Figure 5.3 GDP-β-S, a G protein inhibitor, blocked D2 inhibition of NMDA responses. **A**, whole cell current recording with GDP-β-S (0.5 mM) and ATP (1 mM) in the pipette solution. This trace illustrates the largest change observed in the presence of GDP-β-S. NMDA (10 μM) and glycine (10 μM) were applied for 2 minutes, followed by 5 minutes quinpirole (1 μM) and SCH-23390 (10 nM), and finally NMDA (10 μM), glycine (10 μM), quinpirole (1 μM) and SCH-23390 (10 nM) for 2 minutes. The holding current was -100 pA prior to the control NMDA responses. The holding current was -120 pA prior to the control NMDA responses. **B**, The mean current (± SE) in the presence of intracellular GDP-β-S (0.5 mM) of the first NMDA response compared to the second response in the presence of quinpirole and SCH-23390, (n=7, $p > 0.05$).

Cell number	I_{H2} (pA)	NMDA (pA)	I_{H2} (pA)	NMDA + quinpirole (pA)	% change	R_s (MΩ)	C_m (pF)
#2-31-8-04	-17	275.0	-27	220.0	-20.0	26.9	45.0
#3-31-8-04	-8	221.9	-32	187.5	-15.5	39.9	18.2
#4-31-8-04	-50	281.4	-18	300.0	6.6	49.8	19.0
#1-1-9-04	-20	90.7	-30	37.5	-58.6	69.9	22.3
#3-1-9-04	-120	343.8	-100	300.0	-12.7	32.5	13.8
#4-1-9-04	-12	218.8	-13	200.0	-8.6	48.5	15.0
#6-1-9-04	-29	575.0	-72	250.0	-56.5	68.7	17.5
Count	7	7	7	7	7	7	7
Mean	-36.6	286.6	-41.7	213.6	23.6	48.0	21.5
SE	14.9	56.4	10.9	33.9	9.3	6.3	4.0

Table 5.4 G protein was required for D2 inhibition of NMDA receptor activities. GDP-β–S (0.5 mM), replaced GTP in the pipette solution. Details of each whole cell recording from 7 neurons are illustrated, which include the holding currents (I_H), the steady state NMDA currents in the absence and in the presence of quinpirole (1 μM) and SCH-23390 (10 nM), the series resistance (R_s) and the capacitance of each cell (C_m). Comparing the NMDA (10 μM) and glycine (10 μM) responses in the absence and presence of quinpirole and SCH-23390 shows that quinpirole did not produce a significant change in the NMDA receptor whole-cell currents in the presence of the G-protein inhibitor, GDP-β–S ($p>0.05$ in both paired t-test and a randomization test).There is no significant difference between the holding current prior to the NMDA response in the presence of quinpirole (I_{H2}) and the holding currents prior to the control NMDA response (I_{H1}) ($p = 0.64$)

depolarizing pulses ranging from −80 mV to +20 mV in 10 mV increments. The first transient inward current was observed around -60 mV. The current reached its peak in 10 ms after the beginning of each step pulse and decayed rapidly back to the holding current (Figure 5.4A). With further depolarization the peak amplitude increased (Figure 5.4 B), and in most of the experiments the Ba^{2+} current reached its maximal amplitude at the potential of 0 mV yet some at -10 mV. After the peak inward current, as the depolarizing step increased the amplitude of Ba^{2+} currents gradually decreased.

5.2.3.1 Quinpirole 40 nM did not affect calcium currents in the striatum

Figure 5.4 *B* represents the I–V relationships of Ba^{2+} currents from six medium spiny neurons in the absence and in the presence of quinpirole (40 nM) and SCH-23390 (10 nM), and there is no significant difference between the averaged Ba^{2+} currents in the presence and in the absence of quinpirole (40 nM). Therefore this lower concentration of quinpirole did not affect the Ba^{2+} currents significantly ($n = 6$, $p > 0.05$).

5.2.3.2 Quinpirole 1 μM reduced the calcium currents in the striatum

A large reduction was found in the Ba^{2+} currents when increasing the quinpirole concentration to 1 μM (Figure 5.5A). The average peak Ba^{2+} current at 0 mV were reduced from 215 ± 54 pA to 148 ± 39 pA ($n= 8$, $p<0.05$). However, when the quinpirole-induced inhibition of Ba^{2+} currents was looked at detail, there were no significant changes until the voltage step reached -10 mV.

Figure 5.4

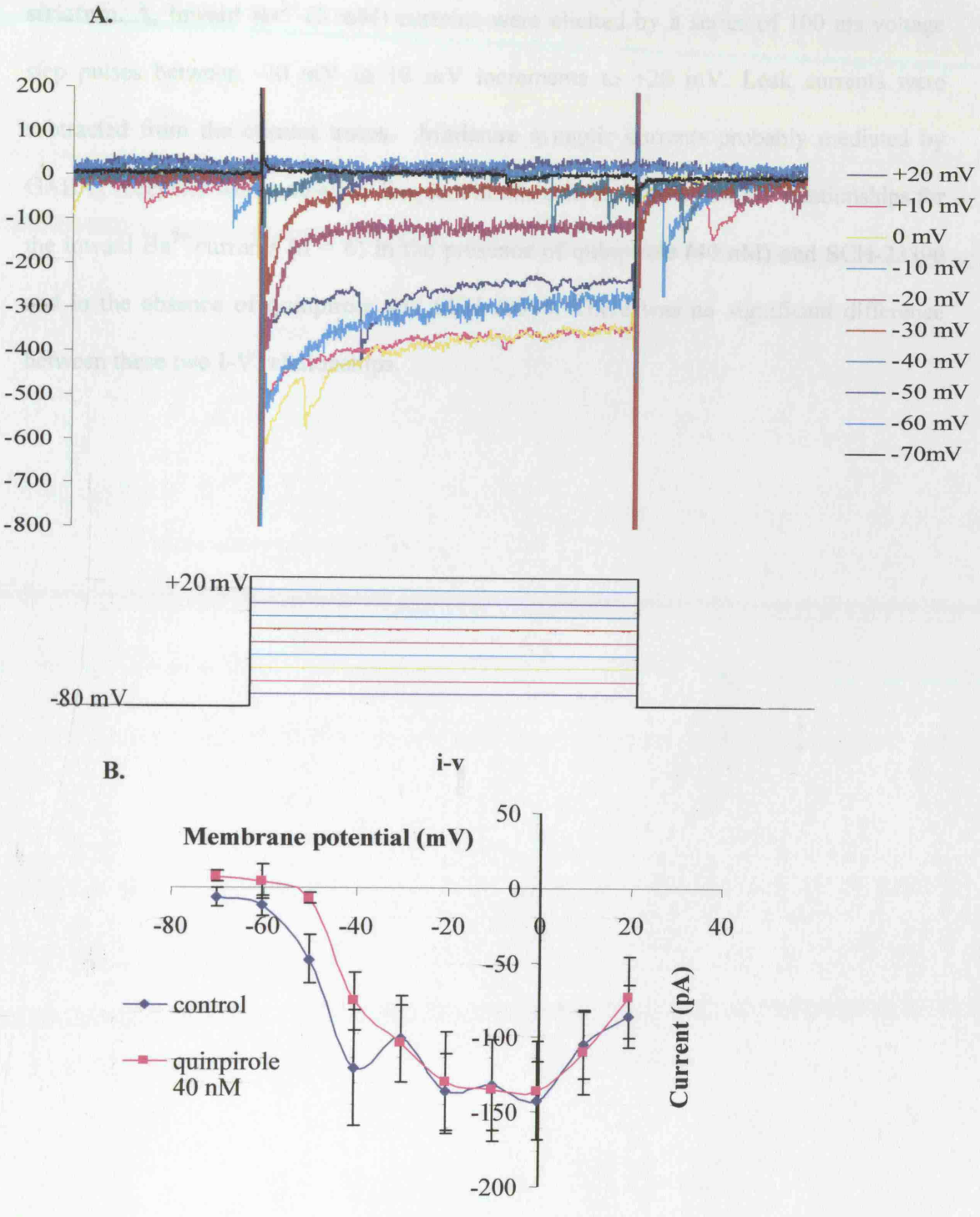
A.
200
100
0
-100
-200
-300
-400
-500
-600
-700
-800
+20 mV
+10 mV
0 mV
-10 mV
-20 mV
-30 mV
-40 mV
-50 mV
-60 mV
-70mV
+20 mV
-80 mV
B.
i-v
Membrane potential (mV)
50
0
-50
-100
-150
-200
-80
-60
-40
-20
0
20
40
control
quinpirole
40 nM
Current (pA)

Figure 5.4 Quinpirole (40 nM) has no significant effect on calcium currents in the striatum. A, Inward Ba^{2+} (5 mM) currents were elicited by a series of 100 ms voltage step pulses between -70 mV in 10 mV increments to +20 mV. Leak currents were subtracted from the current traces. Miniature synaptic currents probably mediated by $GABA_A$ receptors were unusually frequent in this cell. **B,** Whole-cell I-V relationships for the inward Ba^{2+} currents (n = 6) in the presence of quinpirole (40 nM) and SCH-23390 and in the absence of quinpirole and SCH-23390. There was no significant difference between these two I-V relationships.

Figure 5.5

A. Control

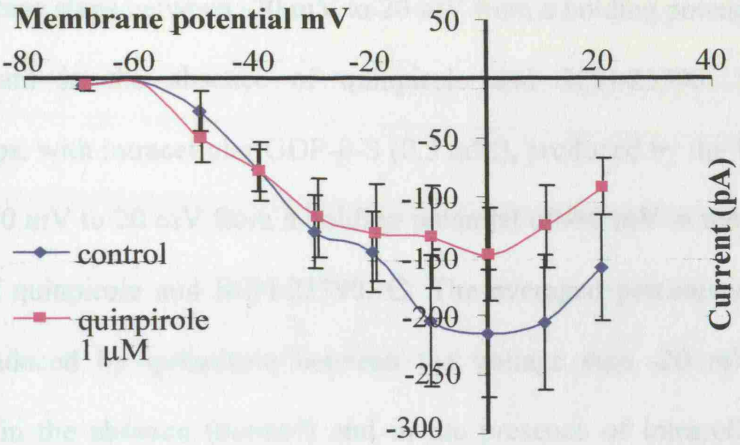

B. GDP-β-S

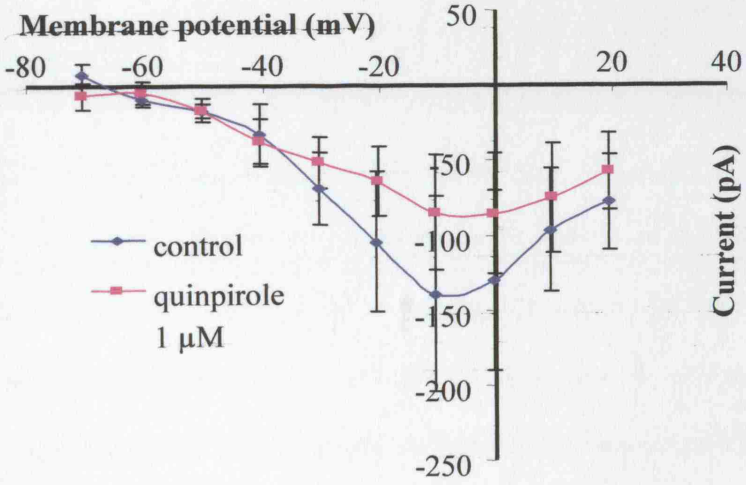

C. Percentage inhibition

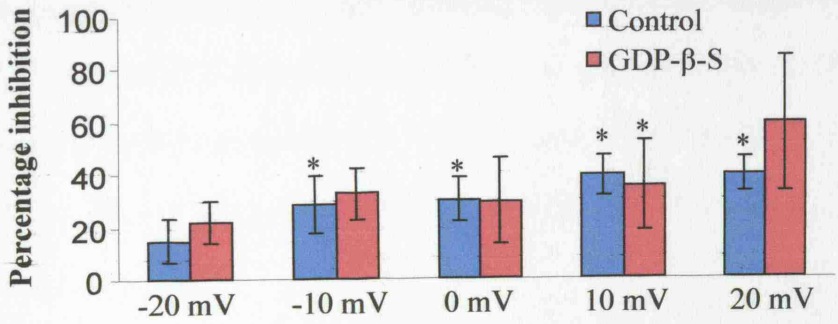

Figure 5.5 Quinpirole (1 μM) suppressed Ba^{2+} currents through Ca^{2+} channels, and this effect was G protein-dependent. A: Whole-cell I-V relationships produced by the 10 mV voltage steps between -70 mV to 20 mV from a holding potential of -80 mV in the presence and in the absence of quinpirole and SCH-23390. B: Whole-cell I-V relationships, with intracellular GDP-β-S (0.5 mM), produced by the 10 mV voltage steps between -70 mV to 20 mV from a holding potential of -80 mV in the presence and in the absence of quinpirole and SCH-23390. C: The averaged percentage inhibition of Ba^{2+} currents induced by quinpirole between the voltage step -20 mV to +20 mV was compared in the absence (control) and in the presence of intracellular GDP-β-S. The asterisk represents a significant percentage inhibition.

Intracellular GTP (1mM) was substituted with a general G protein inhibitor, GDP-β-S (0.5 mM) in 8 neurons. In the presence of GDP-β-S, quinpirole 1 μM did not inhibit the Ba^{2+} currents significantly during most voltage steps (Figure 5.4B), and a significant difference was only found when neurons was depolarized to 10 mV (n = 8).

Therefore, in my experiments the calcium channels, which require larger depolarization for activation, were weakly inhibited by D2 receptor activation, and this inhibition was dependent on G protein activation. These results suggest that 1μM quinpirole was sufficient to activate D2 receptors in these experiments.

5.3 Discussion

Dopamine D2 receptors are widely expressed in the striatum (Missale et al., 1998) and have been found in most enkephalin containing medium spiny neurons (Le Monie and Blotch, 1995). In the basal ganglia circuitry, D2 receptors mediate the dopaminergic synaptic transmission from the substantia nigra pars compacta to inhibit the striatal GABAergic efferent neurons in the indirect pathway. Moreover, when the D2 receptor gene is disrupted, an abnormal synaptic plasticity is found in the striatum (Calabresi et al., 1997). In the presence of magnesium, high-frequency stimulation of corticostriatal fibers produces NMDA-receptor-dependent LTP rather than LTD which is found in wild type striatal slices. Therefore D2 receptors play an important role in modification of striatal synaptic excitability.

Cepeda et al. (1993) reported that the D2 receptor antagonist, quinpirole significantly reduced NMDA-evoked responses in striatal neurons of adult rats. In prefrontal cortex, reduction of NMDA-evoked currents and NMDA receptor-mediated EPSCs has also been found when D4 receptors are activated, and this D4 inhibition of NMDA receptor was dependent on the inhibition of protein kinase A and activation of protein phosphatase 1 (PP1) (Wang et al., 2003).

In this project, D2 receptor activation by a D2 agonist, quinpirole (40 nM or 1 μM) decreased NMDA receptor whole-cell currents in most striatal neurons; however, statistically significant attenuation was only found when a higher concentration (1 μM) of quinpirole was applied. This suggests D2 receptors inhibit NMDA receptors in a concentration-dependent manner. Moreover a general G protein inhibitor, GDP-β-S, successfully abolished the significant inhibition induced by D2 activation suggesting a G-protein-dependent mechanism underlies the D2 attenuation of NMDA receptors in the striatum.

Dopamine D2-like receptors are characterized by their inhibition of adenylate cyclase via Gi proteins (Onali et al., 1985) and consequently less cAMP accumulation which results in less PKA activity in the central nervous system. DARPP-32 is phosphorylated by PKA, and its phosphorylation forms are a potent inhibitor of PP1 which causes NMDA receptor dephosphorylation (Greengard 2001). Thus D2 activation in the striatum may result in less DARPP-32 phosphorylation and more PP1 activity, which ultimately inhibits NMDA receptor activity by dephosphorylation.

Activation of D2 receptors have been shown to reduce L-type Ca^{2+} currents in striatal medium spiny neurons (Hernandez-Lopez et al., 2000; Olson et al., 2005) and N-type Ca^{2+} currents in globus pallidus neurons (Stefani et al., 2002) via G protein activation. In my experiment, D2 receptor activation by quinpirole (1 μM) inhibited the high-voltage activated Ca^{2+} channel (HVA) currents, and the attenuation was mediated by G-protein activation indicating a G protein-dependent mechanism. In addition, similar to D2 receptor effects on NMDA responses, 40 nM quinpirole had no effect on HVA currents, and this implied 40 nM quinpirole may not be enough to activate sufficient D2 receptors in these brain slices.

Chapter 6

Discussion

6.1 Summary

The striatum is the main input structure of the basal ganglia. Glutamatergic afferents from the cerebral cortex, the thalamus and the limbic system mainly target medium spiny neurons (Parent and Hazrati, 1995a) and form synapses primarily at the heads of dendritic spines (Smith et al., 1994; Yung and Bolam, 2000). Medium spiny neurons are also innervated by dopaminergic inputs from the pars compacta of the substantia nigra which form synapses with dendritic elements (Smith et al., 1994; Yung and Bolam 2000). Integration of glutamatergic and dopaminergic synaptic transmission is crucial for normal striatal motor, cognitive and emotional functions. The aim of my project described in this thesis was to investigate how dopamine receptors modulate NMDA receptor activity in medium spiny neurons and to investigate the mechanisms underlying this regulation.

Dopamine has complex effects on striatal neurons. Dopamine D1 receptors are abundant in the substance P containing projection neurons which send GABAergic inputs to the internal globus pallidus, whereas D2 receptors are enriched in enkephalin medium spiny neurons which project to the external globus pallidus (Le Moine et al., 1995; Le Moine et al., 1991). According to the conceptual model of the basal ganglia circuitry (Albin et al., 1989; Alexander and Crutcher 1990), dopamine D1 receptors are functionally excitatory in the medium spiny neurons which send GABAergic inputs to internal globus pallidus,

and result in more inhibition in the internal globus pallidus and via the direct pathway ultimately facilitates thalmo-cortical circuits. However dopamine via D2 receptors also dampens striatal GABAergic inputs to external globus pallidus and this eventually also facilitates thalmo-cortical circuits via the indirect pathway.

NMDA receptors are one of the major ionotropic glutamate receptors mediating excitatory synaptic transmission in the striatum. Thanks to this high permeability for Ca^{2+}, activation of NMDA receptors elevates intracellular Ca^{2+}. The transient increase of cytoplasmic Ca^{2+} activates a number of Ca^{2+}-dependent enzymes and triggers a series of intracellular events such as long-lasting modifications of synaptic strength. Nevertheless, excessive stimulation of the NMDA receptors causes a massive influx of extracellular Ca^{2+} that leads to cell death.

In chapter 3 I showed that NMDA receptor whole-cell currents were inhibited by D1 receptor activation in striatal medium spiny neurons. This modulation was G protein-independent and mediated by a non-receptor Src family tyrosine kinase. Dynamin-dependent endocytosis was essential in order to observe this D1 effect on the NMDA receptor whole-cell current. Moreover, in chapter 4, application of a D1 agonist to outside-out patches did not affect the NMDA receptor single channel properties suggesting a receptor number change in the cell surface could underlie the D1 inhibition of whole-cell currents. These results suggest activation of D1 receptors can depress the strength of striatal excitation by decreasing NMDA receptor activity. Perhaps D1 receptor inhibition of NMDA receptors may reduce the strength of glutamate transmission from the cerebral cortex and therefore influence the impact of the direct pathway (relative to

the indirect pathway) in the basal ganglia circuitry. This may suggest a way for the striatum to balance activity in the direct and indirect pathways.

In chapter 5, experiments were carried out to test the effect of D2 receptor activation on NMDA responses in medium spiny neurons. Unlike D1 receptors, D2 receptor decreased NMDA receptor whole-cell currents via G protein activation. Hence dopamine may act on D2 receptors in the indirect pathway of the basal ganglia circuitry to weaken the efficacy of excitatory projections from the cerebral cortex partly via inhibition of NMDA receptors.

6.2 Important differences between my results and other publications

6.2.1 Potentiation or inhibition

The classical adenylate cyclase pathway involving G_S G protein stimulation has been the most popular hypothesis suggested by Greengard's group to interpret D1 receptor modulation of NMDA receptors (Blank et al., 1997; Snyder et al., 1998; Greengard, 2001). They suggested D1 receptor activation increases AC activity via G protein stimulation. Consequently more cAMP is accumulated which augments PKA phosphorylation of DARPP-32. The phosphorylated form of DARPP-32 is crucial for the D1 receptor to increase NMDA receptor activity because it inhibits PP1 dephosphorylation of NMDA receptors (Wang et al., 1994).

However, this mechanism was not evident in my experiments. First instead of D1 enhancement of NMDA receptor currents, I observed a D1 inhibition in striatal medium spiny neurons. Secondly D1 inhibition of NMDA receptor currents could not be either abolished by intracellular application of GDP-β–S (an inhibitor of G protein function) or occluded by GTP-γ–S (an irreversible activator of G proteins), which strongly suggests that D1 receptor activation attenuates NMDA receptor currents by a G protein-independent mechanism. Finally, the PKA inhibitor H-89 did not affect D1 inhibition. Therefore, my results imply a mechanism other than the G protein-dependent classic pathway for D1 modulation of NMDA receptor activity in striatal medium spiny neurons from 7 day-old rats.

Ca^{2+} has also been nominated for D1 modulation of NMDA receptors. Cepeda's group (Cepeda et al., 1998a) showed that L-type Ca^{2+} channel blockers reduced D1-induced potentiation in medium spiny neurons suggesting an involvement of L-type Ca^{2+} conductance in D1 receptor potentiation of NMDA receptor currents. However, there experiments are complicated by the voltage-dependence of both the NMDA response and the Ca^{2+} current. Moreover, Chen et al. (2004) suggested the major effect of D1 receptors on NMDA responses is the inhibition of Ca^{2+}-dependent inactivation of NMDA receptor channels, and thus calmodulin and PKC were involved in D1 potentiation of NMDA receptor currents in prefrontal cortex instead of PKA or PP1. In my experiments intracellular calcium was buffered with EGTA, a slow calcium buffer which never the less might occlude some mechanisms that are calcium dependent.

Interestingly most of those studies showing D1 enhanced NMDA receptor responses were performed in older animals (Table 6.1). For example, Blank et al. (1997) injected striatal mRNA from adult rats into oocytes; Cepeda et al. (1998a) used 12- to 18-day old rats; and Flores-Hernandez carried out these experiments on 21- to 40-day old rats. As I mentioned in the introduction, the expression patterns of NMDA receptor subunits are undergoing strict developmental regulation in the brain. Additionally, variant NMDA receptor complexes have been found at different stage of synapses formation (Kennth et al., 1999; Li et al., 1998). Therefore developmental changes in NMDA receptors may account for the dissimilar effects of D1 receptor modulation, and more importantly this indicates a changing role of dopamine receptors in synaptic modifications during developmnet.

6.2.2 NR2A or NR2B

The D1 inhibition of NMDA receptor currents observed in my experiments is consistent with that of Lee et al. (2002) (Table 6.1). They demonstrated that D1 inhibition of the peak amplitude of NMDA currents was not dependent on G protein activation, but D1 inhibition was significantly reduced when direct protein – protein interactions between the C-terminus of the D1 receptor (D1-t3) and the C-terminus of the NR2A subunit were interrupted by an intracellular peptide. Moreover, according to their results the carboxyl tail of NR2B could not form a complex with the D1 receptor directly.

Interestingly, by postnatal day 7, NR2B exhibits strongest expression among the NR2 family in the striatum, while NR2A mRNA only weakly appears (Monyer et al., 1994; Portera-Cailliau et al., 1996). It may be these receptors are located at synapses and are only a small proportion of the total whole-cell receptors at this stage. In my experiments,

I could not find evidence for the presence of functional NR2A subunits in the striatum of 7 day old rats as well. Thus another mechanism, other than direct protein-protein interactions between NR2A and D1 receptors, may dominate D1 inhibition of striatal NMDA receptors in 7 day-old rats.

6.2.3 Mechanism of D1 inhibition and hypotheses

In chapter 4, the single channel results suggested a cell surface receptor number change underlying the D1 inhibition of NMDA receptor whole cell currents and confirmed the SKF-82958 has no direct effect on the NMDA receptor. Moreover both the non-receptor Src tyrosine kinase and dynamin-dependent endocytosis were essential for D1 inhibition of NMDA receptor responses in my experiment. Therefore it is likely that D1 receptor modulation of the NMDA receptor activity occurs via an influence on receptor internalization.

NMDA receptor NR2 subunits have one PDZ-binding motif and one tyrosine phosphorylation motif (YEKL 1472) at the C-terminal, which influence receptor internalization (Wenthold et al., 2003). NR2B has been reported to be the most prominently tyrosine phosphorylated protein in the postsynaptic density (Moon et al., 1994), and the main site of tyrosine phosphorylation of NR2B is Y1472 (Nakazawa et al., 2001). In addition the tyrosine motif has been shown to bind to AP-2 adaptor complexes allowing a rapid internalization of surface NMDA receptors (Bonifacino and Dell'Angelica 1999; Lavezzari et al., 2003). Moreover in recombinant NR1/NR2A

receptors, dephosphorylation of a ring formed with tyrosine 842 in NR2A and tyrosine 837 in NR1 has been suggested to reduce the number of functional NMDA receptor channels by allowing AP-2 binding (Vissel et al., 2001). Roche et al (2001) demonstrated that the YEKL motif regulates a robust endocytosis of NMDA receptors in cultured neurons and there was a developmental decline in NMDA receptor endocytosis as neurons mature. This is consistent with a decrease of NR2B subunits together with an increase of NR2A subunits while neurons are maturing (Watanabe et al., 1993; Wenzel et al., 1997; Monyer et al., 1994; and Laurie et al., 1997).

Developmental change in NR2 subunit expression appears to influence the surface stability of NMDA receptors (Lavezzari et al., 2004). Lavezzari et al. (2004) showed NR2B subunits exhibited more robust endocytosis than NR2A subunits and, instead of a tyrosine-based endocytic motif (YEKL) in NR2B subunits, NR2A endocytosis was regulated by a dileucine motif (leucine 1320) at the NR2A C-terminal. They suggested that the extrasynaptic location of NR2B subunits may be the reason for the NR2B robust endocytosis as these receptors may not be stabilized by contact with the synaptic scaffolding protein PSD-95. Subsequently they tested endocytosis at earlier developmental times in hippocampal neurons while synapses are still developing; NR2A and NR2B underwent similar endocytosis, and truncation of the dileucine motif did not affect the NR2A endocytosis significantly suggesting NR2A subunits may use variant endocytosis motifs at different developmental stages. Therefore, non-receptor tyrosine kinases may play a key role in regulating NMDA receptor internalization especially for NR2B containing receptors at earlier brain developmental stages.

PSD-95 is abundant in the postsynaptic density (PSD) and is a membrane associated guanylate kinase-like protein (MAGUKs), contributing to anchoring NMDA receptors at the synapse (Wenthold et al., 2003; Chung et al., 2004; and Lin et al., 2004). PSD-95 associates with the last four amino acids (ESDV) of the NR2 subunit (Kornau et al., 1995; Niethammer et al., 1996) and this binding site is very close to Y1472 (Nakazawa et al., 2001), the main site of tyrosine phosphorylation. Roche et al (2001) suggested that tyrosine phosphorylation of the NMDA receptor could inhibit the receptor's interaction with PSD-95. They concluded that the disruption of the NMDA receptor-PSD-95 complex destabilized the NMDA receptor, thereby allowing receptor internalization. Similarly phosphorylation of NR2B subunits at a serine residue (Ser1480) has been show to disrupt the PSD association with NMDA receptors and decrease NR2B expression on the cell surface (Chung et al., 2004).

So I suggest in my experiments that tyrosine kinase phosphorylation of the C-terminal of NR2B subunits may interfere with PSD-95 anchoring of NMDA receptors. As a result, fewer NMDA receptors remain on the cell surface producing smaller whole cell currents after D1 receptor activation, and more NMDA receptors internalize via the dynamin dependent pathway (Figure 6.1).

Figure 6.1 A hypothesis for dopamine receptor modulation of NMDA receptors in the striatum

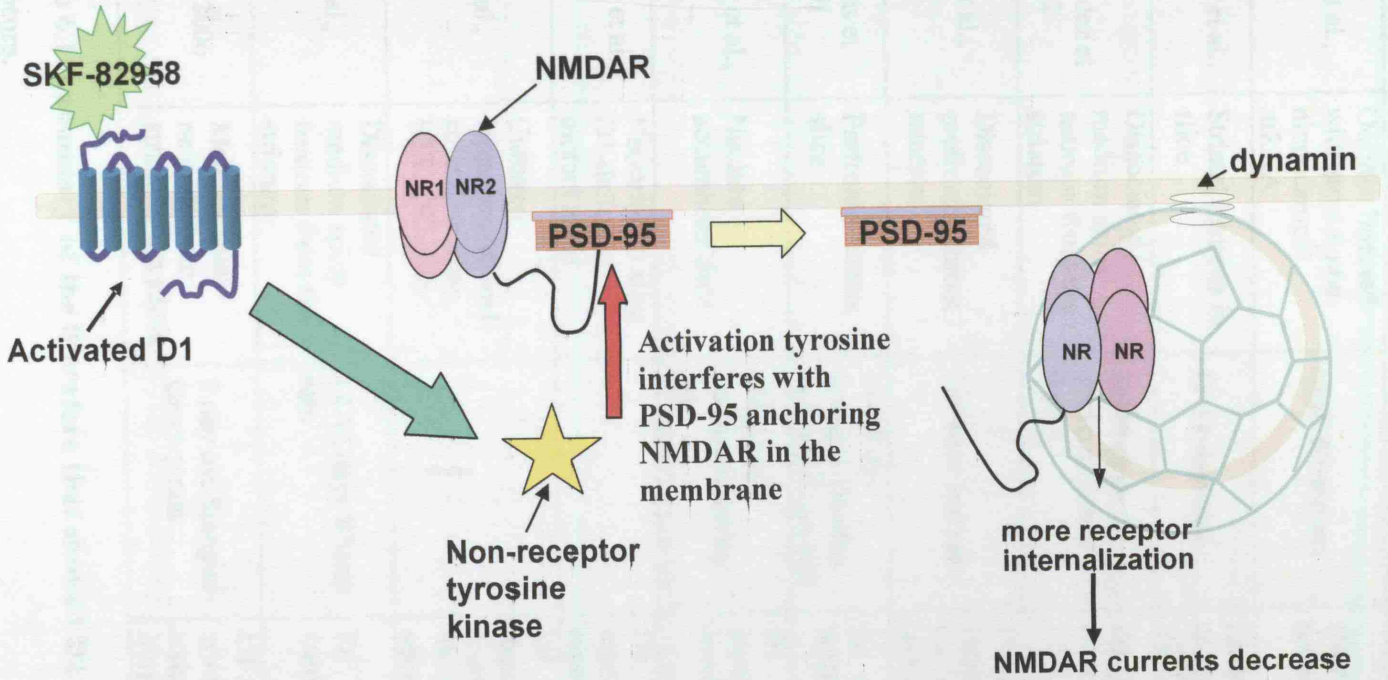

The hypothesis: When the D1 receptor is activated, it may activate non-receptor tyrosine kinase although the pathway mediating this is not clear. The activation of non-receptor tyrosine kinase may disrupt the association of the NMDA receptor with PSD-95, and then the NMDA receptor can be released from the cell surface. Consequently more NMDA receptors traffic to intracellular compartments via dynamin-dependent endocytosis, and the NMDA receptor whole-cell currents decrease.

Authors	Neuron type	Animal age	D1 receptor modulation of NMDA receptors
Blank et al., 1997	Oocytes injected with striatal and hippocampal mRNA	adult Wistar rats	DARPP-32 mediated cAMP-dependent potentiation of NMDA responses.
Cepeda et al., 1998	Striatal neurons in slice	12-18 days rats	L-type Ca^{2+} channel contributed to D1 receptor-induced potentiation of NMDA whole-cell current.
Flores-Hernandez et al., 2002	Dissociated medium spiny neurons from the striatum	21-40 days Sprague-Dawley rats	D1 potentiation of NMDA whole-cell current was mediated by DARPP-32 but not L-type Ca^{2+} channels.
Chen et al., 2004	Dissociated prefrontal cortex neurons	3-5 week old rats	D1 potentiation of NMDA whole-cell current involved PKC and reduction of Ca^{2+}/Calmodulin-dependent inactivation of NMDA receptors
Seamans et al., 2001	Prefrontal cortex slice	14-20 day Sprague-Dawley or Long-Evan rats	D1 activation selectively increased the NMDA component of EPSCs.
Synder et al., 1998	Nucleus accumbens slice	150g-200g Sprague-Dawley rats	D1 activation increased NR1 phosphorylation. DARPP-32 and PKA involved.
Levine et al., 1996	Neostriatum slice D1-deficient mutant mice		D1 agonist increased responses mediated by activation of NMDA receptors.
Lee et al., 2002	Cultured hippocampal and striatal neurons, HEK-293 cells		D1 inhibition of NMDA currents was dependent on direct protein-protein interaction between the C-terminus of the D1 receptor (D1-t3) and the NR2A subunit.
Lin et al., 2003	Dissociated medium spiny neurons from the striatum	14-12 days Wistar rats	D1 agonist reduced NMDA induced currents.
Tong, 2006	Medium spiny neurons from striatal brain slices	7 day old Sprague-Dawley rats	D1 activation inhibited NMDA receptor whole-cell current by G protein-independent but tyrosine kinase and dynamin-dependent pathway.

Table 6.1 A summary of the literature that showed D1 receptor modulation of NMDA receptors.

6.3 Future experiments

6.3.1 Biochemical measurement of surface-expressed receptors

Although the results from single-channel recordings and dynamin inhibitory peptide experiments strongly support the hypothesis that D1 receptor inhibition of the NMDA whole-cell current is caused by increasing the internalization of NMDA receptors, it would be very helpful to directly investigate the exact change of NMDA receptor surface expression biochemically.

In striatum brain slices, the biotin-avidin system can be utilized to recognize all surface proteins (Wang et al., 2003), and the amount of NR1 protein on the cell surface can then be detected with electrophoresis followed by western blotting using an NR1 antibody. In order to investigate the effect of D1 activation on NR1 surface expression, striatal slices will be treated with D1 agonist SKF-82958 before using the biotin-avidin system to measure changes in the proportion of surface receptors compared to intracellular receptors.

6.3.2 D1 modulation of NMDA receptors in adult rat striatum

Conflicting results have been demonstrated for D1 receptor modulation of NMDA receptors in the striatum in rats of different ages. D1 modulation of NMDA receptors might be a developmental phenomenon. NMDA receptor expression is strictly controlled during development. NR2B is enriched in the striatum in the first postnatal week, while NR2A expression is gradually increased during the second and third postnatal weeks. Dopamine

receptors may selectively regulate the different NMDA receptor complexes by variant mechanism depending on the developmental stage.

Although I found D1 receptor activation had inconsistent effects on the NMDA receptor currents in striatal neurons from 3 week-old rats, more experiments could be carried out at higher D1 receptor agonist concentrations with adult rats. Flores-Hernandez et al. (2002) showed in 21-40 day old rats that the D1 agonist SKF-81297 enhanced NMDA currents in a concentration dependent manner, and the EC50 for this D1 effect was about 300 nM.

6.3.3 D1 modulation of the NMDA component of EPSCs

Although whole-cell currents can reflect both synaptic and extrasynaptic receptor activity, they have been reported to be mainly dominated by the extrasynaptic population (Tovar and Westbrook, 1999). Moreover distinct subunit compositions of NMDA receptors have been found in synapses and extrasynaptic areas. NR2B subunits are predominant at extrasynaptic sites, whereas NR2A subunits mainly occur in the synapses (Li et al., 1998; Tovar and Westbrook, 1999).

Hence there might be differential regulation of synaptic and extrasynaptic receptors by dopamine receptors because of intrinsic receptor properties and determined by their location. For instance, D1 agonist has been shown to increase the NMDA component of excitatory postsynaptic currents (EPSCs) in prefrontal cortex and the hippocampus (Yang, 2000; Seamans et al., 2000). Hence, it would be very interesting to investigate dopamine

receptor modulation of synaptic NMDA receptors by recording the NMDA component of EPSCs in the striatum, which will help to understand the interaction between the glutamatergic and dopaminergic input at the single cell level in the striatum.

6.3.4 Animal models of Parkinson's disease

In Parkinson's disease, the loss of dopamine-producing neurons in the substantia nigra pars compacta (SNc) results in a radical depletion of dopamine in the striatum as well as functional changes in the whole basal ganglia network (Lotharius and Brundin, 2002; Hornykiewicz, 2000). Under this pathological condition, both NMDA receptors and dopamine receptors may function abnormally because of an imbalance between glutamate and dopamine mediated synaptic transmission. Striatal dopamine denervation has been shown to alter NR1 subunit expression (Betarbet et al., 2004; Lai et al., 2003) and elevate NR2A subunit expression (Oh et al., 1999). Therefore, to test dopamine receptor modulation of NMDA receptor activity under dopaminergic denervation in Parkinson's animal models will be important in relation to the clinical significance of this work.

References

Afifi AK, Bergman BA (1998) Functional Neuroanatomy, M'Graw-Hll, New York

Aizman O, Brismar H, Uhlen P, Zettergren E, Levey AI,Forssberg H,Greengard P,Aperia A (2000) Anatomical and physiological evidence for D1 and D2 dopamine receptor colocalization in neostriatal neurons. Nat Neurosci. 3:226-30.

Akiyama T, Ishida J, Nakagawa S, Ogawara H, Watanabe S, Itoh N, Shibuya M, Fukami Y (1987) Genistein, a specific inhibitor of tyrosine-specific protein kinases. J Biol Chem. 262:5592-5.

Albin RL, Young AB, Penney JB (1989). The functional anatomy of basal ganglia disorders. Trends Neurosci. 12:366-75

Albin RL (1995) The pathophysiology of Chorea/Ballism and Parkinsonism. Parkinsonism & Related Disorders 1:3-11

Alexander GE, Crutcher, ME (1990) Functional architecture of basal ganglia circuits: neural substrates of parallel processing. Trends Neurosci 13, 266-271

Ali DW, Salter MW (2001) NMDA receptor regulation by Src kinase signalling in excitatory synaptic transmission and plasticity. Curr Opin Neurobiol. 11:336-42.

Anson LC, Chen PE, Wyllie DJ, Colquhoun D, Schoepfer R. (1998) Identification of amino acid residues of the NR2A subunit that control glutamate potency in recombinant NR1/NR2A NMDA receptors. J Neurosci. 18:581-9.

Arundine M, Tymianski M. (2004) Molecular mechanisms of glutamate-dependent neurodegeneration in ischemia and traumatic brain injury. Cell Mol Life Sci.61:657-68.

Beckstead RM. (1985) Complementary mosaic distributions of thalamic and nigral axons in the caudate nucleus of the cat: double anterograde labeling combining autoradiography and wheat germ-HRP histochemistry.Brain Res. 335:153-9.

Behe, P., Wyllie, D.J., Nassar, M., Schoepfer, R., Colquhoun, D. (1995). Determination of NMDA NR1 subunit copy number in recombinant NMDA receptors. Proceedings of the Royal Society, London, B, 262: 205-213.

Behe P, Colquhoun D, Wyllie DJ: (1999) Activation of single AMPA- andNMDA-type glutamate-receptor channels. In Ionotropic Glutamate Receptors in the CNS. Edited by Jonas P, Monyer H. Springer; Berlin:175-218.

Benquet P, Gee CE, Gerber U (2002) Two distinct signaling pathways upregulate NMDA receptor responses via two distinct metabotropic glutamate receptor subtypes. J Neurosci. 22:9679-86.

Benveniste M, Mayer ML (1991) Kinetic analysis of antagonist action at N-methyl-D-aspartic acid receptors. Two binding sites each for glutamate and glycine. Biophys J. 59:560-73.

Betarbet R, Poisik O, Sherer TB, Greenamyre JT (2004) Differential expression and ser897 phosphorylation of striatal N-methyl-d-aspartate receptor subunit NR1 in animal models of Parkinson's disease. Exp Neurol. 187:76-85.

Blahos J 2nd, Wenthold RJ. (1996) Relationship between N-methyl-D-aspartate receptor NR1 splice variants and NR2 subunits. J Biol Chem. 271:15669-74.

Blandini F, Nappi G, Tassorelli C, Martignoni E (2000) Functional changes of the basal ganglia circuitry in Parkinson's disease. Prog Neurobiol. 62:63-88.

Blank T, Nijholt I, Teichert U, Kugler H, Behrsing H, Fienberg A, Greengard P, Spiess J (1997) The phosphoprotein DARPP-32 mediates cAMP-dependent potentiation of striatal N-methyl-D-aspartate responses. Proc Natl Acad Sci U S A 94:14859-64.

Bliss TV, Collingridge GL. (1993) A synaptic model of memory: long-term potentiation in the hippocampus. Nature. 361:31-9.

Bolam JP, Hanley JJ, Booth PA, Bevan MD. (2000) Synaptic organisation of the basal anglia. J Anat. 196:527-42.

Bonifacino JS, Dell'Angelica EC (1999) Molecular bases for the recognition of tyrosine-based sorting signals. J Cell Biol. 145:923-6.

Brickley SG, Misra C, Mok MH, Mishina M, Cull-Candy SG (2003) NR2B and NR2D subunits coassemble in cerebellar Golgi cells to form a distinct NMDA receptor subtype restricted to extrasynaptic sites. J Neurosci. 23:4958-66.

Calabresi P, Pisani A, Mercuri NB, Bernardi G (1992) Long-term Potentiation in the Striatum is Unmasked by Removing the Voltage-dependent Magnesium Block of NMDA Receptor Channels. Eur J Neurosci. 4:929-935.

Calabresi P, Saiardi A, Pisani A, Baik JH, Centonze D, Mercuri NB, Bernardi G, Borrelli E. (1997) Abnormal synaptic plasticity in the striatum of mice lacking dopamine D2 receptors. J Neurosci.17:4536-44.

Calabresi P, Centonze D, Gubellini P, Pisani A, Bernardi G. (2000a) Acetylcholine-mediated modulation of striatal function. Trends Neurosci. Mar;23:120-6.

Calabresi P, Centonze D, Bernardi G. (2000b) Electrophysiology of dopamine in normal and denervated striatal neurons. Trends Neurosci. 23:S57-63.

Calabresi P, Gubellini P, Centonze D, Picconi B, Bernardi G, Chergui K, Svenningsson P, Fienberg AA, Greengard P (2000c) Dopamine and cAMP-regulated phosphoprotein 32 kDa controls both striatal long-term depression and long-term potentiation, opposing forms of synaptic plasticity. J Neurosci. 20:8443-51.

Canteras NS, Shammah-Lagnado SJ, Silva BA, Ricardo JA. (1990) Afferent connections of the subthalamic nucleus: a combined retrograde and anterograde horseradish peroxidase study in the rat. Brain Res 513, 43-59

Carroll RC, Beattie EC, Xia H, Luscher C, Altschuler Y, Nicoll RA, Malenka RC, von Zastrow M.(1999) Dynamin-dependent endocytosis of ionotropic glutamate receptors. Proc Natl Acad Sci U S A. 96:14112-7.

Centonze D, Picconi B, Gubellini P, Bernardi G, Calabresi P (2001) Dopaminergic control of synaptic plasticity in the dorsal striatum. Eur J Neurosci. 13:1071-7.

Centonze D, Grande C, Saulle E, Martin AB, Gubellini P, Pavon N, Pisani A, Bernardi G, Moratalla R, Calabresi P (2003) Distinct roles of D1 and D5 dopamine receptors in motor activity and striatal synaptic plasticity. J Neurosci. 23:8506-12.

Cepeda C, Buchwald NA, Levine MS (1993) Neuromodulatory actions of dopamine in the neostriatum are dependent upon the excitatory amino acid receptor subtypes activated. Proc Natl Acad Sci U S A. 1993 Oct 15;90(20):9576-80.

Cepeda C, Colwell CS, Itri JN, Chandler SH, Levine MS (1998a) Dopaminergic modulation of NMDA-induced whole cell currents in neostriatal neurons in slices: contribution of calcium conductances. J Neurophysiol 79:82-94.

Cepeda C, Colwell CS, Itri JN, Gruen E, Levine MS (1998b) Dopaminergic modulation of early signs of excitotoxicity in visualized rat neostriatal neurons. Eur J Neurosci. 10:3491-7.

Charpier S, Deniau JM (1997) In vivo activity-dependent plasticity at cortico-striatal connections: evidence for physiological long-term potentiation.Proc Natl Acad Sci U S A. 94:7036-40.

Chatterton JE, Awobuluyi M, Premkumar LS, Takahashi H, Talantova M, Shin Y, Cui J, Tu S, Sevarino KA, Nakanishi N, Tong G, Lipton SA, Zhang D (2002) Excitatory glycine receptors containing the NR3 family of NMDA receptor subunits. Nature. 415:793-8.

Chazot PL, Stephenson FA (1997) Molecular dissection of native mammalian forebrain NMDA receptors containing the NR1 C2 exon: direct demonstration of NMDA receptors comprising NR1, NR2A, and NR2B subunits within the same complex. J Neurochem. 69:2138-44.

Chen G, Greengard P, Yan Z (2004) Potentiation of NMDA receptor currents by dopamine D1 receptors in prefrontal cortex. Proc Natl Acad Sci U S A 101:2596-600.

Chen PE, Wyllie DJ. (2006) Pharmacological insights obtained from structure-function studies of ionotropic glutamate receptors. Br J Pharmacol. [Epub ahead of print]

Chesselet MF, Delfs JM (1996) Basal ganglia and movement disorders: an update. Trends Neurosci 19:417-22.

Choi DW (1994) Glutamate receptors and the induction of excitotoxic neuronal death. Prog Brain Res. 100:47-51.

Chung HJ, Huang YH, Lau LF, Huganir RL (2004) Regulation of the NMDA receptor complex and trafficking by activity-dependent phosphorylation of the NR2B subunit PDZ ligand. J Neurosci. 24:10248-59.

Ciabarra AM, Sullivan JM, Gahn LG, Pecht G, Heinemann S, Sevarino KA. (1995) Cloning and characterization of chi-1: a developmentally regulated member of a novel class of the ionotropic glutamate receptor family. J Neurosci.15:6498-508.

Colquhoun D, Sigworth FJ (1995). Fitting and statistical analysis of single-channel records. In Single-Channel Recording, 2nd Edition, edited by Sakmann, B. & Neher, E., pp 483-587. Plenum Press, New York.

Conn PJ Pin JP (1997) Pharmacology and functions of metabotropic glutamate receptors. Annu Rev Pharmacol Toxicol.37:205-37.

Cull-Candy S, Brickley S, Farrant M.(2001) NMDA receptor subunits: diversity, development and disease. Curr Opin Neurobiol. 11:327-35.

Cull-Candy SG, Leszkiewicz DN (2004) Role of distinct NMDA receptor subtypes at central synapses. Sci STKE. 255:re16.

Das S, Sasaki YF, Rothe T, Premkumar LS, Takasu M, Crandall JE, Dikkes P, Conner DA, Rayudu PV, Cheung W, Chen HS, Lipton SA, Nakanishi N. (1998) Increased NMDA current and spine density in mice lacking the NMDA receptor subunit NR3A. Nature. 393:377-81.

DeLong MR (1990) Primate models of movement disorders of basal ganglia origin. Trends Neurosci. 13:281-5.

Dingledine R, Borges K, Bowie D, Traynelis SF. (1999) The glutamate receptor ion channels. Pharmacol Rev. 51:7-61.

Dunah AW, Luo J, Wang YH, Yasuda RP, Wolfe BB. (1998) Subunit composition of N-methyl-D-aspartate receptors in the central nervous system that contain the NR2D subunit. Mol Pharmacol. 53:429-37.

Dunah AW, Standaert DG (2001) Dopamine D1 receptor-dependent trafficking of striatal NMDA glutamate receptors to the postsynaptic membrane. J Neurosci. 21:5546-58.

Dunah AW, Standaert DG (2003) Subcellular segregation of distinct heteromeric NMDA glutamate receptors in the striatum. J Neurochem. 85:935-43.

Dunah AW, Sirianni AC, Fienberg AA, Bastia E, Schwarzschild MA, Standaert DG (2004) Dopamine D1-dependent trafficking of striatal N-methyl-D-aspartate glutamate receptors requires Fyn protein tyrosine kinase but not DARPP-32. Mol Pharmacol 65:121-9.

Durand GM, Bennett MV, Zukin RS. (1993) Splice variants of the N-methyl-D-aspartate receptor NR1 identify domains involved in regulation by polyamines and protein kinase C. Proc Natl Acad Sci U S A. 90:6731-5.

Dzubay JA, Jahr CE. (1996) Kinetics of NMDA channel opening. J Neurosci. 16:4129-34.

Edwards F.A, Konnerth A, Sakmann B, Takahashi, T. (1989) A slice preparation for patch clamp recordings from synaptically connected neurons of the mammalian central nervous system. Pflugers Archives European Journal of Physiology, 414: 600-612.

Edwards F.A, Konnerth A., (1992) Patch-clamping cells in sliced tissue preparations. Methods in Enzymology, 207: 208-222

Ehlers, M.D., Tingley, W.G., Huganir, R.L. (1995). Regulated subcellular distribution of the NR1 subunit of the NMDA receptor. Science, 269: 1734-1737.

Flores-Hernandez J, Cepeda C, Hernandez-Echeagaray E, Calvert CR, Jokel ES, Fienberg AA, Greengard P, Levine MS (2002) Dopamine enhancement of NMDA currents in dissociated medium-sized striatal neurons: role of D1 receptors and DARPP-32. J Neurophysiol 88:3010-20.

Forsythe ID, Westbrook GL. (1988) Slow excitatory postsynaptic currents mediated by N-methyl-D-aspartate receptors on cultured mouse central neurones. J Physiol. 396:515-33.

Fremeau RT Jr, Duncan GE, Fornaretto MG, Dearry A, Gingrich JA, Breese GR, Caron MG (1991) Localization of D1 dopamine receptor mRNA in brain supports a role in cognitive, affective, and neuroendocrine aspects of dopaminergic neurotransmission. Proc Natl Acad Sci U S A. 88:3772-6.

Freund TF, Powell JF, Smith AD. (1984) Tyrosine hydroxylase-immunoreactive boutons in synaptic contact with identified striatonigral neurons, with particular reference to dendritic spines. Neuroscience. 13:1189-215.

Furukawa H, Singh SK, Mancusso R, Gouaux E. (2005) Subunit arrangement and function in NMDA receptors. Nature. 438:185-92.

Gerfen CR, Engber TM, Mahan LC, Susel Z, Chase TN, Monsma FJ Jr, Sibley DR. (1990) D1 and D2 dopamine receptor-regulated gene expression of striatonigral and striatopallidal neurons. Science. 250:1429-32.

Gernot Riedel, Bettina Platt, Jacques Micheau (2003) Glutamate receptor function in learning and memory Behavioural Brain Research 140 1-47

Gibb, A.J. & Colquhoun, D. (1992). Activation of N-Methyl-D-Aspartate receptors by L-glutamate in cells dissociated from adult rat hippocampus. Journal of Physiology, 456: 143-179.

Gibb, A.J. & Colquhoun, D. (1991). Glutamate activation of a single NMDA receptor-channel produces a cluster of channel openings. Proceedings of the Royal Society, London B., 456: 143-179.

Gibb, A.J. & Edwards, F. A. (1994). Pacth clamp recording from cells in sliced tissues. In Microelectrode Techniques, 2nd Edition, Edited by Odgen, D., pp. 255-274.

Goebel DJ, Poosch MS.(1999) NMDA receptor subunit gene expression in the rat brain: a quantitative analysis of endogenous mRNA levels of NR1Com, NR2A, NR2B, NR2C, NR2D and NR3A. Brain Res Mol Brain Res. 69:164-70.

Gotz T, Kraushaar U, Geiger J, Lubke J, Berger T, Jonas P (1997) Functional properties of AMPA and NMDA receptors expressed in identified types of basal ganglia neurons. J Neurosci 17:204-15.

Greengard P (2001) The neurobiology of slow synaptic transmission. Science 294:1024-30.

Groenewegen HJ, Berendse HW.(1990) Connections of the subthalamic nucleus with ventral striatopallidal parts of the basal ganglia in the rat. J Comp Neurol.294:607-22.

Grosshans DR, Clayton DA, Coultrap SJ, Browning MD (2002) LTP leads to rapid surface expression of NMDA but not AMPA receptors in adult rat CA1. Nat Neurosci.5:27-33.

Hallett PJ, Standaert DG (2004) Rationale for and use of NMDA receptor antagonists in Parkinson's disease. Pharmacol Ther 102:155-74.

Hamill O. P, Marty A., Neher E, Sakmann B, Sigworth, F. J. (1981) Improved patch clamp techniques for high resolution current recording from cells and cell-free membrane patches. Pflügers Archives, 391: 85-100.

Hanke JH, Gardner JP, Dow RL, Changelian PS, Brissette WH, Weringer EJ, Pollok BA, Connelly PA. (1996) Discovery of a novel, potent, and Src family-selective tyrosine kinase inhibitor. Study of Lck- and Fyn-dependent T cell activation. J Biol Chem. 271:695-701.

Hardingham GE, Bading H (2003).The Yin and Yang of NMDA receptor signalling. Trends Neurosci. 26:81-9.

Hassani OK, Mouroux M, Feger J. (1996) Increased subthalamic neuronal activity after nigral dopaminergic lesion independent of disinhibition via the globus pallidus. Neuroscience. 72:105-15

Hassani, O.K., Feger, J., Yelnik, J., Francois, C., (1997) Evidence for a dopaminergic innervation of the subthalamic nucleus in the rat. Brain Res 749, 88-94

Hatton CJ, Paoletti P. (2005) Modulation of triheteromeric NMDA receptors by N-terminal domain ligands. Neuron.46(2):261-74.

Hedreen, J.C., (1999) Tyrosine hydroxylase-immunoreactive elements in the human globus pallidus and subthalamic nucleus. J. Comp. Neurol 409, 400-410.
Hernandez-Lopez S, Tkatch T, Perez-Garci E, Galarraga E, Bargas J, Hamm H, Surmeier DJ (2000) D2 dopamine receptors in striatal medium spiny neurons reduce L-type Ca2+ currents and excitability via a novel PLC[beta]1-IP3-calcineurin-signaling cascade. J Neurosci. 20:8987-95.

Heuss C, Scanziani M, Gahwiler BH, Gerber U (1999) G-protein-independent signaling mediated by metabotropic glutamate receptors. Nat Neurosci. 2:1070-7.

Hollmann, M., Boulter, J., Maron, C., Beasley, L., Sullivan, J., Pecht, G., Heinemann, S. (1993). Zinc potentiates agonist-induced currents at certain splice variants of the NMDA receptor. Neuron, 10: 943-954.

Honer M, Benke D, Laube B, Kuhse J, Heckendorn R, Allgeier H, Angst C, Monyer H, Seeburg PH, Betz H, Mohler H (1998) Differentiation of glycine antagonist sites of N-methyl-D-aspartate receptor subtypes. Preferential interaction of CGP 61594 with NR1/2B receptors. J Biol Chem.;273:11158-63.

Hornykiewicz, O (2000) Parkinson Disease. In: Encyclopedia of Life Sciences. John Wiley & Sons, Ltd: Chichester http://www.els.net/

Hossain MA (2005) Molecular mediators of hypoxic-ischemic injury and implications for epilepsy in the developing brain. Epilepsy and behavior 7 204-213.

Hrabetova S, Serrano P, Blace N, Tse HW, Skifter DA, Jane DE, Monaghan DT, Sacktor TC (2000) Distinct NMDA receptor subpopulations contribute to long-term potentiation and long-term depression induction. J Neurosci. 20:RC81.

Hsu CY, Persons PE, Spada AP, Bednar RA, Levitzki A, Zilberstein A (1991) .Kinetic analysis of the inhibition of the epidermal growth factor receptor tyrosine kinase by Lavendustin-A and its analogue. J Biol Chem.266:21105-12.

Huh KH, Wenthold RJ. (1999) Turnover analysis of glutamate receptors identifies a rapidly degraded pool of the N-methyl-D-aspartate receptor subunit, NR1, in cultured cerebellar granule cells. J Biol Chem. 274:151-7.

Jain M, Armstrong RJ, Barker RA, Rosser AE. (2001) Cellular and molecular aspects of striatal development. Brain Res Bull.55:533-40

Jin DH, Jung YW, Ko BH, Moon IS (1997) Immunoblot analyses on the differential distribution of NR2A and NR2B subunits in the adult rat brain. Mol Cells. 7:749-54.

Johnson JW, Ascher P (1987) Glycine potentiates the NMDA response in cultured mouse brain neurons. Nature. 325:529-31.

Jones S, Gibb AJ (2005) Functional NR2B- and NR2D-containing NMDA receptor channels in rat substantia nigra dopaminergic neurones. J Physiol. 569(Pt 1):209-21. Epub 2005 Sep 1.

Kawaguchi Y. (1997) Neostriatal cell subtypes and their functional roles. Neurosci Res. 27:1-8.

Kebabian John W, Frank I. Tarazi, Nora S. Kula and Ross J. Baldessarini.(1997) Compounds selective for dopamine receptor subtypes. Drug Discovery Today 2:333-340

Kelley AE, Domesick VB, Nauta WJ. (1982)The amygdalostriatal projection in the rat--an anatomical study by anterograde and retrograde tracing methods. Neuroscience. 7:615-30.

Kennedy MB, Beale HC, Carlisle HJ, Washburn LR (2005) Integration of biochemical signalling in spines. Nat Rev Neurosci. 6:423-34.

Kim E, Sheng M (2004) PDZ domain proteins of synapses. Nat Rev Neurosci. 5:771-81.

Kittler JT, Delmas P, Jovanovic JN, Brown DA, Smart TG, Moss SJ (2000) Constitutive endocytosis of GABAA receptors by an association with the adaptin AP2 complex modulates inhibitory synaptic currents in hippocampal neurons. J Neurosci. 20:7972-7.

Kohr G, Seeburg PH (1996) Subtype-specific regulation of recombinant NMDA receptor-channels by protein tyrosine kinases of the src family. J Physiol. 492:445-52.

Kornau HC, Schenker LT, Kennedy MB, Seeburg PH (1995) Domain interaction between NMDA receptor subunits and the postsynaptic density protein PSD-95. Science. 269:1737-40.

Koroshetz WJ, Freese A, DiFiglia M. (1990) The correlation between excitatory amino acid-induced current responses and excitotoxicity in striatal cultures. Brain Res. 521:265-72.

Kotecha SA, Oak JN, Jackson MF, Perez Y, Orser BA, Van Tol HH, MacDonald JF. (2002) A D2 class dopamine receptor transactivates a receptor tyrosine kinase to inhibit NMDA receptor transmission. Neuron. 35:1111-22.

Krupp JJ, Vissel B, Thomas CG, Heinemann SF, Westbrook GL (2002). Calcineurin acts via the C-terminus of NR2A to modulate desensitization of NMDA receptors. Neuropharmacology 42:593–602.

Kuner T, Schoepfer R (1996) Multiple structural elements determine subunit specificity of Mg2+ block in NMDA receptor channels. J Neurosci. 16:3549-58.

Kuner T, Wollmuth LP, Karlin A, Seeburg PH, Sakmann B (1996) Structure of the NMDA receptor channel M2 segment inferred from the accessibility of substituted cysteines. Neuron:343-52.

Kuppenbender KD, Albers DS, Iadarola MJ, Landwehrmeyer GB, Standaert DG. (1999) Localization of alternatively spliced NMDAR1 glutamate receptor isoforms in rat striatal neurons. J Comp Neurol. 415:204-17.

Kuppenbender KD, Standaert DG, Feuerstein TJ, Penney JB Jr, Young AB, Landwehrmeyer GB. (2000) Expression of NMDA receptor subunit mRNAs in neurochemically identified projection and interneurons in the human striatum. J Comp Neurol. 419:407-21.

Kuryatov A, Laube B, Betz H, Kuhse J. (1994) Mutational analysis of the glycine-binding site of the NMDA receptor: structural similarity with bacterial amino acid-binding proteins. Neuron. 12:1291-300.

Lai SK, Tse YC, Yang MS, Wong CK, Chan YS, Yung KK (2003) Gene expression of glutamate receptors GluR1 and NR1 is differentially modulated in striatal neurons in rats after 6-hydroxydopamine lesion. Neurochem Int. 43:639-53.

Landwehrmeyer GB, Standaert DG, Testa CM, Penney JB Jr, Young AB. (1995) NMDA receptor subunit mRNA expression by projection neurons and interneurons in rat striatum. J Neurosci. 15(7 Pt 2):5297-307.

Laube B, Hirai H, Sturgess M, Betz H, Kuhse J. (1997) Molecular determinants of agonist discrimination by NMDA receptor subunits: analysis of the glutamate binding site on the NR2B subunit. Neuron. 18:493-503.

Laurie DJ, Putzke J, Zieglgansberger W, Seeburg PH, Tolle TR (1995) The distribution of splice variants of the NMDAR1 subunit mRNA in adult rat brain. Brain Res Mol Brain Res. 32:94-108.

Laurie DJ, Bartke I, Schoepfer R, Naujoks K, Seeburg PH (1997) Regional, developmental and interspecies expression of the four NMDAR2 subunits, examined using monoclonal antibodies Brain Res Mol Brain Res. 51:23-32.

Lavezzari G, McCallum J, Lee R, Roche KW (2003) Differential binding of the AP-2 adaptor complex and PSD-95 to the C-terminus of the NMDA receptor subunit NR2B regulates surface expression. Neuropharmacology. 45:729-37.

Lavezzari G, McCallum J, Dewey CM, Roche KW (2004) Subunit-specific regulation of NMDA receptor endocytosis. J Neurosci. 24(28):6383-91.

Le Moine C, Normand E, Bloch B (1991) Phenotypical characterization of the rat striatal neurons expressing the D1 dopamine receptor gene. Proc Natl Acad Sci U S A. 88:4205-9.

Le Moine C, Bloch B (1995) D1 and D2 dopamine receptor gene expression in the rat striatum: sensitive cRNA probes demonstrate prominent segregation of D1 and D2 mRNAs in distinct neuronal populations of the dorsal and ventral striatum. J Comp Neurol. 355:418-26.

Lee FJ, Xue S, Pei L, Vukusic B, Chery N, Wang Y, Wang YT, Niznik HB, Yu XM, Liu F (2002) Dual regulation of NMDA receptor functions by direct protein-protein interactions with the dopamine D1 receptor. Cell 111:219-302.

Lei G, Xue S, Chery N, Liu Q, Xu J, Kwan CL, Fu YP, Lu YM, Liu M, Harder KW, Yu XM (2002) Gain control of N-methyl-D-aspartate receptor activity by receptor-like protein tyrosine phosphatase alpha. EMBO J 21:2977-89.

Lerma J. (2003) Roles and rules of kainate receptors in synaptic transmission. Nat Rev Neurosci. 4:481-95.

Lester RA, Jahr CE (1992) NMDA channel behavior depends on agonist affinity. J Neurosci. 12:635-43.

Levine MS, Altemus KL, Cepeda C, Cromwell HC, Crawford C, Ariano MA, Drago J, Sibley DR, Westphal H (1996) Modulatory actions of dopamine on NMDA receptor-mediated responses are reduced in D1A-deficient mutant mice. J Neurosci. 16:5870-82.

Li JH, Wang YH, Wolfe BB, Krueger KE, Corsi L, Stocca G, Vicini S (1998) Developmental changes in localization of NMDA receptor subunits in primary cultures of cortical neurons. Eur J Neurosci. 10:1704-15.

Li L, Fan M, Icton CD, Chen N, Leavitt BR, Hayden MR, Murphy TH, Raymond LA (2003) Role of NR2B-type NMDA receptors in selective neurodegeneration in Huntington disease. Neurobiol Aging. 24:1113-21

Lieberman DN, Mody I (1994) Regulation of NMDA channel function by endogenous Ca2+-dependent phosphatase. Nature 369:235–239.

Lin JY, Dubey R, Funk GD, Lipski J (2003) Receptor subtype-specific modulation by dopamine of glutamatergic responses in striatal medium spiny neurons. Brain Res 959:251-625.

Lin Y, Skeberdis VA, Francesconi A, Bennett MV, Zukin RS (2004) Postsynaptic density protein-95 regulates NMDA channel gating and surface expression. J Neurosci. 24:10138-48.

Lipton SA, Rosenberg PA. (1994) Excitatory amino acids as a final common pathway for neurologic disorders. N Engl J Med.330:613-22.

Lotharius J, Brundin P. (2002) Pathogenesis of Parkinson's disease: dopamine, vesicles and alpha-synuclein. Nat Rev Neurosci.3:932-42.

Lu WY, Xiong ZG, Lei S, Orser BA, Dudek E, Browning MD, MacDonald JF (1999) G-protein-coupled receptors act via protein kinase C and Src to regulate NMDA receptors. Nat Neurosci. 2:331-8.

Lujan R, Shigemoto R, Lopez-Bendito G. (2005) Glutamate and GABA receptor signalling in the developing brain. Neuroscience. 130:567-80.
Luscher C, Xia H, Beattie EC, Carroll RC, von Zastrow M, Malenka RC, Nicoll RA (1999) Role of AMPA receptor cycling in synaptic transmission and plasticity. Neuron. 24:649-58.

Mayer ML, Westbrook GL, Guthrie PB. (1984) Voltage-dependent block by Mg2+ of NMDA responses in spinal cord neurones. Nature. 309:261-3.

Matsuda K, Fletcher M, Kamiya Y, Yuzaki M (2003) Specific assembly with the NMDA receptor 3B subunit controls surface expression and calcium permeability of NMDA receptors. J Neurosci. 23:10064-73.

McHaffie JG, Stanford TR, Stein BE, Coizet V, Redgrave P (2005) Subcortical loops through the basal ganglia. Trends Neurosci. 28:401-7.

McManus O.B, Blatz A.L, Magleby K.L (1987). Sampling, log binning, fitting, and plotting durations of open and shut intervals from single channels and the effects of noise. Pflügers Archives, 410: 530-553.

Meador-Woodruff JH, Mansour A, Healy DJ, Kuehn R, Zhou QY, Bunzow JR, Akil H, Civelli O, Watson SJ Jr (1991) Comparison of the distributions of D1 and D2 dopamine receptor mRNAs in rat brain. Neuropsychopharmacology.5:231-42.

Memo M, Missale C, Carruba MO, Spano PF (1986) Pharmacology and biochemistry of dopamine receptors in the central nervous system and peripheral tissue. J Neural Transm Suppl. 22:19-32.

Missale C, Nash SR, Robinson SW, Jaber M, Caron MG (1998) Dopamine receptors: from structure to function. Physiol Rev. 78:189-225.

Monyer H, Burnashev N, Laurie DJ, Sakmann B, Seeburg PH (1994) Developmental and regional expression in the rat brain and functional properties of four NMDA receptors. Neuron.12:529-40.

Moon IS, Apperson ML, Kennedy MB.(1994) The major tyrosine-phosphorylated protein in the postsynaptic density fraction is N-methyl-D-aspartate receptor subunit 2B. Proc Natl Acad Sci U S A.91:3954-8.

Mori H, Masaki H, Yamakura T, Mishina M.(1992) Identification by mutagenesis of a Mg(2+)-block site of the NMDA receptor channel. Nature. 358:673-5.

Moriyoshi, K., Masu, M., Ishii, T., Shigemoto, R., Mizuno, N., Nakanishi, S. (1991) Molecular cloning and characterization of the rat NMDA receptor, Nature, 354: 31-37.

Morishita W, Connor JH, Xia H, Quinlan EM, Shenolikar S, Malenka RC (2001) Regulation of synaptic strength by protein phosphatease 1. Neuron 32:1133-48.

Mott DD, Doherty JJ, Zhang S, Washburn MS, Fendley MJ, Lyuboslavsky P, Traynelis SF, Dingledine R.(1998) Phenylethanolamines inhibit NMDA receptors by enhancing proton inhibition. Nat Neurosci. 1:659-67.

Mottola DM, Laiter S, Watts VJ, Tropsha A, Wyrick SD, Nichols DE, Mailman RB (1996) Conformational analysis of D1 dopamine receptor agonists: pharmacophore assessment and receptor mapping. J Med Chem 39:285-96.

Nakazawa T, Komai S, Tezuka T, Hisatsune C, Umemori H, Semba K, Mishina M, Manabe T, Yamamoto T (2001) Characterization of Fyn-mediated tyrosine phosphorylation sites on GluR epsilon 2 (NR2B) subunit of the N-methyl-D-aspartate receptor. J Biol Chem. 276:693-9.

Niethammer M, Kim E, Sheng M (1996) Interaction between the C terminus of NMDA receptor subunits and multiple members of the PSD-95 family of membrane-associated guanylate kinases. J Neurosci. 16:2157-63.

Nishi M, Hinds H, Lu HP, Kawata M, Hayashi Y (2001) Motoneuron-specific expression of NR3B, a novel NMDA-type glutamate receptor subunit that works in a dominant-negative manner. J Neurosci. 21:RC185.

Nong Y, Huang YQ, Ju W, Kalia LV, Ahmadian G, Wang YT, Salter MW (2003) Glycine binding primes NMDA receptor internalization. Nature. 422:302-7.

Nowak L, Bregestovski P, Ascher P, Herbet A, Prochiantz A. (1984) Magnesium gates glutamate-activated channels in mouse central neurones. Nature. 307:462-5.

Okada Y, Miyamoto T, Toda K (2003) Dopamine modulates a voltage-gated calcium channel in rat olfactory receptor neurons. Brain Res. 968:248-55.

Oh JD, Vaughan CL, Chase TN. (1999) Effect of dopamine denervation and dopamine agonist administration on serine phosphorylation of striatal NMDA receptor subunits. Brain Res. 821:433-42.

Olson PA, Tkatch T, Hernandez-Lopez S, Ulrich S, Ilijic E, Mugnaini E, Zhang H, Bezprozvanny I, Surmeier DJ (2005) G-protein-coupled receptor modulation of striatal CaV1.3 L-type Ca2+ channels is dependent on a Shank-binding domain. J Neurosci. 25:1050-62

Onali P, Olianas MC, Gessa GL (1985) Characterization of dopamine receptors mediating inhibition of adenylate cyclase activity in rat striatum. Mol Pharmacol.28:138-45.

Onoda T, Iinuma H, Sasaki Y, Hamada M, Isshiki K, Naganawa H, Takeuchi T, Tatsuta K, Umezawa K (1989) Isolation of a novel tyrosine kinase inhibitor, lavendustin A, from Streptomyces griseolavendus. J Nat Prod. 52:1252-7.

Ozawa S, Kamiya H, Tsuzuki K. (1998) Glutamate receptors in the mammalian central nervous system. Prog Neurobiol. 54:581-618.

Paoletti P, Ascher P, Neyton J (1997) High-affinity zinc inhibition of NMDA NR1-NR2A receptors. J Neurosci. 17:5711-25.

Parent A, Hazrati LA, (1995a) Functional anatomy of the basal ganglia. Part I: the cortico – basal ganglia –thalamo-cortical loop. Brain res. Rev 20, 91-127.

Perez-Otano I, Schulteis CT, Contractor A, Lipton SA, Trimmer JS, Sucher NJ, Heinemann SF.(2001) Assembly with the NR1 subunit is required for surface expression of NR3A-containing NMDA receptors. J Neurosci.21:1228-37.

Perez-Otano I, Ehlers MD. (2005) Homeostatic plasticity and NMDA receptor trafficking. Trends Neurosci. 28:229-38.

Portera-Cailliau C, Price DL, Martin LJ (1996) N-methyl-D-aspartate receptor proteins NR2A and NR2B are differentially distributed in the developing rat central nervous system as revealed by subunit-specific antibodies. J Neurochem. 66:692-700.

Purves Dale, Augustine George J, Fitzpatrick David, Katz Lawrence C, laMantia Anthony-Samuel, McNamara James O, Williams S.Mark (2001) Neuroscience second edition. Sunderland MA: Sinauer Associates, Inc.

Qian A, Buller AL, Johnson JW. (2005) NR2 subunit-dependence of NMDA receptor channel block by external Mg2+.J Physiol.562(Pt 2):319-31

Riedel G, Platt B, Micheau J. (2003) Glutamate receptor function in learning and memory. Behav Brain Res. 140:1-47

Roche KW, Standley S, McCallum J, Dune Ly C, Ehlers MD, Wenthold RJ (2001) Molecular determinants of NMDA receptor internalization. Nat Neurosci. 4:794-802.

Rutter AR, Stephenson FA (2000) Coexpression of postsynaptic density-95 protein with NMDA receptors results in enhanced receptor expression together with a decreased sensitivity to L-glutamate. J Neurochem. 75:2501-10.

Rycroft BK, Gibb AJ (2002) Direct effects of calmodulin on NMDA receptor single-channel gating in rat hippocampal granule cells. J Neurosci.22:8860-8.

Rycroft BK, Gibb AJ (2004) Inhibitory interactions of calcineurin (phosphatase 2B) and calmodulin on rat hippocampal NMDA receptors. Neuropharmacology 47:505-14.

Sakurada K, Masu M, Nakanishi S. (1993) Alteration of Ca2+ permeability and sensitivity to Mg2+ and channel blockers by a single amino acid substitution in the N-methyl-D-aspartate receptor. J Biol Chem. 268:410-5.

Salter MW (1998) Src, N-methyl-D-aspartate (NMDA) receptors, and synaptic plasticity. Biochem Pharmacol. 56:789-98.

Schmid SL (1997) Clathrin-coated vesicle formation and protein sorting: an integrated process. Annu Rev Biochem. 66:511-48.

Seamans JK, Durstewitz D, Christie BR, Stevens CF, Sejnowski TJ (2001) Dopamine D1/D5 receptor modulation of excitatory synaptic inputs to layer V prefrontal cortex neurons. Proc Natl Acad Sci U S A. 98:301-6.

Sheng M, Cummings J, Roldan LA, Jan YN, Jan LY (1994) Changing subunit composition of heteromeric NMDA receptors during development of rat cortex. Nature 368:144-7.

Sheng M, Pak DT (2000) Ligand-gated ion channel interactions with cytoskeletal and signaling proteins. Annu Rev Physiol. 62:755-78.

Sheng M, Sala C. (2001) PDZ domains and the organization of supramolecular complexes. Annu Rev Neurosci. 24:1-29

Sibley DR (1999) New insights into dopaminergic receptor function using antisense and genetically altered animals. Annu Rev Pharmacol Toxicol. 39:313-41.

Sigworth F.J, Sine S.M (1987). Data transformations for improved display and fitting of single-channel dwell time histograms. Biophysical Journal, 52: 1047-1054.

Smith, Y., Parent, A., (1988). Neurons of the subthalamic nucleus in primates display glutamate but not GABA immunoreactivity. Brain Res 453, 353-356.

Smith Y, Bennett BD, Bolam JP, Parent A, Sadikot AF (1994) Synaptic relationships between dopaminergic afferents and cortical or thalamic input in the sensorimotor territory of the striatum in monkey. J Comp Neurol.344:1-19.

Smith (1998) Microcircuitry of the direct and indirect pathway of the basal ganglia Neuroscience Vol 86 353-387

Snyder GL, Fienberg AA, Huganir RL, Greengard P. (1998) A dopamine/D1 receptor/protein kinase A/dopamine- and cAMP-regulated phosphoprotein (Mr 32 kDa)/protein phosphatase-1 pathway regulates dephosphorylation of the NMDA receptor. J Neurosci. 18:10297-303.

Snyder EM, Philpot BD, Huber KM, Dong X, Fallon JR, Bear MF (2001) Internalization of ionotropic glutamate receptors in response to mGluR activation. Nat Neurosci. 4:1079-85

Standaert DG, Testa CM, Young AB, Penney JB Jr (1994) Organization of N-methyl-D-aspartate glutamate receptor gene expression in the basal ganglia of the rat. J Comp Neurol. 343:1-16.

Standaert DG, Friberg IK, Landwehrmeyer GB, Young AB, Penney JB Jr. (1999) Expression of NMDA glutamate receptor subunit mRNAs in neurochemically identified projection and interneurons in the striatum of the rat. Brain Res Mol Brain Res. 64:11-23.

Stefani A, Spadoni F, Martorana A, Lavaroni F, Martella G, Sancesario G, Bernardi G. (2002) D2-mediated modulation of N-type calcium currents in rat globus pallidus neurons following dopamine denervation Eur J Neurosci. 15:815-25.

Stephenson FA (2001) Subunit characterization of NMDA receptors. Curr Drug Targets. 2:233-9.

Stern P, Behe P, Schoepfer R, Colquhoun D. (1992) Single-channel conductances of NMDA receptors expressed from cloned cDNAs: comparison with native receptors. Proc Biol Sci. 250:271-7.

Sun YJ, Rose J, Wang BC, Hsiao CD (1998)The structure of glutamine-binding protein complexed with glutamine at 1.94 A resolution: comparisons with other amino acid binding proteins. J Mol Biol. 278:219-29.

Surmeier DJ, Song WJ, Yan Z. (1996) Coordinated expression of dopamine receptors in neostriatal medium spiny neurons. J Neurosci. 16:6579-91.

Takahashi, T. (1978). Intracellular recording from visually identified motoneurons in rat spinal cord slices. Proceedings of the Royal Society, London, B, 202: 417-421.

Tanner CM (1992) Epidemiology of Parkinson's disease.Neurol Clin. 10:317-29.

Tezuka T, Umemori H, Akiyama T, Nakanishi S, Yamamoto T (1999) PSD-95 promotes Fyn-mediated tyrosine phosphorylation of the N-methyl-D-aspartate receptor subunit NR2A. Proc Natl Acad Sci U S A. 96:435-40.

Tovar KR, Westbrook GL (1999) The incorporation of NMDA receptors with a distinct subunit composition at nascent hippocampal synapses in vitro. J Neurosci.19:4180-8.

Traynelis SF, Hartley M, Heinemann SF. (1995) Control of proton sensitivity of the NMDA receptor by RNA splicing and polyamines. Science. 268:873-6.

Traynelis SF, Burgess MF, Zheng F, Lyuboslavsky P, Powers JL. (1998) Control of voltage-independent zinc inhibition of NMDA receptors by the NR1 subunit. J Neurosci. 18:6163-75.

Wang LY, Orser BA, Brautigan DL, MacDonald JF.(1994) Regulation of NMDA receptors in cultured hippocampal neurons by protein phosphatases 1 and 2A. Nature 369:230-2.

Wang X, Zhong P, Gu Z, Yan Z.(2003) Regulation of NMDA receptors by dopamine D4 signaling in prefrontal cortex. J Neurosci. 23:9852-61.

Watanabe M, Inoue Y, Sakimura K, Mishina M (1993) Distinct distributions of five N-methyl-D-aspartate receptor channel subunit mRNAs in the forebrain. J Comp Neurol. 338:377-90

Webster R.A. (2001) Neurotransmitters Drugs and Brain Function John Wiley & sons Ltd, Chichester

Wenthold RJ, Prybylowski K, Standley S, Sans N, Petralia RS (2003) Trafficking of NMDA receptors Annu Rev Pharmacol Toxicol. 43:335-58.

Wenzel A, Fritschy JM, Mohler H, Benke D (1997) NMDA receptor heterogeneity during postnatal development of the rat brain: differential expression of the NR2A, NR2B, and NR2C subunit proteins. J Neurochem. 68:469-78.

Weiss, D.S. & Magleby, K.L. (1989). Gating scheme for single GABA-activated Cl- channels determined from stability plots, dwell-time distributions, and adjacent-interval durations. Journal of Neuroscience, 9: 1314-1324.

Williams K. (1993) Ifenprodil discriminates subtypes of the N-methyl-D-aspartate receptor: selectivity and mechanisms at recombinant heteromeric receptors. Mol Pharmacol. 44:851-9

Wong AC, Shetreat ME, Clarke JO, Rayport S (1999) D1- and D2-like dopamine receptors are co-localized on the presynaptic varicosities of striatal and nucleus accumbens neurons in vitro. Neuroscience. 89:221-33

Wood MW, VanDongen HM, VanDongen AM.(1995) Structural conservation of ion conduction pathways in K channels and glutamate receptors Proc Natl Acad Sci U S A. 92:4882-6.

Wyllie DJ, Behe P, Nassar M, Schoepfer R, Colquhoun D. (1996) Single-channel currents from recombinant NMDA NR1a/NR2D receptors expressed in Xenopus oocytes. Proc Biol Sci. 263:1079-86.

Wyllie DJ, Behe P, Colquhoun D (1998) Single-channel activations and concentration jumps: comparison of recombinant NR1a/NR2A and NR1a/NR2D NMDA receptors.. J Physiol. 510 (Pt 1):1-18.

Vicini S, Wang JF, Li JH, Zhu WJ, Wang YH, Luo JH, Wolfe BB, Grayson DR (1998) Functional and pharmacological differences between recombinant N-methyl-D-aspartate receptors..J Neurophysiol. 79:555-66

Vissel B, Krupp JJ, Heinemann SF, Westbrook GL. (2001) A use-dependent tyrosine dephosphorylation of NMDA receptors is independent of ion flux. Nat Neurosci. 4:587-96.

Xie X, Dale TJ, John VH, Cater HL, Peakman TC, Clare JJ. (2001) Electrophysiological and pharmacological properties of the human brain type IIA Na+ channel expressed in a stable mammalian cell line. Pflugers Arch. 441:425-33.

Xiong ZG, Pelkey KA, Lu WY, Lu YM, Roder JC, MacDonald JF, Salter MW (1999) Src potentiation of NMDA receptors in hippocampal and spinal neurons is not mediated by reducing zinc inhibition. J Neurosci 19:37.

Yamamoto, C. (1975). Recording of electrical activity from microscopically identified neurons of the mammalian brain. Experientia, 31: 309-311.

Yang SN (2000) Sustained enhancement of AMPA receptor- and NMDA receptor-mediated currents induced by dopamine D1/D5 receptor activation in the hippocampus: an essential role of postsynaptic Ca2+. Hippocampus. 10:57-63.

Yu XM, Askalan R, Keil GJ 2nd, Salter MW (1997) NMDA channel regulation by channel-associated protein tyrosine kinase Src. Science. 275:674-8.

Yung KK, Bolam JP. (2000) Localization of dopamine D1 and D2 receptors in the rat neostriatum: synaptic interaction with glutamate- and GABA-containing axonal terminals. Synapse. 38:413-20.

Zeron MM, Hansson O, Chen N, Wellington CL, Leavitt BR, Brundin P, Hayden MR, Raymond LA (2002) Increased sensitivity to N-methyl-D-aspartate receptor-mediated excitotoxicity in a mouse model of Huntington's disease. Neuron. 33:849-60.

Zheng F, Gingrich MB, Traynelis SF, Conn PJ (1998) Tyrosine kinase potentiates NMDA receptor currents by reducing tonic zinc inhibition. Nat Neurosci.1:185-91.